TECHNICAL MEMORANDUM

815

Assimilating observations sensitive to cloud and precipitation

Alan Geer, Maike Ahlgrimm, Peter Bechtold, Massimo Bonavita, Niels Bormann, Stephen English, Mark Fielding, Richard Forbes, Robin Hogan, Elias Hólm, Marta Janisková, Katrin Lonitz, Philippe Lopez, Marco Matricardi, Irina Sandu, Peter Weston

Research Department

Abstract

Satellite radiances were originally used only in clear-sky conditions, but now they can be assimilated in cloudy and precipitating areas with the 'all-sky' approach. This has significantly increased the influence of microwave humidity-related observations, which now contribute around 20% of observation impact (measured using adjoint techniques) and improve medium-range scores by around 3%. Much of the benefit comes through 4D-Var tracing, which infers dynamical initial conditions from observed humidity, cloud and precipitation. Initial conditions can be further improved by extending all-sky assimilation to temperature-sounding microwave and infrared radiances, though there are still many challenges, and observation operators need more development. Research will be undertaken to assimilate new types of data, such as satellite-based cloud and precipitation radar, and satellite radiances at frequencies not previously used (e.g. sub-mm or solar). The use of ground-based precipitation radar, rain gauges and lightning imagers is also being developed. All these observations bring new information, not just on the location and mixing ratio of hydrometeors, but also on sub-grid variability (such as the cloud overlap), particle shape and size distribution, and even on particle orientation.

To support these new observations will require an increasingly accurate representation of moist physical processes. The forecast model will start to represent more details of the microphysics and sub-grid distribution of cloud and precipitation, and crucially, these new variables and the assumptions behind them will start to be constrained directly by observational data, using it in the most optimal way, e.g. in its original form as a radiance or a backscatter. By helping to improve the modelling of cloud and precipitation, cloud and precipitation-sensitive observations will give benefit at all forecast ranges. A further important step will be to archive more of the variables required by cloud and precipitation observation operators (for example, hourly precipitation accumulations, or the mixing ratios of convective precipitation) to support forecast validation and verification against observations. The data assimilation system must also continue to provide the right tools, including a move towards cloud control variables. Also the tangent-linear and adjoint representations of the moist physical processes must evolve in tandem with the forecast model itself.

Contents

1 Introduction

1.1 Overview

The assimilation of cloud and precipitation became a theoretical possibility with the advent of variational assimilation in the 1990s. However, given the limited predictability of cloud and precipitation and the often non-linear and discontinuous nature of moist atmospheric processes, it has been difficult to develop this into a practical capability. ECMWF has invested over many years in developing the necessary scientific tools and in finding the best way to make use of observations sensitive to cloud and precipitation, with several previous papers to its Science Advisory Committee (SAC) covering the subject (e.g. Hólm et al., 2002; Bauer et al., 2006c; English et al., 2013). Furthermore, reviews show that most NWP centres are developing the capability (Bauer et al., 2011; Geer et al., 2017b). At ECMWF, the development of assimilation for satellite radiances in all-sky (i.e. clear, cloudy and precipitating) conditions has substantially increased their impact.

These microwave observations are made at a variety of frequencies: 'imaging' channels partly see the surface and were originally used at ECMWF for sensing column-integrated humidity over the ocean; humidity sounding channels are sensitive to broad layer humidity through the troposphere. These channels also have strong sensitivity to cloud and precipitation, from the lowest frequencies which are most sensitive to heavy rain, the mid frequencies which see cloud liquid water, and the higher frequencies that see larger frozen particles such as snow and hail. In the past, all observations affected by cloud and precipitation had to be discarded, and these observations were not major contributors to forecast quality. Now, with the move to all-sky assimilation, these observations provide around 20% of all observation impact in operational forecasts (Geer et al., 2017a, Fig. 1; more details in Sec. 1.4). Although much of the benefit comes from being able to use humidity-sensitive observations in the presence of cloud, information on cloud and precipitation coming from these radiances is also being used to constrain and infer dynamical variables, thus improving forecasts (Geer et al., 2014). A further benefit has been to help to constrain and develop the cloud and precipitation parametrisations in the forecast model; this can help improve cloud and precipitation forecasts at all forecast ranges.

The recent success of all-sky microwave assimilation gives a chance to review ECMWF's broader strategy for assimilating observations sensitive to cloud and precipitation. As will be demonstrated, we are just at the start of an era in which cloud and precipitation-related observations will become an increasingly important part of operational weather forecasting. Around 75% of satellite radiances can still only be assimilated in clear-sky conditions. All-sky assimilation has not yet been implemented for temperature sounding microwave radiances, or for any infrared radiances, and current efforts demonstrate how challenging it will be to achieve this. However, these efforts are strongly motivated by the current impact of all-sky assimilation of microwave water-vapour sensitive radiances. As well as the existing satellite radiance data, observations sensitive to cloud and precipitation are available from an increasing number of sensors such as cloud and rain radar (both satellite-based and ground-based), rain gauges and lightning sensors, as well as satellite radiances at wavelengths that have not previously been assimilated for NWP, such as solar (including visible) wavelengths and mm-waves, which provide new information on cloud ice and cloud water. Hence, this paper to SAC will cover not just the current and future development of all-sky radiance assimilation, but the wider use of observations sensitive to cloud and precipitation.

The development of all-sky assimilation has benefitted greatly from collaborations and funding from external partners. EUMETSAT supports the work at ECMWF through its fellowship program and the NWP Satellite Application Facility (NWP-SAF) collaboration which (with the Met Office, Météo France and new partner DWD) has developed the RTTOV (Radiative Transfer for TOVS) radiative transfer
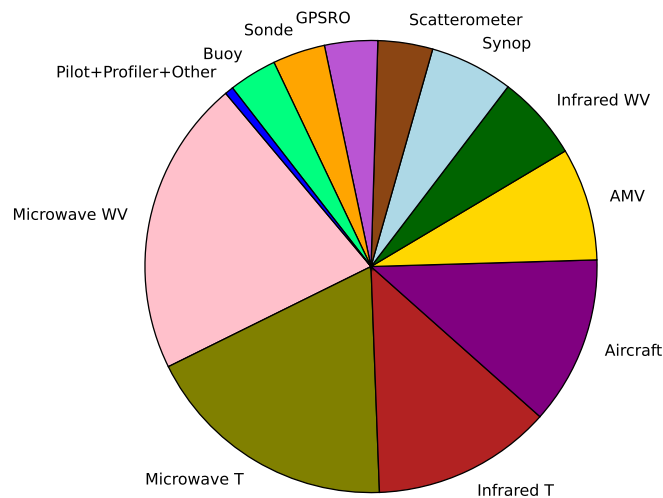
Figure 1: Forecast sensitivity to observation impact (FSOI) measuring the reduction in 24 h forecast error provided by different observation groups in the Cycle 43r3 esuite, given as a percentage of the total FSOI, from 15 April to 15 June 2017. The "Microwave WV" category provides 21% of FSOI; this covers the imaging and/or sounding channels from 12 instruments sensitive to water vapour (WV), cloud and precipitation, most of which are assimilated in all-sky conditions. "Microwave T" and "Infrared T" cover temperature (T) sounding channels in (mostly) clear-sky conditions from respectively 7 and 4 instruments.

model. ESA supports development of satellite radar assimilation for the forthcoming EarthCARE[1] satellite. Moreover, many external scientists have visited to help develop new capabilities. For example scientists from Japan Meteorological Agency (JMA) and Météo France have, respectively, added all-sky GCOM-W AMSR2 and Megha-Tropiques SAPHIR to our system (Kazumori et al., 2016; Chambon and Geer, 2017). Further, the large number of space-based observations that are now available, as well as the observing capabilities being developed for future launches, have depended on funding from space agencies around the world. Within ECMWF, cloud and precipitation assimilation is an inter-disciplinary activity that involves far more than the development of the observations and their observation operators. It has also depended on developments in the modelling of cloud and precipitation and the data assimilation techniques that link model and observations together. Hence, following this introduction (which will motivate the work further, and cover all-sky assimilation and its development history in a little more depth) this paper to SAC has three main sections, the first covering the full variety of cloud and precipitation-sensitive observations, and the following sections covering the modelling and data assimilation aspects. A final short section outlines the links between data assimilation and the forecast verification of cloud and precipitation-sensitive observations.

1.2 Motivation

In their review of the state of the art across different NWP centres, Geer et al. (2017b) expand on four main reasons to assimilate cloud- and precipitation-sensitive observations for weather forecasting:

1. **Extracting mass, wind and humidity in the presence of cloud:** Being able to assimilate satellite

---

[1]Satellite and sensor acronyms are explained in a glossary at the end of this document

radiances in all-sky conditions increases the coverage of satellite sounding observations, even if the cloud and precipitation information content is ignored. For example, cloud can be treated as a sink variable initialised from a prior retrieval as is currently done at ECMWF for overcast infrared radiances (e.g. McNally, 2009). Even if just the moisture and/or temperature information is used, four-dimensional variational assimilation (4D-Var) can infer much about the dynamical state (e.g. mass and wind) through background error covariances and through the 4D-Var tracing of humidity, just as it does for clear-sky observations (e.g. Peubey and McNally, 2009).

2. **Extracting mass, wind and humidity from cloud and precipitation:** Modern data assimilation techniques make it possible to infer information from cloud and precipitation itself. The 4D-Var tracing effect comes from the adjoint of the continuity equation in the presence of a tracer gradient (e.g. Riishøjgaard, 1996; Allen et al., 2013). However, the more complex equations that describe the formation of cloud and precipitation can also be used to infer winds, temperature and humidity even if that is more difficult in practice (see next sub-section). Better initialisation of mass and wind fields then leads to improved forecasts through to the medium range.

3. **Initialising cloud and precipitation:** Especially for nowcasting and regional forecasting, analysing the correct placement of cloud and precipitation is itself of great interest. There are reasons to do this in medium-range forecasting, too: we can hope that in stable continental winter high-pressure systems, once cloud (or its absence) has been analysed correctly, the benefit would persist for some days in the forecasts (e.g. Schomburg et al., 2015). To initialise both tropical and extratropical cyclones, the observed position and intensity of cloud and rain bands is likely to be important. At ECMWF, although we do not have cloud or precipitation control variables, we do initialise cloud and precipitation in the 4D-Var assimilation window using the strong constraint of the forecast model.

4. **Improved modelling of cloud and precipitation:** Confronting forecast models with cloud and precipitation-related observations is an optimal way to understand model biases and help develop better moist physics parametrisations. This is often referred to as the model-to-satellite approach (as opposed to the retrieval approach) and it is a natural output of a data assimilation for weather forecasting. For example, all-sky microwave departures reveal biases in modelled clouds in maritime stratocumulus regions and in cold air outbreaks (e.g. Kazumori et al., 2016). The bias in cold air outbreaks has been tracked to a lack of supercooled water in the model, helping to develop a possible solution (Forbes et al., 2016). Improving the moist physics representation in forecast models benefits medium-range forecasts through the influence of latent heating and radiation processes, and also improves cloud and precipitation forecasts themselves.

Of these reasons, the first three lead to direct improvements in the initial conditions. In the all-sky assimilation of microwave humidity-sensitive radiances at least the first two can be seen to benefit ECMWF forecasts (Geer et al., 2014, 2017a). The fourth reason, the indirect effect, is an area where we expect to see much future benefit, and it will be a running theme through this paper. Assumptions about the microphysical details of cloud and precipitation such as sub-grid overlap and heterogeneity, hydrometeor size distributions and habits are critical to getting accurate simulated radiances and reflectivities. They are also critical to the quality of the moist physics in the forecast model, as well as to the radiation modelling (see this year's other SAC special topic paper, ECMWF, 2017). But different assumptions are being made in different parts of the Integrated Forecasting System (IFS). A long-term goal is to achieve microphysical consistency across the moist physical and radiation processes in the forecast model, as well as in the observation operators. This topic is also of much interest in wider all-sky research (e.g. Galligani et al., 2017; Sieron et al., 2017).

Microphysical consistency will be difficult to achieve in practice, but it has great potential. For exam-
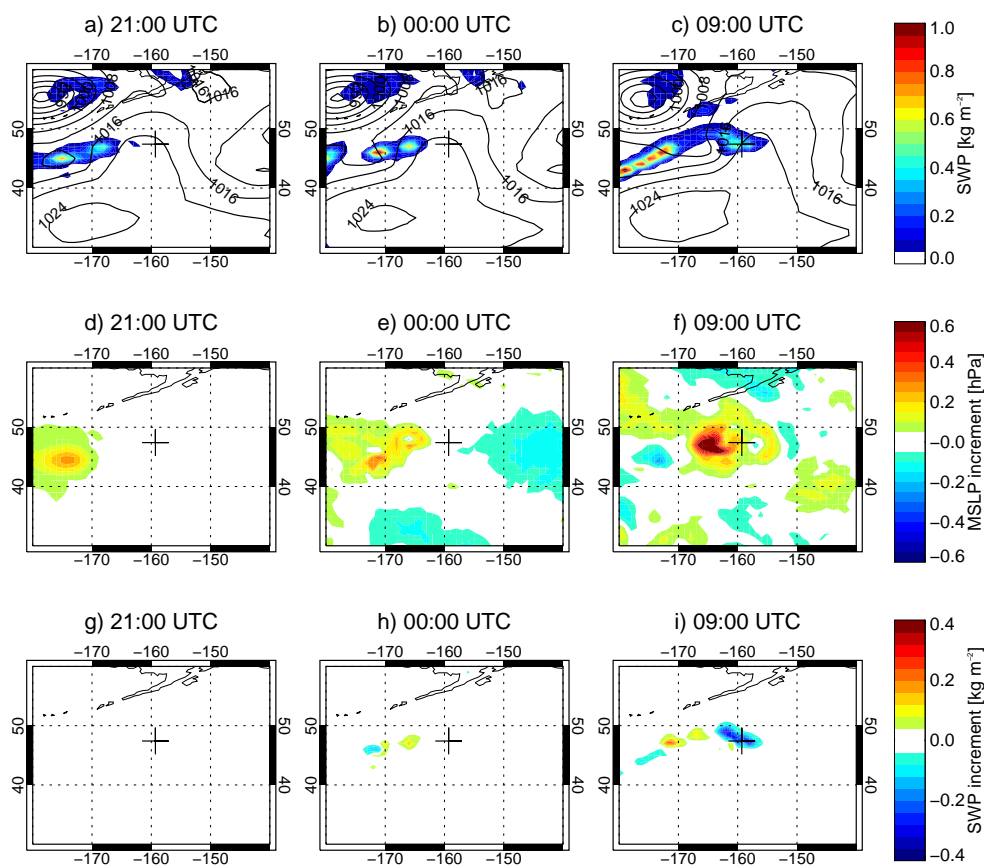
Figure 2: Model fields through the assimilation window (21 UTC - 09 UTC) in single observation of Geer et al. (2014, their case J): (a-c) First guess mean sea-level pressure (MSLP, line contours, in hPa) and snow water path (SWP, filled contours); (d-f) Increments in MSLP; (g-i) Increments in SWP. The cross shows the location of the Metop-B MHS observation, which was made at 08:00 UTC.

ple, infrared observations constrain the sub-grid cloud fraction and cloud-top height, visible observations constrain the cloud optical depth (and hence the particle effective radius), microwave observations give the total column weight of cloud, sub-mm observations will give rich detail on the ice microphysics, such as particle orientation and shape, and finally lidar and radar give the vertical locations of these clouds. So one great hope of cloud and precipitation assimilation is that we can provide a fuller observational constraint on the microphysics and sub-grid modelling and can achieve much more physical realism within both the forecast model and the observation operators. A probably unattainable but ideal goal of this process could be called 'microphysical closure', when there is no further possibility of making incorrect assumptions, or allowing hidden or compensating biases to accumulate, because almost everything is constrained by observations.

1.3 Extracting mass and wind from precipitation: a single-observation study

Single observation test cases show the ability of incremental 4D-Var to fit observed cloud and precipitation by modifying the moist and dynamical initial conditions. Figure 2 examines the increments resulting from a single all-sky MHS observation at 183 GHz. This frequency, originally intended for humidity sounding, is now also used for its strong sensitivity to the precipitation-sized frozen particles character-

Figure 3: FSOI in the ECMWF operational system from June 2012 to October 2016, averaged in 25-day bins, normalised so total impact is 100%.

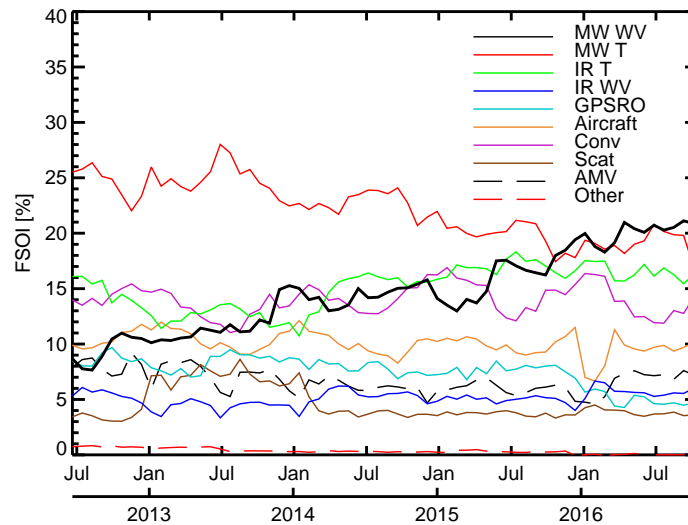istic of deep convection and heavy frontal precipitation. In this example the first guess departures have indicated that the model first guess is over-predicting frozen hydrometeors ('snow') on the leading edge of a developing front. To fit this observation, the pressure of the developing low-pressure system has been increased by around 0.2 hPa at the beginning of the assimilation window, leading to a less intense snowfall along the front that develops 8 hours later. Importantly, no increments are made to the water vapour (not shown) or snow at the beginning of the assimilation window; instead it is the dynamical initial conditions that are adjusted. At midlatitudes, these kind of results have been repeated in many case studies (e.g. Bauer et al., 2010; Geer et al., 2014). In the tropics, in deep convection, many single-observation case studies are similarly successful, but some occasionally fail to fit the observations. This may be due to the difficulty of modelling convection in the tropics, including its diurnal cycle (Sec. 3). However, these case studies support the basic ability of a 4D-Var system to assimilate cloud and precip-itation, and illustrate a mechanism of '4D-Var tracing' that relies on much more physics than just tracer advection.

1.4   Current impact of all-sky microwave radiances

Figure 3 shows the sensitivity of 24 h forecast errors to assimilated observations calculated using an adjoint-based technique (Forecast Sensitivity to Observation Impact, FSOI, Langland and Baker, 2004; Cardinali, 2009). Between 2012 and 2016, the impact of microwave humidity, cloud and precipitation sensitive observations ('MW WV') has increased from 8% to 21% of the total observational impact, mainly coming from applying all-sky assimilation to microwave humidity sounding channels. The first clear increase in the timeseries (September 2013) comes from activating ATMS in clear skies (Bormann et al., 2013). But from then on the increases come from all-sky assimilation: activation of all-sky mi-crowave humidity channels from SSMIS (Geer, 2013; Baordo and Geer, 2016) in November 2013, and the transition of MHS from a clear-sky to an all-sky approach (Geer et al., 2014) in May 2015. More recently, smaller increases have come from activating the all-sky assimilation of new microwave im-agers AMSR2 and GMI (Kazumori et al., 2016; Lean et al., 2017) and the novel sounders MWHS-2 (Lawrence et al., 2016) and SAPHIR (Chambon and Geer, 2017). As illustrated by Geer et al. (2014),

26–Feb–2015 to 13–Sep–2015 from 380 to 399 samples. Verified against own–analysis.
Confidence range 95% with AR(2) inflation and Sidak correction for 4 independent tests
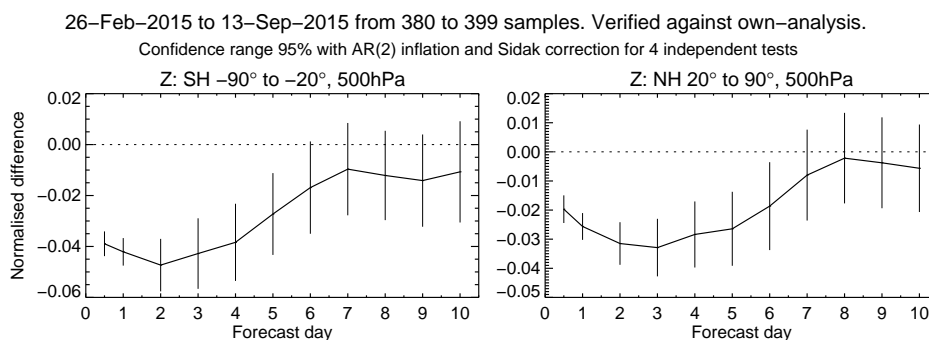

Figure 4: Normalised change in RMS error in 500hPa geopotential in the SH and NH coming from the addition of 7 all-sky microwave humidity instruments in an ECMWF system representative of the operational configuration in mid-2015 (hence measuring the combined impact of clear-sky, cloudy and precipitation-affected microwave humidity observations). Confidence range 95%.

some improvements have come from better use of clear-sky data as well as from the addition of cloud and precipitation-affected observations. As of 2017, a total of 10 microwave humidity-sensitive instruments are being assimilated through the all-sky route (and two more, MWHS and ATMS, await conversion to all-sky).

The leading all-sky microwave sensor is the SSMIS on DMSP F-17, which combines microwave imaging and humidity sounding channels and has near global utilisation (ocean, sea-ice and land including snow-covered land surfaces). On its own it provides around 3.5% of FSOI, a similar level of impact to the most important satellite temperature-sounding instruments, such as AMSU-A and CrIS (temperature channels exist on SSMIS, but are not used at ECMWF). The impact of the all-sky microwave humidity sensors is also seen in the medium-range, using observing system experiments (OSEs). Figure 4 shows that adding 7 all-sky microwave sensors into the otherwise full observing system improves forecasts by around 3% up to day 5.

1.5 Development of all-sky assimilation at ECMWF

All-sky assimilation builds on many developments at ECMWF over the last 20 years[2]. First it relies on the ability of the 4D-Var assimilation system to infer dynamical information from humidity. In the earlier 3D-Var approach, humidity-related observations had no effect on the quality of the ECMWF day-5 forecast (Bengtsson and Hodges, 2005). But with a 4D-Var experiment equivalent to the operational system from 2004, Andersson et al. (2007) showed that activating all humidity-sensitive observations (i.e. clear-sky infrared and microwave satellite data, plus conventional data) reduced day-5 midlatitude temperature and wind forecast errors by around 1% – 3%. Peubey and McNally (2009) showed that, unlike 3D-Var, a 4D-Var system could extract dynamical information from humidity-sensitive radiances using the tracer-advection mechanism.

Although 4D-Var provides a framework for exploiting cloud and precipitation-sensitive observations, along similar lines to the use of humidity observations, the immediate application of these ideas in operational forecasting was hindered by practical and theoretical difficulties (e.g. Fillion and Errico, 1997; Errico et al., 2000). For example the 'zero-gradient problem' means that cloud and precipitation observations cannot be assimilated when cloud or precipitation is missing in the first guess. Despite the

---

[2]A more detailed version of this section is found in Geer et al. (2017a)

possible difficulties, it was noted that meteorologically sensitive areas are often cloudy (McNally, 2002) and ECMWF invested significant resources towards developing cloud and precipitation assimilation (e.g. Hólm et al., 2002; Andersson et al., 2005). For microwave radiance assimilation, one key development was the computationally efficient, scattering-capable radiative transfer code (Bauer, 2001; Chevallier and Kelly, 2002; Smith et al., 2002; Bauer et al., 2006d) that is now available as the RTTOV-SCATT package within RTTOV. However, the most critical early developments were the tangent-linear and adjoint moist physics models that link a change in the 4D-Var control variables with a change in cloud and precipitation fields (Janisková et al., 1999; Tompkins and Janisková, 2004; Lopez and Moreau, 2005). These moist physics developments were justified by the need to improve the quality of the tangent-linear approximation to the full nonlinear atmospheric model beyond what was achievable with a purely adiabatic approach (Mahfouf, 1999) but their additional potential for enabling cloud and precipitation assimilation was clear. However, it was still not obvious how to use cloud and precipitation-sensitive observations in the data assimilation system.

ECMWF explored a great variety of strategies for using cloud and precipitation-sensitive observations, including the assimilation of cloud retrievals from MODIS and precipitation retrievals from microwave imager radiances (e.g. Chevallier and Kelly, 2002; Moreau et al., 2003; Marécal and Bauer, 2002; Lopez and Bauer, 2007; Benedetti et al., 2005; Lopez and Moreau, 2005). One problem with many of these early studies was the use of cloud and precipitation retrievals. This is problematic because the error statistics of these observations can be far from Gaussian, because of the zero-gradient issue, and also because of the sub-optimal analysis that can result from assimilating retrievals (e.g. Andersson et al., 1991; Joiner and Da Silva, 1998; Migliorini et al., 2008). It was seen that radiances have a more continuous sensitivity to humidity, cloud and precipitation, and departure statistics can be more Gaussian (Moreau et al., 2004; Bauer et al., 2006a). However, there was still caution around operational use of cloud and precipitation-sensitive observations. Hence the first operational assimilation at ECMWF, starting in 2005, used cloud- and precipitation-affected microwave imager radiances with an initial 1D-Var retrieval to infer total column water vapour (TCWV) from the radiances (Bauer et al., 2006a). Then the TCWV retrievals were assimilated in 4D-Var, giving a '1D+4D-Var' approach (Bauer et al., 2006b), intended to keep any problems of nonlinearity or non-Gaussianity outside of the main assimilation system.

Other solutions to the problems of nonlinearity and non-Gaussianity were found, allowing some additional use of cloud and precipitation-sensitive observations in the ECMWF operational system. For infrared radiances, limited use of cloud-affected data was introduced, focusing on the clear-air signal above the 'surface' provided by an unbroken cloud top (McNally, 2009; Lupu and McNally, 2012). The direct assimilation of surface rain rate composites from radars and rain gauges over the U.S.A. was also implemented by Lopez (2011) using 6-hour precipitation accumulations to improve linearity, and a logarithmic transform of the rain accumulations to improve Gaussianity.

It was still hoped to be able to directly assimilate cloud and precipitation-affected radiances into 4D-Var, with a main motivation being to avoid the theoretical sub-optimality of 1D+4D-Var (Lopez and Bauer, 2007; Geer et al., 2007, 2008). Further, the 1D+4D-Var technique suffered from biases which led ERA-Interim to underestimate global rainfall for the years when cloud and precipitation-affected microwave imager data were assimilated (Dee et al., 2011). There were several, partly cancelling biases involved, of which the largest was excessive rainfall in the simplified moist physics used in the 1D-Var retrieval. However, a more fundamentally important, counter-balancing bias was also present, in the asymmetric treatment of observations when they are divided up into a 'clear' and 'rainy' stream (Geer et al., 2008). The only way to eliminate artificial biases coming from the clear-sky approach is to assimilate all observations using a cloud- and precipitation-capable observation operator throughout: a single 'all-sky' radiance assimilation.

It was important to show that 4D-Var assimilation can handle nonlinearity associated with cloud and precipitation, but in principle an incremental 4D-Var system has an advantage in assimilating radiances. Even if there is no initial sensitivity to cloud or precipitation in the forecast model, at least the atmospheric humidity can be adjusted in the first minimisation to better fit the radiances, therefore creating cloud or precipitation in a subsequent linearisation trajectory. This avoids the zero-gradient problem. The accuracy of the cloud and precipitation tangent-linear (TL) approximation was investigated by Bauer et al. (2010) who showed that even if it is not good for the initial large increments it becomes increasingly good in subsequent re-linearisations. In one example, it was shown that ECMWF incremental 4D-Var can create convection to match all-sky microwave humidity observations, even when it does not exist in the first guess.

The transition of the microwave imager assimilation to all-sky came in two stages. It was first implemented with an observation error model that inflated observation errors as a function of distance from gridpoint centre, trying to account for representation error (Bauer et al., 2010; Geer et al., 2010). However, this was a poor predictor for observation error, and much better results were obtained using the average of observed and simulated cloud amount, known as a 'symmetric' observation error model (Geer and Bauer, 2010, 2011, with 'cloud amount' more precisely being an approximate retrieval of the square of the cloud optical depth at the relevant frequency). Although cloud and precipitation features are generally well represented by the forecast model, often their intensity or location is slightly wrong when compared to observations; all these errors are referred to as 'mislocation'. The distance between an observation and a model grid-point had little effect on the size of the first-guess departures for distances less than 100 km, because cloud and precipitation features are not fully predictable over 12 h on that scale. Wherever cloud and precipitation is present, mislocation errors dominate and produce large first-guess departure variances. These errors are generally considered as representation error, and hence it is appropriate to include them in the observation error model. There is usually a clear relationship (often linear or quadratic) between the inferred 'cloud amount' and the size of these variances. A main benefit of the new error model was to produce nearly Gaussian first-guess departures, addressing another of the possible problems with cloud and precipitation assimilation.

Figure 5 illustrates the link between the mislocation error and the assigned observation error. In panel a, heavy precipitation in a mesoscale convective system just south of the island of Sumatra has caused high observed 19 GHz brightness temperatures between 8°S and 13°S, over a distance of roughly 500 km. The forecast model's first guess represents the same convective system, but it is incorrectly restricted between 10°S and 13°S. As shown in panel b, this gives a typical 'dipole' pattern of first guess departures, even if the error itself is more complicated than a simple displacement. These dipoles, of different shapes and scales, are a major feature of any map of cloud and precipitation first guess departures. The analysis, based on all observations including the all-sky data, is able to extend the area of precipitation to match observations, though in this case it fails to reduce precipitation between 10°S and 13°S where it is too intense in the model. The observation error model inflates observation errors (also shown on panel b) across the region where precipitation is present in either the observations or the first guess.

The initial use of all-sky observations focused on the microwave imaging channels, and the main subsequent development was the extension to the moisture sounding channels at 183 GHz on sensors like SSMIS, MHS and MWHS-2, which has provided significant benefits to medium-range forecasts over the last 4 years (Geer, 2013; Geer et al., 2014; Lawrence et al., 2016). This was only possible after substantial observation operator biases were addressed. These biases came from an inadequate representation of scattering from frozen particles (Geer and Baordo, 2014). Instead using a discrete-dipole-based representation of scattering properties of snow particles (Liu, 2008), cloud and precipitation observations could be simulated with more realism at AMSU-A frequencies like 52.8 GHz but also up to 183 GHz,
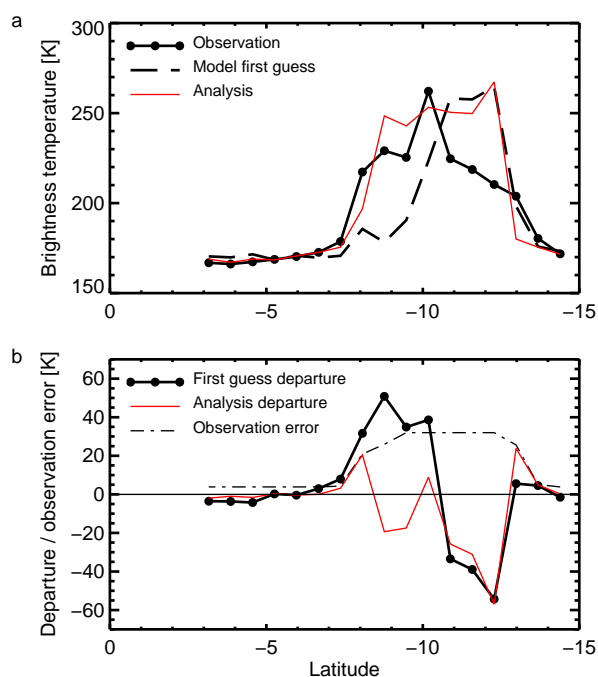
Figure 5: Assimilating SSMIS F17 channel 19h observations in the presence of precipitation displacement and intensity errors: a) Observed, modelled and analysed brightness temperatures (high brightness temperatures correspond to precipitation); b) First guess departure, analysis departures, and observation error. A N-S transect has been taken at 100°E through observations valid at 00Z on 3rd May 2016.

making the humidity sounding channels viable candidates for all-sky assimilation. A further vital step was the development of all-sky dynamic emissivity retrievals (Karbou et al., 2006; Baordo and Geer, 2016) helping to use the data over land and sea-ice surfaces.

1.6   Status at other NWP centres

In conjunction with the international symposium on data assimilation (ISDA) 2016, NWP centres working on all-sky assimilation have reviewed their status and plans (Geer et al., 2017b). Many centres already use some form of cloud and precipitation assimilation operationally, and others are working towards it:

- **Météo France:** Infrared radiances are assimilated in some cloudy areas, using a prior retrieval of cloud (Pangaud et al., 2009). The operational mesoscale NWP system (AROME) includes the assimilation of ground-based radar reflectivities (Caumont et al., 2010; Wattrelot et al., 2014). This relies on a '1D Bayesian' technique to retrieve a water vapour pseudo-variable for assimilation in the main analysis, which is useful when TL and adjoint (AD) moist physics are not available, but potentially subject to the limitations of the 1D+4D-Var approach noted at ECMWF. There are projects to develop cloud and precipitation-affected radiance assimilation in a 1D Bayesian or 1D-Var framework with applications to both local and global models (Guerbette et al., 2016; Martinet et al., 2013). However, the long-term plan is to use the ensemble variational (EnVar) assimilation framework to allow direct radiance assimilation with EnVar replacing the need for TL and AD forecast models.

- **Met Office:** Infrared observations are assimilated in some cloudy areas (Pavelin et al., 2008),

similar to Météo-France. Ongoing work aims to introduce all-sky assimilation of microwave humidity-related observations, starting with improvements to the handling of cloud and precipitation increments (Migliorini et al., 2017).

- **DWD:** The local-area NWP system (KENDA) is the focus of developments at DWD, with its Local Ensemble Transform Kalman Filter (LETKF) assimilation technique avoiding the need for TL and AD physics development. For regional forecasting, cloud is a main assimilation target, and the direct assimilation of both infrared and visible radiances is under development (Harnisch et al., 2016; Schomburg et al., 2015; Scheck et al., 2016). All these techniques will be developed with the intention to use them in the both the global and the local NWP system.

- **JMA:** With tropical cyclones (TC) as a forecasting priority, direct all-sky infrared and microwave radiance assimilation is under development along similar lines to that at ECMWF (e.g. Okamoto, 2017). Promising results have been seen in the TC analysis, with all-sky microwave observations able to positively influence TC structure and development.

- **NCEP:** Since May 2016, NCEP have operationally assimilated AMSU-A temperature-sensitive radiances in an all-sky framework, although they do not use the data in precipitation (Zhu et al., 2016). This has removed a spurious low-level moisture bias that was caused by the earlier clear-sky framework. Ongoing developments will extend the all-sky framework to more microwave data, and to infrared (e.g. Bi et al., 2016).

2 Observations

2.1 Introduction: a wealth of data

There is a growing variety of observations giving information on cloud and precipitation. First are observations already routinely available to ECMWF, including typical satellite radiances that are (or were previously) assimilated only in clear-sky situations, but which have great sensitivity to different aspects of cloud and precipitation. This category also includes things like the rain gauge accumulations that are standard part of synoptic reports, but have until now only been used for offline verification. Hence, one reason to assimilate cloud and precipitation-sensitive observations is simply to make better use of existing data. But beyond this, user requirements, including those of NWP and weather science, have been driving a large increase in the provision of cloud and precipitation-related measurements by space agencies. This includes the ESA EarthCARE mission which will be launched in 2019 and will provide cloud radar and lidar, as well as the novel EUMETSAT ICI instrument, which will be launched as part of the second-generation Metop programme in 2022, and will sense ice cloud at sub-mm frequencies. Lightning sensors are being launched on US and European geostationary platforms, and other international partners such as NASA and JAXA have already launched the Global Precipitation Measurement (GPM) mission. At ECMWF we already use the microwave imager from GPM but the dual-frequency precipitation radar (DPR) on the same satellite would be interesting to assimilate. Finally there are existing observation types, such as ground-based rain radar, where NWP users will need to work harder to encourage provision of appropriately quality-controlled, near-real time observations for weather forecasting. We do already operationally assimilate ground-based radar-gauge composite precipitation observations over the USA, but observational coverage needs to be extended to Europe and other areas, and the direct assimilation of reflectivities needs to be developed.

This section will survey the available observations, along with the current state of their development at

ECMWF, or the potential for future development. Even if not intended for operational assimilation in the first instance, passive monitoring of these new observations should provide improved diagnostics of the quality of cloud and precipitation in the forecast model. At the end we will summarise the priorities and timelines relating to this very diverse set of observations.

2.2   Microwave imaging and humidity sounding channels

As described in Sec. 1 the assimilation of radiances from microwave imagers under all-sky conditions has been operational at ECMWF since 2005, first using a 1D+4D-Var approach and then from 2009 using direct all-sky radiance assimilation (Bauer et al., 2010). More recently, microwave humidity sounding channels have been added in all-sky conditions, giving a significant increase in forecast impact (Geer et al., 2014, 2017a). Imaging channels are assimilated over ocean surfaces, only between 60°S and 60°N, for frequencies of around 19 GHz, 23 GHz, 37 GHz and 90 GHz. These observations are sensitive to the ocean surface and to total column water vapour across all frequencies. Sensitivity to hydrometeors varies strongly with frequency: low microwave window frequencies (e.g. 5 - 20 GHz) sense predominantly the column-integrated rain, whereas mid window frequencies (e.g. 30 - 90 GHz) are more sensitive to cloud liquid water. There is also sensitivity to scattering from large frozen particles (e.g. snow and graupel in deep convection) around 90 GHz. Humidity sounding channels are found at higher frequencies still, around 183 GHz, where the sensitivity to large frozen particles is stronger. Because they are not so sensitive to the surface, the humidity-sounding channels can be assimilated over most ocean, sea-ice and land surfaces, giving near-global coverage. In some situations, all-sky humidity radiances are affected by systematic errors between observations and model (Geer et al., 2011; Kazumori et al., 2016; Lonitz and Geer, 2017, see also Sec. 3). We have not been able to correct these biases with Variational Bias Correction (VarBC; Dee, 2004; Auligné et al., 2007) given their complex and sensitive dependencies on the local conditions. Hence, some situation-dependent screening is necessary, mainly in high-latitude cold-air outbreaks (Lonitz and Geer, 2015).

Currently microwave imaging channels are assimilated from three sensors: the SSMIS onboard of DMSP-F17 (SSMIS-F17), along with AMSR2 and GMI. Other satellites and sensors are available with similar channels, but we have not seen benefit from using more than three sensors actively. Rather the additional data seems to start degrading forecasts instead. In contrast, all additional data from humidity sounding channels has benefitted forecast quality (including the recent addition of SAPHIR and GMI humidity channels; Chambon and Geer, 2017; Lean et al., 2017). Hence we try to use all available sensors with humidity sounding channels, a total of 9 so far (SSMIS from F17 and F18, MHS from Metop-A, Metop-B, NOAA-18 and NOAA-19, plus MWHS-2, SAPHIR and GMI). The significant impact of the humidity-sounding channels means that even apparently small upgrades are worth pursuing. For example the improved use of all-sky humidity sounding observations near coastlines, which will go into Cycle 45r1, will bring significant forecast improvements.

For the future, the broad aims are to use more channels, and to extend the use of microwave imaging channels over land surfaces. The addition of the 150 GHz and 166 GHz channels will help constrain humidity increments better in the vertical (Lean et al., 2017). The addition of frequencies below those currently used, such as 10 GHz, will bring more information on tropical rain over oceans, and the required developments (such as more exact treatment of coastlines and spatial response functions) will support potential future assimilation of sea-ice, SST and snow cover. Finally, although radiative transfer modelling for imaging channels is significantly more difficult over land, there is still substantial information on frozen particles, so that we could improve analyses of snowfall over land. There will also be benefits from addressing observation error correlations in the error model, particularly as this may be necessary

to support the use of additional channels (see Sec. 4.4). Also there are still major improvements that can be made in the observation operator for all-sky microwave radiances; these will be described in Sec. 3.6. Lowering errors in the observation operator should allow more weight to be put on the observations, and will support developments in the forecast modelling of microphysics and sub-grid heterogeneity. Finally, the maximum limit of assimilating three microwave imagers needs to be investigated further: whether it is an issue of situation-dependent systematic error (e.g. Kazumori et al., 2016), or whether it is a more fundamental issue like the possible generation of gravity waves that degrade the stratosphere (Lean et al., 2017) it indicates that we still need to improve the data assimilation and modelling framework to be able to use cloud and precipitation-sensitive observations better.

2.3 Microwave temperature sounding channels

Microwave temperature sounding radiances are currently the second most influential part of the observing system, providing around 18% of FSOI (Fig. 1). We assimilate AMSU-A instruments from six satellites (MetOp-A and B, NOAA-15, 18 and 19, Aqua) as well as ATMS from Suomi-NPP, which provides similar capabilities. Up to 10 temperature channels are assimilated from each instrument, giving a set of broad-layer temperature weighting functions peaking from around 5 km up to 60 km. The majority of forecast impact comes from constraining the large scales. Currently cloud- and precipitation-affected radiances are screened, resulting in a loss of up to 25% of the data from the most important tropospheric sounding channels. All-sky assimilation would bring additional temperature information in meteorologically active areas, as well as information on frozen hydrometeors similar to that from the humidity sounding channels. We could also assimilate AMSU-A channel 4 for the first time. This peaks lower than the existing channels and as a result is strongly affected by cloud liquid water; if used in an all-sky approach it could bring valuable new information on both cloud and temperature in the lowermost troposphere. Previous attempts to assimilate AMSU-A radiances in the presence of cloud and precipitation gave mixed results and exposed limitations in the scattering optical properties used in the radiative transfer model (Geer et al., 2012). This led to the development of improved particle scattering properties (Geer and Baordo, 2014), leading to a much better accuracy of simulated all-sky radiances at AMSU-A and ATMS frequencies. Hence we have again started to look at moving AMSU-A into the all-sky framework.

Testing of all-sky AMSU-A is done in three stages, the first two of which are illustrated in Fig. 6. A first stage assesses the impact of changing to the all-sky infrastructure, without activating all-sky assimilation (this is known as 'clear-sky in all-sky'). There are minor scientific differences between the two approaches, including different thinning and treatment of surface skin-temperature. This first stage results in small degradations to temperature and humidity forecasts throughout the atmosphere, indicated by the degraded fits to most ATMS channels in the figure. This shows that the existing framework for assimilating microwave temperature data in clear-skies is highly tuned and some of its refinements need to be transferred into the all-sky framework. Next, comparing the second stage to the first stage gives a clean test of the impact of all-sky assimilation. This improves temperature and moisture in the troposphere but further degrades the stratosphere. In the third stage (not shown), adding the assimilation of AMSU-A channel 4 improves first guess fits to microwave imagers indicating improved short range forecasts of humidity, cloud and precipitation. However, there are also degradations in longer range temperature and geopotential height forecasts indicating our system is not yet able to make good use of AMSU-A channel 4.

It is possible that adding too much new information on cloud liquid water from AMSU-A might be hitting similar problems to those seen when adding more all-sky microwave imager data. For example, the
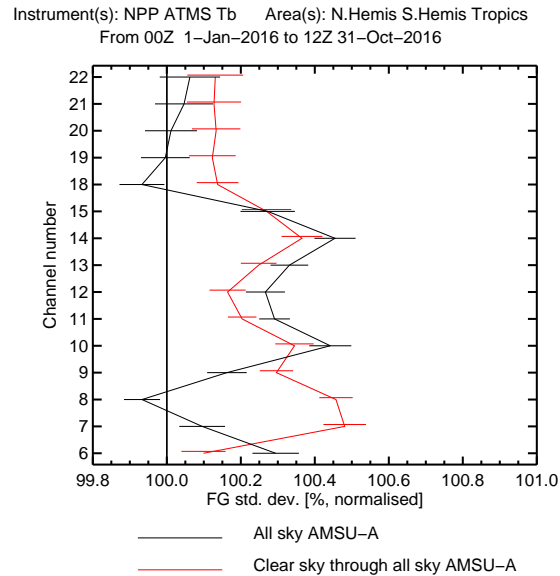
Figure 6: Change in first guess fits to ATMS channels from AMSU-A 'clear-sky through all-sky' and all-sky experiments against an AMSU-A clear-sky control which is represented by the 100% line.

slight degradations of the stratosphere in Fig. 6 are reminiscent of those shown by Lean et al. (2017) when adding all-sky GMI microwave imager channels. There may also be issues specific to doing all-sky assimilation for temperature channels. For example there may be greater vulnerability to the zero-gradient problem, due to the lack of humidity sensitivity. Increments may be aliased into temperature fields in the absence of cloud in the first guess, which, unlike humidity increments, will probably not create cloud in subsequent re-linearisations. A further possible issue is that reliably separating the required temperature increments from those to the cloud hydrometeors may demand too much from the existing background error modelling. However, we have seen that moving existing AMSU-A channels to all-sky framework could bring forecast benefits, but only if further work is done to transfer over some of the refinements of the existing clear-sky approach (for example by matching the thinning strategy). Even if the initial benefits of all-sky AMSU-A radiance assimilation are small, we can expect them to grow as the assimilation system becomes better able to make use of cloud information, and it will simplify the system if all radiances go through the all-sky approach. Instruments like AMSU-A will remain an influential part of the observing system, with new AMSU-A, ATMS, MWTS-2 and MWS instruments all planned for launch in the next five years.

2.4 Between microwave and infrared: sub-mm

An under-exploited region of the spectrum is found between the highest frequencies of conventional microwave channels (up to 190 GHz, which corresponds to a wavelength of 1.6 mm) and the far-infrared end of the range of typical infrared radiometers like IASI (which go down to 2000 GHz or equivalently up to 15 μm). This region is sometimes referred to as the sub-mm and it contains water vapour and oxygen lines that provide sounding capabilities similar to those at conventional microwave frequencies, as well as window channels offering additional information on cloud and precipitation (Klein and Gasiewski, 2000; Prigent et al., 2006; Buehler et al., 2007; Birman et al., 2017). The unique contribution of these frequencies is a strong sensitivity to the amount, size distribution, and likely also the shape and orientation of cloud ice particles. This has encouraged EUMETSAT to include an Ice Cloud Imager (ICI) on its

next generation polar satellites, which will observe selected frequencies between 183 GHz and 664 GHz. Further, there are many proposals for using constellations of small cheap 'cubesats' that will make use of this spectral range. A cubesat can provide only a small aperture (order 10 cm) making it hard to provide a small-enough field-of-view on the surface at frequencies lower than around 200 GHz. To prepare for ICI's launch in 2022, and to be able to assimilate any cubesat data that may become available, ECMWF will develop capabilities to assimilate these radiances.

A preliminary capability for simulating clear-sky ICI radiances is already available in RTTOV v12, including surface emissivity calculations (Prigent et al., 2016). The capability for all-sky simulations is awaiting developments such as the generation of particle scattering optical properties databases; these are not yet available for frequencies above 300 GHz but EUMETSAT is procuring them. The need for new particle scattering models for ICI will require us to revisit the simulation of particle scattering at microwave frequencies, which were last updated for RTTOV-SCATT by Geer and Baordo (2014), who chose a smooth and idealised 'sector' snowflake (Liu, 2008) to represent frozen precipitation particles. To produce accurate results at higher frequencies will require more complex shape models, so as to continue representing features on scales down to the wavelength of the radiation. Similarly, cloud ice particles, which are currently modelled simply as spheres, will instead need detailed non-spherical modelling. Finally, the effects of oriented particles will need to be modelled (since for a fixed particle size, the higher the frequency, the more the extinction depends on the area rather than the mass of a particle). All these developments will also improve radiative transfer simulations at the microwave frequencies we already use, so they will help improve the existing all-sky assimilation.

2.5   Infrared

Hyperspectral infrared sounders like IASI, AIRS and CrIS observe the temperature and moisture profile with much greater vertical resolution than is possible with current microwave instruments. Cloud-detection is key to making good use of current infrared observations; no centre has yet assimilated them in all-sky conditions, except for a limited use of cloudy scenes with a prior retrieval of cloud parameters (e.g. Pavelin et al., 2008; McNally, 2009; Pangaud et al., 2009). For a mid-tropospheric channel, only around 20% of scenes will be identified as cloud-free; the rest have to be discarded, generally in the most meteorologically sensitive areas (McNally, 2002). Figure 7 illustrates the additional coverage to be gained, especially in the midlatitude storm-tracks, with all-sky assimilation of a typical mid-tropospheric water vapour channel. These channels are much more sensitive to cirrus cloud than are the microwave equivalents, but otherwise they have similar radiative transfer, and could provide similar benefit in an all-sky approach. If the impact of these infrared channels could be raised to that of the all-sky microwave humidity-sensitive channels (Fig. 1) it could substantially benefit medium-range forecasts. The infrared temperature-sounding and window channels will be left for now: these are likely to be more challenging, due to the dominating influence of cloud.

ECMWF has been working towards all-sky IR assimilation since the possibilities were first examined by Chevallier and Kelly (2002) and Chevallier et al. (2004). An important step was the extension of RTTOV to simulate cloudy infrared radiances including a parametrisation of scattering effects (Matricardi, 2005). An all-sky framework has been developed, including the development of a symmetric error model similar to the one used for microwave observations (Okamoto et al., 2014). However, progress has been hindered by the slow speed and high memory requirements of RTTOV when simulating cloudy IR brightness temperatures. As will be illustrated in Sec. 3 the infrared is strongly sensitive to variations in cloud fraction and overlap as a function of altitude. The all-sky microwave module RTTOV-SCATT can use just two sub-columns to represent these effects with acceptable accuracy in the microwave (Geer et al.,
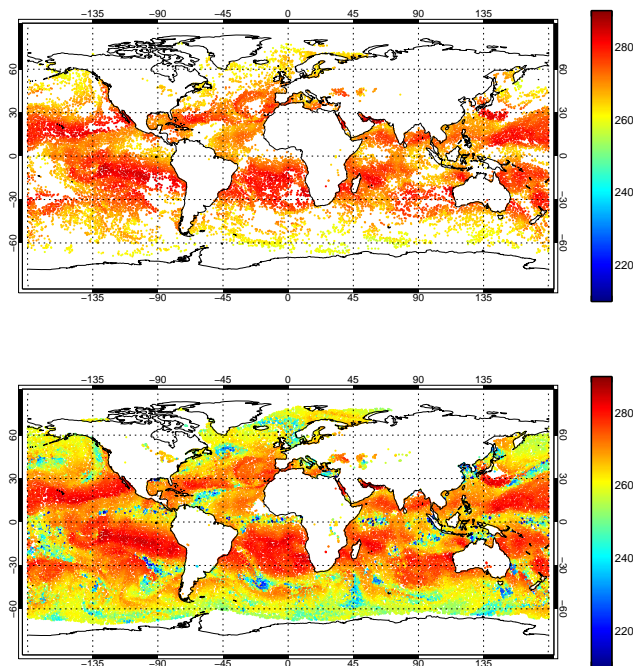
Figure 7: IASI observations available for assimilation in channel 2889 (a mid-tropospheric water vapour sounding channel) after cloud screening (top panel) or in an all-sky framework (bottom panel). Colour scale indicates the brightness temperature in Kelvin.

2009), but in contrast the infrared module needs up to around 100 sub-columns. As a workaround, a two sub-column approach has been devised, which uses a single cloudy column that occupies a fraction of the grid-box equal to the maximum cloud fraction in the upper-troposphere (this scheme is sometimes referred to as CMSS for Cfrac Max Simple Streams). This allows much faster simulation of upper-tropospheric water vapour channels, but it is highly inaccurate for lower-peaking channels.

The most recent testing of all-sky infrared attempts to move the 7 upper-troposphere water vapour channels of IASI from a clear-sky to an all-sky approach, bringing the additional coverage shown in Fig. 7. The operational assimilation of IASI now uses an observation error covariance matrix to represent inter-channel error correlations, with significant benefits to forecast scores (Bormann et al., 2016). Hence it has been necessary to extend this for all-sky assimilation in order to represent the increased inter-channel error correlation and the larger error standard deviations found in cloudy conditions (see Sec. 4.) Initial results of all-sky assimilation are mixed. For example Fig. 8 compares the impact on fits to ATMS data coming from assimilating the 7 IASI water vapour channels in either the existing clear-sky framework, or in the all-sky framework. While the clear-sky assimilation improves first guess fits, mainly in the channels sensitive to water vapour (ATMS channels 18–22), the all-sky assimilation does not do as well, and it also apparently degrades the temperature forecast from the troposphere to the stratosphere (ATMS channels 5–15). These problems appear to come from noise being added to the analysis that dissipates during the forecast. This noise is still present after 12 hours, but medium-range forecast scores are not degraded. This suggests that the all-sky assimilation is generating additional, possibly unwanted, increments in temperature and moisture fields in order to fit observed cloud features, as already seen with the assimilation of all-sky microwave imagers (e.g. Geer and Bauer, 2010; Kazumori et al., 2016). In order to reduce these spurious increments, we either need to improve the quality of the radiative transfer

Instrument(s): NPP ATMS Tb   Area(s): N.Hemis S.Hemis Tropics
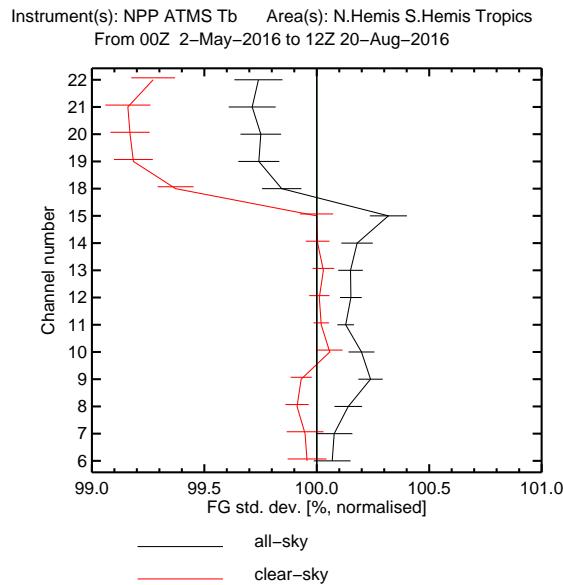From 00Z 2–May–2016 to 12Z 20–Aug–2016

Figure 8: Normalised change in standard deviation of first guess ATMS departures, when seven IASI upper-tropospheric channels are activated in either a clear-sky or an all-sky framework, in the context of the otherwise full observing system, which is represented by the 100% line.

modelling or the forecast model, so as to avoid state-dependent systematic errors that could be aliased into the analysis, or we need to change the filtering properties of the data assimilation system, so that spurious increments are suppressed. This might be achieved with further development of the observation error model, but might also require changes to the background error modelling or to the tangent-linear forecast model.

2.6 Solar

Solar radiances provide potentially very useful information on clouds, including on cloud optical depth, which is complementary to the thermal-infrared and microwave radiances. However, accurate modelling of solar radiances is much more expensive than at longer wavelengths because of (a) the presence of a discrete source (the sun), and (b) much weaker absorption which leads to the radiance field being more sensitive to the details of the particle scattering pattern. For this reason, their use has so far been limited to experimental assimilation of cloud optical-depth retrievals from MODIS (Benedetti and Janisková, 2008). We would envisage improved impact on forecast quality if we were able to assimilate radiances directly.

To support the future assimilation of solar radiances, we will need to develop a fast forward model. RTTOV can already compute cloudy radiances at solar frequencies using the highly accurate 1D Discrete Ordinate Method (DOM), but its high computational cost makes it unsuitable for operational forecasting. Hence, the Method for Fast Satellite Image Synthesis (MFASIS, Kostka et al., 2014; Scheck et al., 2016) is being implemented in RTTOV by DWD and the Met Office. MFASIS uses reflectance look-up tables computed using the DOM based solver DISORT. The state of the atmosphere and the geometry is described using 8 parameters (i.e. vertically integrated optical depths and effective particle radii for water and ice clouds, albedo, solar zenith angle, sensor zenith angle and azimuth angle difference) which are sufficient to compute reflectances with an accuracy of a few percent. MFASIS gives good results

compared to DISORT simulations but it is typically 3–4 orders of magnitude faster.

A radiance model that overcomes some limitations of the look-up table approach is the 'Forward-Lobe Two-Stream Radiance Model' (FLOTSAM), being developed at ECMWF to generate retrieval products for model validation. It exploits the fact that particle scattering patterns are frequently dominated by a 'forward lobe' of width around 30°. This enables the radiation field at a given height to be described as the sum of three components: the direct (unscattered) solar beam, a wide beam propagating away from the sun due to scattering by the forward lobe, and a diffuse radiation field that has been scattered enough times to lose memory of the direction to the sun. FLOTSAM also compares well to reference calculations using a DISORT approach, and gives a substantial speed increase. ECMWF will initially use MFASIS as it develops assimilation of solar radiances, but the FLOTSAM model should potentially be brought into RTTOV at a later stage, where it could become part of the standard observation operator framework coordinated by the EUMETSAT NWP-SAF.

2.7   Earth radiation budget

Top-of-the atmosphere (TOA) fluxes from earth radiation budget satellites such as CERES are already extensively used for validation by model developers (e.g. Forbes et al., 2016) as they have strong sensitivity to cloud fraction and optical depth. Given that the model radiation scheme already provides the 'forward operator' as well as the tangent-linear and adjoint to generate TOA fluxes, only a small amount of development work would be required to provide passive monitoring, and potentially assimilation of these instruments. Apart from the current lack of near-real-time satellite data provision, another issue is the mixed sensitivity to different atmospheric variables, which may be hard for an assimilation system to interpret correctly. Nevertheless, the passive monitoring of TOA fluxes remains a low-priority development.

2.8   Spaceborne radar and lidar

Since their advent in the late 1980s, cloud radars have been the workhorse for the study of clouds (e.g., Kollias et al., 2007). By penetrating deep into even the most strongly-precipitating storms, radars see the cloud structure in unrivalled detail. Used in synergy with lidar, they can be used to infer ice and liquid particle concentrations. Space-based observations from active sensors, such as radar and lidar, are not currently assimilated in the ECMWF operational 4D-Var system. The ESA-funded projects on Quantitative Assessment of the Operational Value of Space-Borne Radar and Lidar Measurements of Cloud and Aerosol Profiles (QuARL, Janisková et al., 2010) and EarthCARE assimilation (STSE, Janisková et al., 2014) helped develop an observation operator called ZmVar, and they have shown these observations are useful not only to evaluate the performance of current NWP models in representing clouds, precipitation and aerosols, but they also have potential to be assimilated. Figure 9 illustrates the quality of IFS simulations of the pioneering CloudSat (Stephens et al., 2002) and CALIPSO (Cloud-Aerosol Lidar and Infrared Pathfinder Satellite Observations; Winker et al., 2009) observations. Experimental assimilation of these observations using a 1D-Var+4D-Var technique showed benefit to both the analysis and subsequent short-term forecast (Janisková, 2015).

The immense detail provided by active sensors paradoxically increases the difficulty in their use to initialize a forecast. Many of the challenges in radar or lidar assimilation are shared with passive cloudy observations and some are new. The profiling nature of active sensors adds additional complexity; any mis-match in the positioning of clouds between observation and model is difficult to reconcile. For radar, the forward model is extremely sensitive to assumptions on hydrometeor size (Di Michele et al., 2012).
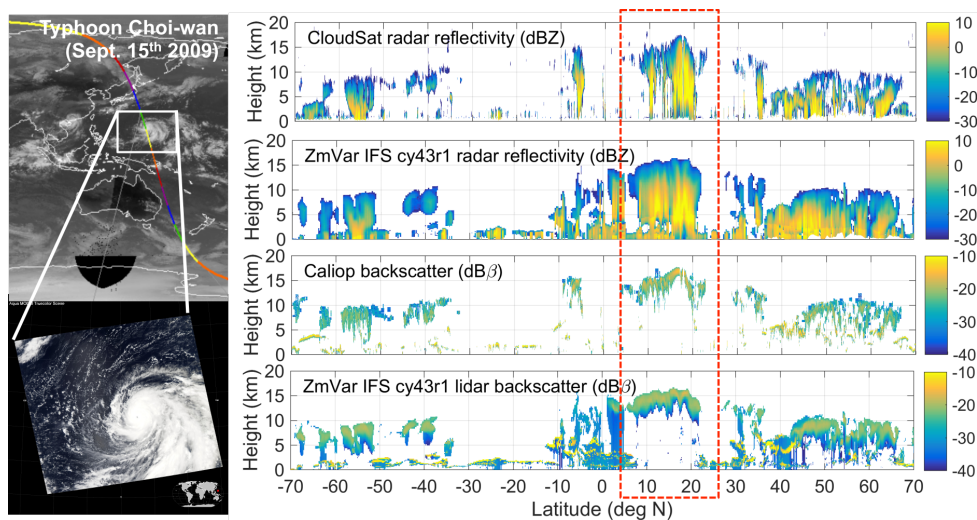
Figure 9: Observed and modelled CloudSat radar reflectivity and CALIPSO lidar backscatter for a satellite transect passing through Typhoon Choi-Wan (red dashed line) on September 15th 2009.

For lidar, any errors in the forward model can compound quickly where the signal is attenuated. As for all cloudy observations, if the model observations depart too far from the real-world measurements, the non-linearity in the model and observation operators can result in a sub-optimal analysis.

Direct assimilation of active observations in 4D-Var is under development to support ingestion of Earth-CARE (Illingworth et al., 2015) cloud radar and lidar observations upon its launch (expected mid-2019). When implemented, this will be the first time profiling observations using radar and lidar have been assimilated in to a global NWP model. Further developments are possible: doppler velocity provided by the EarthCARE radar could be assimilated once fallspeeds are represented within the IFS cloud scheme. It is also hoped to allow assimilation of the Dual-frequency Precipitation Radar (DPR) on GPM, through a collaboration with Météo-France that aims to unify the active and passive microwave observation operators in RTTOV-SCATT. Most of the science base in ZmVar is the same as in RTTOV-SCATT, and moreover, it would become easier to use consistent microphysical assumptions throughout the active and passive observations assimilated at ECMWF.

2.9   Ground-based precipitation radars

Precipitation observations derived from ground-based radars over the U.S.A. have been assimilated directly in the ECMWF operational 4D-Var system since November 2011. The data are NCEP Stage IV surface precipitation composites derived from the American network of ground-based weather radars (NEXRAD) but with rain-gauges used for calibration. Assimilation improves not only the short-range precipitation forecasts, but also the geopotential and temperature forecasts over the North Atlantic and over Europe, several days later (Lopez, 2011). To use precipitation observations successfully required some novel developments: the observations are assimilated as 6-hour accumulations rather than the original hourly precipitation data, which improves the validity of the linear assumption in 4D-Var minimizations. Also a logarithmic transform is applied before assimilation so as to make the distribution of departures more Gaussian, and bias correction relies on VarBC, but with bias predictors formulated as functions of the precipitation amount itself. Figure 10 shows the continuous improvement of forecast precipitation evaluated against NEXRAD observations (due to model upgrades but also to the assimila-
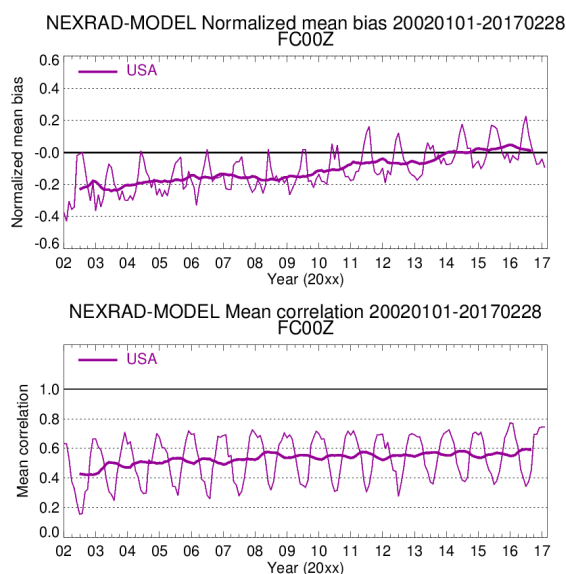
Figure 10: Monthly mean bias (top) and correlation (bottom) of ECMWF operational day-1 forecasts against NEXRAD composites for 6-hour accumulated rainfall over the U.S.A. from January 2002 to February 2017. Both monthly curves (thin line) and one-year running mean (thick line) are shown. The bias is normalized by the monthly precipitation averaged over the model and the NEXRAD observations.

tion of these observations starting 2011), with a reduced mean bias and increasing correlation against the precipitation observations. Snowfall situations have been included in the assimilation from Cycle 43r1 (November 2016) onwards, after being conservatively discarded for many years.

So far, the assimilation of retrieved precipitation composites has been preferred to volume reflectivity data in order to avoid a heavy burden of pre-processing and quality control of data from individual radars. Besides, raw data from individual radars are often much more difficult to obtain due to data policy restrictions, even within Europe. European precipitation radar composites (OPERA) have been continuously evaluated against synoptic station (SYNOP) rain gauges and ECMWF short-range forecasts since 2008. However, despite an obvious improvement over the years, the quality of the European radar composites is still not good enough for operational assimilation, because of recurrent issues of inter-ference contamination (especially over Eastern Europe) and occasional spurious ground clutter echoes. A systematic underestimation of precipitation amounts is apparent, particularly in snowfall situations in the wintertime because of the use of a single reflectivity-precipitation relationship for rain and snow (Saltikoff et al., 2015). A 'partial' assimilation of OPERA composites might be envisaged as soon as sub-regions with better quality can be identified. For the future, assimilation of reflectivities rather than precipitation amounts would give better control of the reflectivity-precipitation relationship, and could be achieved in a unified observation operator framework that also supports spaceborne active and passive applications. This would require the lifting of current access restrictions to raw data, and ideally we would develop access to other large-scale radar composites, such as those from China.

2.10   Precipitation gauges

Precipitation accumulations are routinely measured by worldwide networks of rain gauges, but only those from SYNOP stations have the near-real-time availability that would allow their use in operational

Model (gp7h) CG+IC Flash Rate (input resol. = 9 km)
2016082800 +15 -> +18h

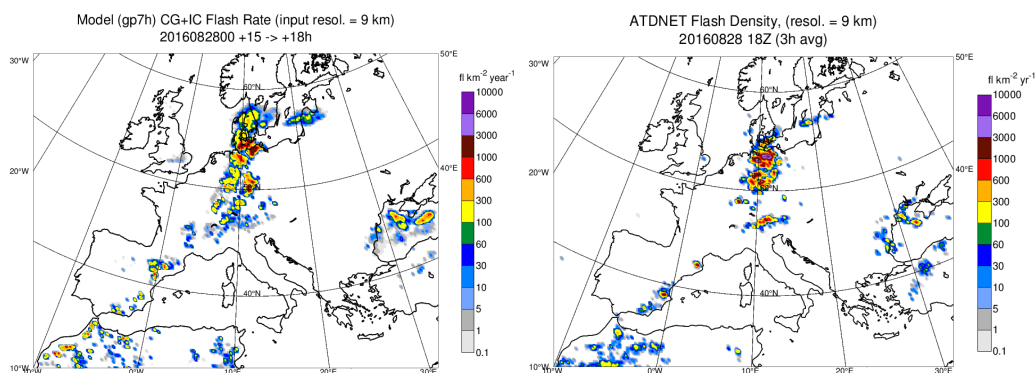ATDNET Flash Density, (resol. = 9 km)
20160828 18Z (3h avg)

Figure 11: Comparison of an 18h forecast of total lightning flash densities (per km² per year) on 28 August 2016 with ATDnet ground-based observations over Europe (data from Met Office), both on the model's 9 km grid. Since the detection efficiency of ATDnet is around 80% for cloud-to-ground flashes and much less for intra-cloud flashes, the numbers are not comparable, but spatially there is good agreement.

data assimilation. The experimental 4D-Var assimilation of worldwide SYNOP rain gauges found limited impact on scores in an operational framework due to the dominating impact of all other observation types already assimilated Lopez (2013). However, it was demonstrated that rain gauge assimilation could be beneficial to atmospheric forecast scores when the coverage in other observation types was restricted to surface pressure data only, as would be the case in an early 20th century reanalysis.

The assimilation of global precipitation gauges is challenging. There is a lack of worldwide standardization in terms of instrument type (shape, design) and instrument height above ground, despite existing WMO recommendations, and the required metadata are hard to obtain or nonexistent. This hinders the accurate estimation of gauge biases, especially in strong wind situations where the aerodynamic influence of the instrument generates 'under-catch'. The potentially huge gap in representativeness between rain-gauge point measurements and model grid-box average precipitation values also needs to be accounted for. This can be addressed partly by observing that the representativeness error generally decreases with accumulation length (hence the assimilation of 6 h accumulations) and also by parametrizing representativeness errors based on precipitation observations from high-resolution rain-gauge networks. Finally, rain gauge accumulation length and end-of-accumulation times can vary between countries and the data assimilation system is flexible enough to handle this, as long as the accumulation time is within the assimilation window. Similar issues can affect rain-gauge verification done using archived forecast accumulations from MARS, but these could be addressed using the revised archiving strategy proposed in Sec. 5.

The operational implementation of rain gauge assimilation has been postponed to address the recent change in the format of the input data (to BUFR) but is otherwise ready for operational assimilation. Including rain gauges into the set of data passively monitored within 4D-Var would make them more useful for forecast verification and model development. There would also be a case to support rain-gauge assimilation under reanalysis activities, given the demonstrated benefits in data-sparse periods like the early 20th century, and in recent decades the possibility to assimilate high-density climatological rain-gauge networks that are not available in near-real-time.

2.11   Lightning

Lightning can disrupt a wide range of human activities, including power supply, forestry and air transport. In the past decades, a growing number of lightning observations have become available from ground-based sensors. Both global (e.g. Vaisala GLD360, ENTLN, WWLLN) and continental-scale networks (e.g. ATDnet, LINET, EUCLID in Europe, NLDN in the U.S.A.) have been installed. These sensors detect the electromagnetic signals (or 'sferics') emitted by lightning discharges at Very-Low-Frequency (VLF), Low-Frequency (LF) or Very-High-Frequency (VHF). Space-borne lightning imagers are also available, and following the pioneering missions OTD (1995-2000) and TRMM-LIS (1998-2013), the next generation of geostationary satellites (US GOES-R GLM and China's FY-4A LMI) will offer full-disk observations of total lightning with an unprecedented temporal sampling. Europe is expected to follow suit with the launch of MTG LI in 2021. A lightning parametrization has been developed for the IFS which includes tangent-linear and adjoint models making it suitable for data assimilation (Lopez, 2016) as well as the forecasting of lightning activity, which could be of great interest to end-users as well as for model validation. Fig. 11 shows the good level of agreement between forecast and ATDnet ground-based observations. Of course, lightning data assimilation comes with many challenges, most of which are related to its intermittent and discrete nature. The successful implementation of lightning 4D-Var assimilation in the coming years will require to adopt a conservative, smooth approach, with the application of some temporal or spatial averaging and a careful screening of observations.

2.12   Summary

A common theme from the assimilation of microwave imaging and temperature-sounding channels, as well as from the infrared humidity channels, is that adding too much cloud and precipitation-sensitive data can generate unwanted increments in the short-range. There can also be degradations to the stratosphere, possibly through the generation of resolved gravity waves. Hence, the problem of assimilating cloud and precipitation observations is far from solved. However, as described in Sec. 1.5 there was no smooth path to the current successful assimilation of all-sky microwave water vapour observations, and a series of improvements in many areas was required, taking years to get right. Hence it is still a high priority to move the remaining 75% of satellite radiances from a clear-sky to an all-sky framework. Operational implementation should be targeted even if the all-sky approach brings no improvement in forecasts compared to the clear-sky framework initially. History shows that forecast benefit can be unlocked by developing the system further once it is operational, for example by adding new satellite channels, or by improving the quality of cloud and precipitation modelling. As more data is added to the all-sky framework, the pay-off for new developments becomes ever larger. For example, a solution to the problem of unwanted short-range increments (perhaps by getting the assimilation system to better filter all-sky-induced gravity waves) might allow the rapid addition of more microwave imager instruments and additional channels from many existing instruments, from AMSU-A to IASI. To benefit from this we need to standardise our satellite radiance framework, both in the IFS and by making sure that all observation operator developments are incorporated in the RTTOV radiative transfer model.

Outside the aim of moving existing radiance observations into the all-sky framework, there are many possibilities for using new observations sensitive to cloud and precipitation. These range from solar radiances to lightning, along with novel cloud and precipitation-sensitive satellite channels on existing instruments. Of these, one immediate priority is the development of EarthCARE radar and lidar assimilation, which is already planned for operational assimilation after launch in 2019. Another short-term priority is the development of the sub-mm observations and the extension of microwave imager usage to 10 GHz. Although operational sub-mm ICI data will only appear from 2022, solving the scientific

challenges (for example, being able to simulate polarised scattering from oriented particles) will bring immediate benefits to the existing all-sky microwave observations. Similarly, the scientific developments for 10 GHz (such as better handling of coastlines, and better treatment of sub-grid heterogeneity in convection) will also benefit existing all-sky usage, and they are a starting point for assimilating earth-system quantities such as sea-ice.

Some developments have a lower priority because they are not expected to bring large benefit to initial conditions. This includes rain gauges and earth radiation budget measurements. However, it would not require great effort to provide an initial passive monitoring capability that would benefit forecast verification and model development. Hence, these developments may not go forward immediately but a small effort at the right time could bring benefits. A final category of developments have a much longer time-frame and would certainly be expected to benefit forecast quality when assimilated. This includes the use of solar radiances, ground-based radar reflectivities and lightning. Here it is important that data providers (as well as the wider research community) know these are realistic targets for operational assimilation in global weather forecasting within the next 10 years, and that we will expect to assimilate quantities close to the original measurement, such as radiances and reflectivities. This will motivate (and ECMWF should also encourage) the development of near-real-time, publicly-accessible data provision for NWP.

3 Modelling

3.1 Introduction

As illustrated in previous sections, the assimilation of cloud and precipitation requires a forecast model that can simulate cloud and precipitation without state-dependent systematic error, as well as observation operators that are capable of accurately transforming the cloud and precipitation profiles (along with the rest of the earth-system state) into observed quantities like radiances, backscatter or accumulated precipitation. Within a 4D-Var framework, it is also necessary to provide tangent-linear and adjoint versions of these models, which are examined in Sec. 4.2. Where there are discrepancies between observations and the model, it is often hard to uniquely attribute the problem to the forecast model or to the observation operator. To diagnose these issues requires detailed collaborative work between the observation and model specialists, and supporting evidence from a number of observing systems. Further, many similar assumptions need to be made about the microphysics (such as particle size distributions) and sub-grid variability (such as the cloud and precipitation overlap) in both model and observation operator. Often these assumptions are inconsistent, even within different parts of the forecast model. For the future it makes sense to think about the observation operators and forecast model as part of a unified system, possibly sharing components such as sub-grid cloud-generators and particle habit models. This section follows that philosophy, placing the issues of forecast modelling and observation modelling side by side.

Section 2 has already given an overview of the observation operators, but it is worth summarizing how the forecast model represents cloud and precipitation. All clouds, plus the stratiform precipitation, are parametrized with prognostic equations for cloud liquid, cloud ice, rain and snow water contents and a sub-grid fractional cloud cover. The cloud scheme represents the sources and sinks of cloud and precipitation due to the major generation and destruction processes, including cloud formation by detrainment from cumulus convection, condensation, deposition, evaporation, collection, melting and freezing. The scheme is based on Tiedtke (1993) but has been developed over the years with an improved representation of liquid-phase, ice-phase and mixed-phase microphysical processes (Tompkins et al., 2007; Forbes

and Tompkins, 2011; Forbes et al., 2011). Each hydrometeor category is represented with one prognostic variable, the grid-box mean specific water content (kg of water/ice per kg of moist air) and hence the parametrization is described as a single-moment scheme (rather than a double-moment scheme which also prognoses particle number concentrations). Particle size distributions, terminal fall speeds and densities are all represented diagnostically based on observational studies. Subgrid heterogeneity is modelled to first order with the subgrid cloud fraction prognostic variable, and various diagnostic assumptions to represent heterogeneity of humidity and in-cloud ice/water and rain/snow water contents.

The moist convection scheme is based on the mass-flux approach and represents deep (including congestus), shallow and mid-level (elevated moist layers) convection. Clouds are represented by a single pair of entraining/detraining plumes which describes updraft and downdraft processes. The scheme, originally described in Tiedtke (1989), has evolved over time and amongst many changes includes a modified entrainment formulation leading to an improved representation of tropical variability of convection (Bechtold et al., 2008), and a modified CAPE closure leading to a significantly improved diurnal cycle of convection (Bechtold et al., 2014). An important part of the scheme is the detrainment of cloud water/ice (and more recently rain and snow) as well as cloud fraction into the prognostic variables treated in the cloud scheme. Hence detrained cloud from the convective updrafts (for example representing convective anvils) is present and has memory in the prognostic cloud variables. This cloud associated with the convection can then interact with the radiation and the grid-scale dynamics through latent heating/cooling. However the cloud associated directly with the convective core is not represented explicitly, but the convective core precipitation fluxes are represented diagnostically.

We will first examine the quality of agreement between model and observations, also illustrating some of the areas where all-sky observations are helping to identify model biases (Sec. 3.2). However, the real target for future improvements is the detailed sub-grid and microphysical properties of cloud and precipitation. In the model, these control things like rate of rain formation, precipitation evaporation and the precipitation rate at the surface. Better control of these parameters should help to correct some of the remaining errors in the forecast model. These parameters also have great influence on the observations. For example, good knowledge of the area-fraction of convective updrafts is important for making accurate simulations in the passive microwave. Section 3.3 will explore some of these detailed modelling issues. Sec. 3.4 describes some of the main assumptions being made across the forecast model and observation operator, illustrating the need for unification of these assumptions. Finally Secs. 3.5 and 3.6 outline the future evolution of the model physics and observation operators to support greater use of cloud and precipitation observations, and to allow those observations to play a bigger role in constraining the forecast model.

3.2   Accuracy of model cloud and precipitation in observation space

An assimilation system is designed to correct random rather than systematic errors. Hence, if there are systematic errors between the simulations and their observed counterparts, and these are assimilated, this can bias the analysis and degrade the forecast (e.g Andersson et al., 1991). When it comes to cloud and precipitation, the agreement between simulations and observations is already good enough to permit assimilation of cloud- and precipitation-sensitive observations in many situations. The visual agreement between simulated and observed cloud in observation space is usually surprisingly good (e.g. Chevallier and Kelly, 2002). Simulated geostationary satellite images (Lupu and Wilhelmsson, 2016) are a popular forecast product that routinely demonstrate the quality of cloud modelling in the IFS. However, long-term monitoring of the actively assimilated cloud- and precipitation-sensitive observations has helped identify important state-dependent systematic errors, some of which can be traced to cloud process modelling, and
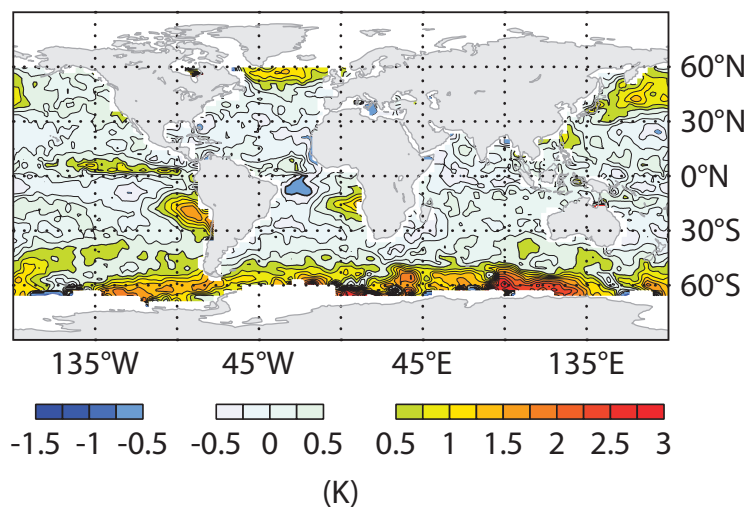
Figure 12: Annual mean of the operational SSMIS microwave 92 GHz brightness temperature first-guess departures (May 2014 to April 2015) from the ECMWF HRES assimilation system (model minus observation).

others which are not fully understood. Some of these biases are large enough to prevent the observations being assimilated in those areas, or even to prevent the assimilation of some channels globally.

Low-frequency microwave observations over ocean have sensitivity to the liquid water path, i.e. the mass of water cloud. There has been a longstanding positive bias in all-sky microwave imager first-guess departures around $50° - 60°$ latitude, which is strongest in winter and particularly in the southern hemisphere (Fig. 12). The bias occurs in cold-air outbreaks, where observed microwave imager radiances are typically warmer than the corresponding model radiances. As discussed in Forbes et al. (2016) the model does not generate sufficient liquid cloud compared to observations, instead preferring to generate ice cloud. Joint work from observation and model scientists showed that modelled detrainment from convection in cold-air outbreaks is not generating sufficient supercooled liquid water. The availability of all-sky first-guess departures helped to identify the problem and find its strong link to lower tropospheric stability (e.g. Lonitz and Geer, 2015; Kazumori et al., 2016). Cloud retrievals from CALIPSO lidar and TOA radiation budget measurements from CERES have also been important in confirming and diagnosing the problem. Improvements have now been made in both large-scale and convective cloud schemes that should become operational with Cycle 45r1, and which are expected to reduce the bias.

A bias is also found in maritime stratocumulus areas, also most likely due to insufficient cloud liquid water (or possibly drizzle) in the forecast model. This is seen in Fig. 12 off the west coasts of S. America and S. Africa. Kazumori et al. (2016) showed the dependence of the first-guess departure biases on the local solar time: biases peak in the early morning, suggesting the forecast model is unable to generate the full amplitude of the morning peak in cloud liquid water typical of maritime stratocumulus. More research is needed to understand the origins of the maritime stratocumulus bias: for example in the observation operator we need to ensure the issue is not associated with drizzle (and hence may be affected by the projection effect, which is not modelled).

The higher-frequency microwave observations help us examine the quality of convection modelling in the IFS. It is still difficult to represent the diurnal cycle of convection and in particular the diurnal cycle over land remains a challenge for models with horizontal resolutions $> 1\text{-}2$ km (Pearson et al., 2014). The strong and rapidly changing surface heat fluxes over land, together with convective inhibition lead to
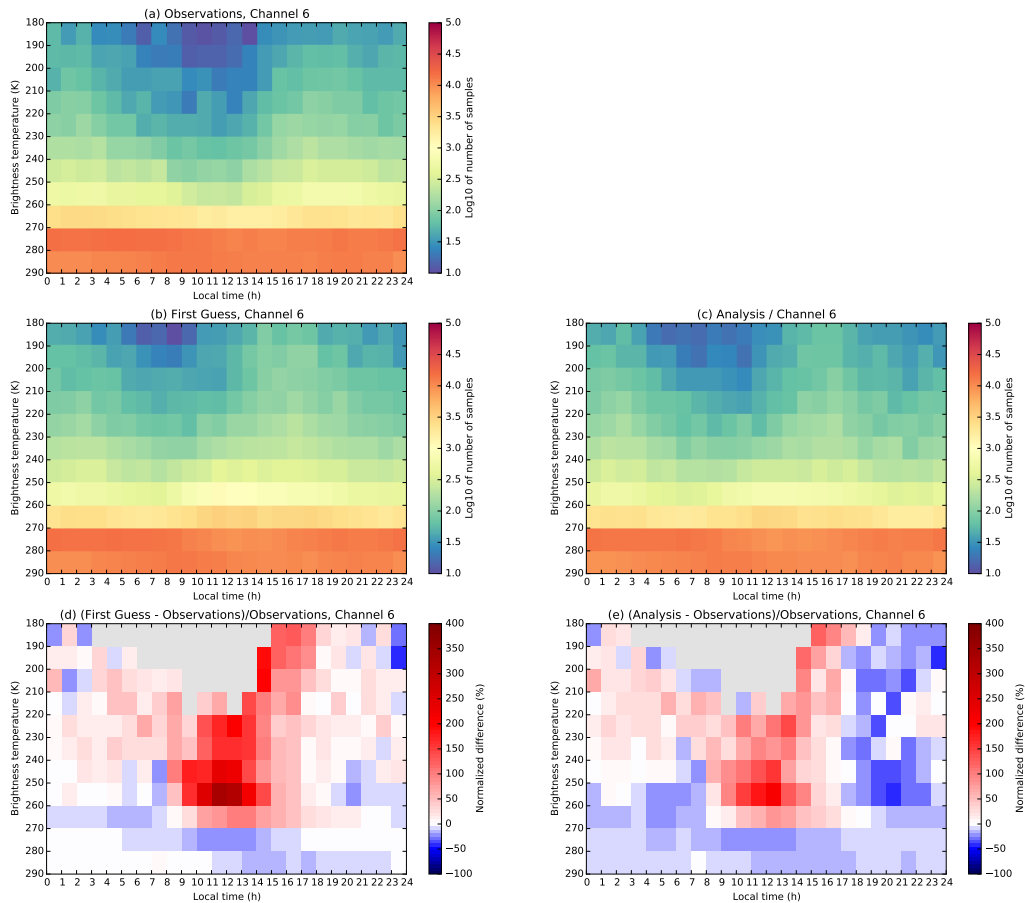
Figure 13: Two-dimensional histograms of observed (a) and simulated (b, first-guess, c, analysis) brightness temperatures for tropical land surfaces from SAPHIR channel 6, taken from Chambon and Geer (2017). The percentage difference between observations and simulations is also shown (d, e). The brightness temperatures are categorized by local time bins and brightness temperature bins over the whole tropics. Low brightness temperatures (e.g. less than 260 K, towards the upper part of the histogram) are associated with large frozen particles in deep convection.
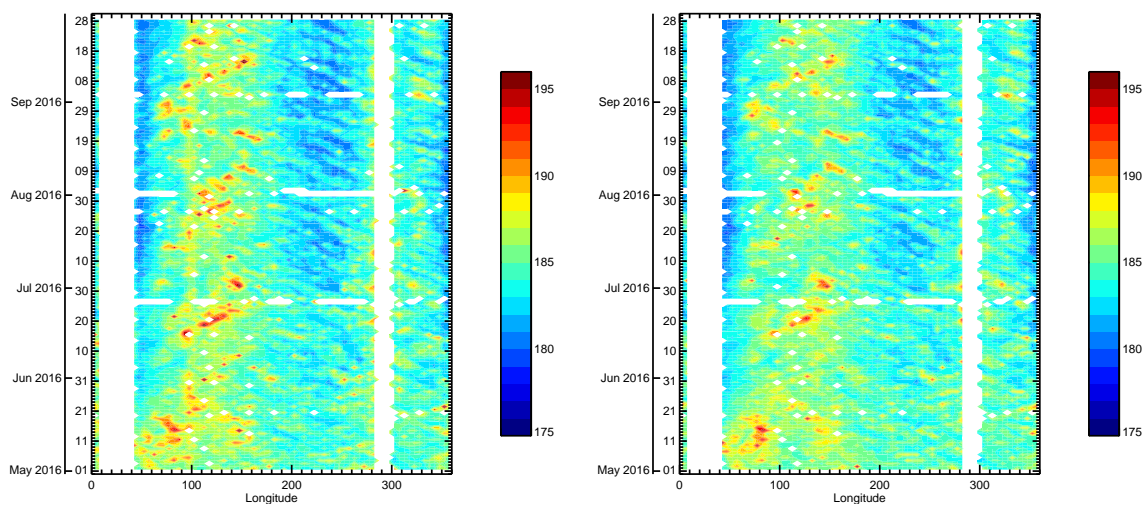
Figure 14: Hovmöller diagrams of all-sky 10 GHz brightness temperatures from AMSR2 during May-September 2016 in the operational system (left) and the first guess (right). Warmer brightness temperatures are associated with rain.

a convection that is not in equilibrium with its forcing, and therefore less predictable. ECMWF forecasts of the diurnal cycle have been much improved recently (Bechtold et al., 2014) and can now realistically represent both the characteristic rainfall maximum in the early morning hours over the oceans and the late afternoon rainfall peak over land. However, Fig. 13 shows there are still disagreements between the modelled and observed diurnal cycles of all-sky 183 GHz SAPHIR brightness temperatures (Chambon and Geer, 2017). These observations are sensitive to scattering from large frozen particles in deep-convective cores. This makes them sensitive to the evolution (glaciation phase) of convective clouds which can precede surface precipitation by 1 to 3 hours. Fig. 13 indicates that the first guess overestimates the occurrence of medium cold brightness temperatures in the 230-260 K range between 10 and 15 local solar time (LST), indicating too-early onset of the glaciation phase of convection. However, the night-time convection (very cold brightness temperatures) is reasonably well simulated. The analysis is able to partly suppress the excessive daytime convection, but at a cost of introducing a night-time bias instead. However, this is not the whole story: ground-based radar measurements see precipitation near the ground, and they show that the modeled convective rainfall decays on average too rapidly after roughly 20 LST so that the convective nighttime precipitation tends to be underestimated (Lopez, 2014). In particular this is seen in the Southern Great Plains and the Sahel region where there are strong night-time mesoscale convective systems that are linked to a nocturnal low-level jet. This illustrates how a range of observations are needed to observe and constrain the diverse processes of cloud formation and precipitation.

One final example will illustrate an area where the IFS is doing well. Convectively-coupled tropical waves modulate tropical rainfall on synoptic to intra-seasonal scales, so an accurate representation of the structure and propagation of these waves is of the highest priority in tropical numerical weather prediction. Since Bechtold et al. (2008) the IFS has greatly improved the prediction of these waves, with the improvements in the Kelvin waves and the Madden-Julian oscillation being the most prominent. The tropical wave features are illustrated in Fig. 14 with the aid of Hovmöller diagrams of the 10 GHz all-sky brightness temperatures during May to September 2016 observed by AMSR2 and as simulated by the first guess. Over the Indian Ocean and West Pacific region (50°E – 150°E) both the observations

and the model produce distinct features that are associated with eastward propagating Kelvin waves and westward propagating Rossby waves, with the anomalies being somewhat larger in the observations. The Rossby (African easterly waves) over the Atlantic ($300°E - 360°E$) are also realistically reproduced by the first guess.

3.3   Sensitivity to sub-grid and microphysical details

Cloud and precipitation-affected radiances are strongly sensitive to sub-grid and microphysical details. This section investigates some of those sensitivities, illustrating how the observations can help constrain the model, but also showing how much detailed work is required to make accurate physical interfaces between the forecast model and the observation operator. To start with, we will look at the sensitivities of all-sky infrared radiances. Compared to the microwave, which is generally sensitive to a large depth of cloud and/or precipitation, and strongly affected by the microphysical details of those hydrometeors, the infrared mostly sees cloud tops and might be expected to be easier to model. However, it is just as dependent on sub-grid and microphysical details: there is strong sensitivity to the cloud's altitude, its phase, the fraction it occupies in the field of view, and to some extent the microphysical details of the cloud. These sensitivities are also often ambiguous – for example, changes in cloud fraction and cloud altitude can have very similar effects on the simulated brightness temperature.

The effects of cloud properties on high-spectral resolution radiances measured by the IASI instrument are examined in Fig. 15 which shows the 'cloud effect', in this case the simulated clear-sky brightness temperatures, minus the brightness temperatures when cloud is added to that scene. The high spectral resolution of IASI can finely resolve the infrared (IR) spectral shape of cloud features. Simulations have been carried out using the RTTOV fast radiative transfer model with the Chou scaling parametrisation for cloud scattering (Matricardi, 2005, 2006). Panel a shows the radiative effect of a water cloud (with a small effective radius representative of maritime conditions) placed at approximately 6 km altitude either as an overcast layer (black) or as two adjacent broken cloud layers corresponding to 50% and 30% fractional cloud coverage (with maximum overlap and with the top still placed at 6 km, red). This shows the dramatic difference when some of the radiance emitted below the cloud can reach the top of the atmosphere. The cloud signal is strongest in the more transparent regions of the spectrum (e.g. the thermal infrared 'window' at 1000 cm^{-1}). Panel b shows the same two possible clouds but this time using the optical properties of a stratus (maritime) water cloud and placing it at an altitude of about 2 km. Compared to panel a, the cloud has much less effect because its lower altitude gives lower thermal contrast with the background. There is also a small effect from changing the optical properties (e.g. a larger effective radius) but the effect of cloud altitude dominates, and there is still a large difference between overcast and layered cloud.

Panel c illustrates the effect of cloud phase on the overcast layer cloud at an altitude of 6 km. For the same mass of cloud, the optical properties are either those of a water cloud (black curve) or a cirrus (red curve) ice cloud. The effective radius is 0.0782 μm for the water cloud and 72 μm for the ice cloud. This, along with the different refractive index of ice compared to water, means that for the same mass of cloud, the radiative effect of ice cloud is much less than water cloud. Finally, for the same ice cloud, panel d varies the effective radius of the ice cloud particles whilst keeping the cloud mass constant. Three values of effective radius are shown, i.e. 25 μm (black curve), 42 μm (red curve) and 72 μm (green curve). The larger the effective radius, the smaller the radiative effect of the cloud. For ice clouds, one should note that radiative effects also depend on ice particle habit and shape; for example the results have been obtained using optical properties for hexagonal columns but would be different for other choices of habit. However, for infrared observations, radiative effects due to variations in effective radius and ice water
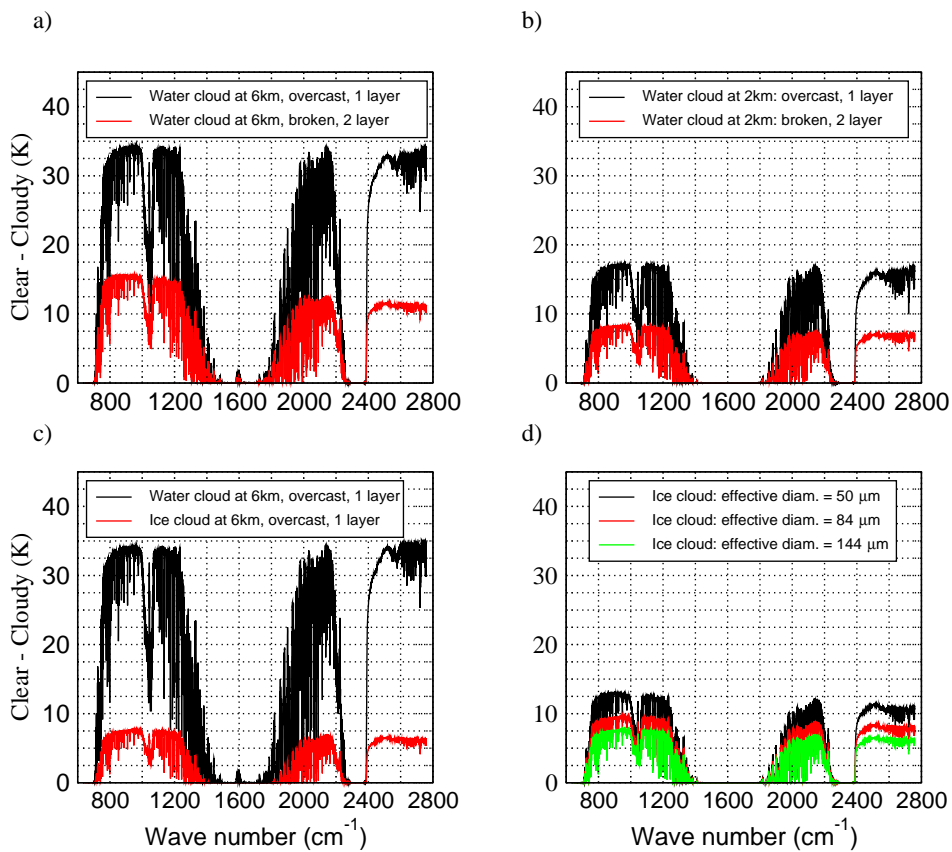
Figure 15: The main sensitivities of cloud-affected infrared radiances are to cloud fraction, cloud top temperature, cloud phase (ice versus water) and, for ice cloud, effective radius. This is demonstrated in a reference profile by: (a) modifying cloud fraction for a liquid water cloud placed at 6 km altitude; (b) placing a cloud of the same mass at 2 km; (c) for the cloud at 6 km, changing phase from water to ice; (d) for the ice cloud at 6 km, changing the effective radius

content tend to dominate over radiative effects due to variations in particle shape and habit.

The infrared observations clearly are sensitive to microphysical details like the effective radius of ice cloud that are not yet predicted by the forecast model, and some of the sensitivities are ambiguous. However, all the other cloud and precipitation observations that we hope to assimilate constrain different aspects of the cloud and precipitation properties. For example, combining microwave, infrared and solar radiances, plus lidar, there should be enough information on cirrus clouds to constrain ice cloud mass, particle size distribution (e.g. the effective radius), cloud top height, and even possibly particle shape and orientation. Further, the data assimilation process allows the forecast model to help constrain some properties, for example the cloud top height, which could be quite well predicted if the temperature and humidity profiles are accurate. A data assimilation system seems the ideal place to combine all this information.

Our second example is the sensitivity of simulated microwave brightness temperatures to the sub-grid and modelling details of convection. The sensitivity to assumptions of particle shape and size distribution is already well known (e.g. Geer and Baordo, 2014). However, due to the nonlinearity of cloud and precipitation radiative transfer, it is also necessary to represent the sub-grid layout of hydrometeors. Of importance is the 'beamfilling effect' (e.g. Kummerow, 1998) where the same weight of hydrometeor can generate a very different observed brightness temperature depending on whether it is spread out across an instrument's field-of-view or more concentrated in one place. The observation operator RTTOV-SCATT already includes a zero-order correction for this effect (Geer et al., 2009) but it needs a reliable estimation of the sub-grid cloud and precipitation fraction from the forecast model (Geer et al., 2009). The nonlinearity of the radiative transfer also leads to the 'projection effect', which can induce differences of 10-20 K in brightness temperatures when, for example, observations are made at a slant-angle through a one or more vertical shafts of precipitation or cloud (Bauer et al., 1998; Bennartz and Greenwald, 2011). This is not yet modelled in RTTOV-SCATT, but is one of the main targets for future development (Sec. 3.6). Finally, there is still ambiguity in how to convert the mass-fluxes simulated by a convection scheme into the mass-mixing ratios needed in the radiative transfer.

These issues have become particularly important with our ambition to assimilate 10 GHz microwave imager observations for heavy (i.e. mainly convective) rain over ocean (Sec. 2.2). These frequencies are sensitive to the melted precipitation in the lower part of a convective system. It has not yet been possible to get good agreement between the histograms of modelled and observed brightness temperature, as illustrated in Fig. 16. Here, brightness temperatures above 190 K are mostly associated with convective rain, with increasing brightness temperature broadly indicating increased precipitation intensity. At the intense end, the agreement between simulations and observations is dependent on the spatial scale of the observations presented to the assimilation system; in this case applying the usual superobbing makes the agreement worse. This could indicate that the super-observation scale is not well-matched to the forecast model scale, but it could also indicate a lack of intense rain in the forecast model. However, the most likely issues are those already described around the sub-field-of-view heterogeneity or the conversion of convective fluxes to mass mixing ratios.

The computation of grid-mean brightness temperatures in convective areas requires the convective area fraction. This is not directly available from the convective mass flux scheme in the forecast model and is set to a value of 5% (Tab. 1, later). A better match to the observations in Fig. 16 can in some cases be obtained by increasing the convective fraction towards 20% in the observation operator. Numerical estimates of this parameter are also somewhat ambiguous, especially in the upper troposphere. Fig. 17 depicts profiles of the convective area fraction for oceanic tropical convection. The results suggest that the assumption of a constant area fraction of a few % up to the melting level is reasonable, but that the area fraction is likely significantly larger in the upper troposphere, in particular for intense continental
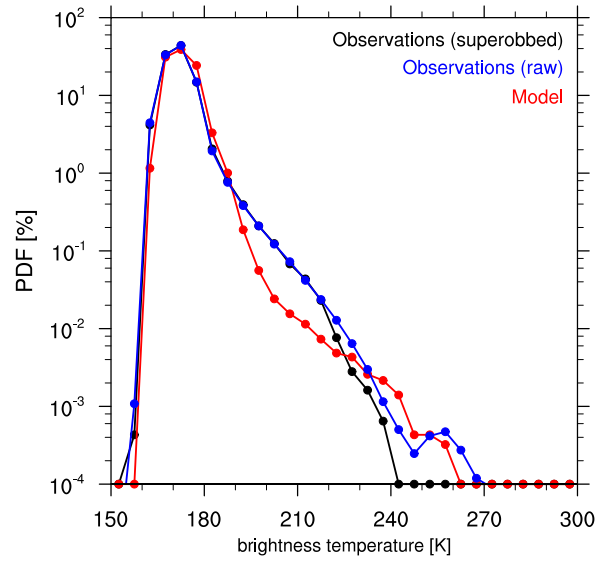
Figure 16: Histogram of over-ocean brightness temperatures from TMI 10 GHz vertically polarised channel covering August 2013 for model (red) and observations (black, superobbed; blue, raw data) with a binning of 5 K.
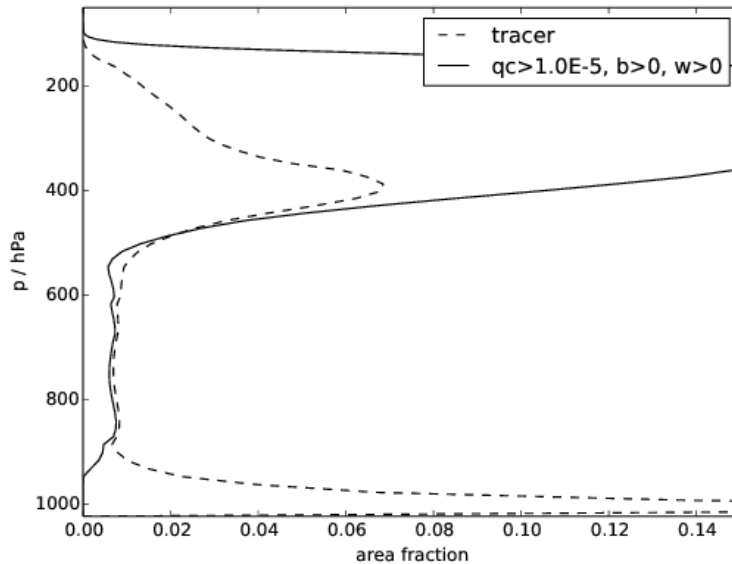
Figure 17: Large Eddy Simulation (LES) profiles of the convective core area fraction for oceanic convection in radiative convective equilibrium (Courtesy M. Whitall, Met Office): tracer tracking method (dashed) and vertical velocity method (solid).
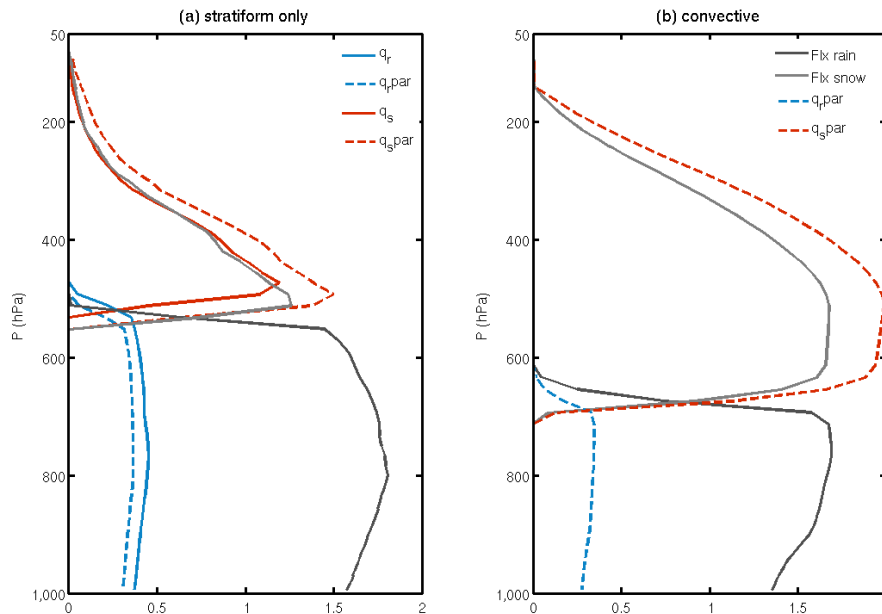
Figure 18: Rain (thick) and snow (thin) precipitation fluxes (black lines, $\mathrm{gm^{-2}s^{-1}}$) as well as prognostic (solid) and parametrized (as in the observation operator, dashed) grid-mean rain and snow mixing ratios (blue and red lines, $\mathrm{g\,kg^{-1}}$) as obtained from single column model simulations of the TWP-ICE campaign near Darwin, Australia. Three-hourly mean profiles are shown during January 24, 2006 from two simulations: without (stratiform only, a) and with the deep convection scheme activated (b).

convection with large anvils. We believe that the currently used $O(5\%)$ values of the convective fraction are valid, at least down to effective model resolutions of $O(5\text{-}10\ \mathrm{km})$. Beyond that the parametrized convective contribution (convective mass fluxes) is anyhow strongly reduced and the contribution from the resolved dynamics/microphysics strongly increases. Hence, an incorrect assumption of convective area fraction is unlikely to be the problem for the $10\,\mathrm{GHz}$ microwave observations (although these LES results suggest we may need to revise the convection fraction used for the glaciated upper levels, which could impact our modelling of higher-frequency microwave observations).

The conversion of the mass-fluxes is another major issue in simulating all-sky radiances. The observation operator converts the stratiform and convective rain and snow precipitation fluxes from the forecast model $(\mathrm{kgm^{-2}s^{-1}})$ into grid-mean specific rain and snow contents $(\mathrm{kg\,kg^{-1}})$ using assumed of fall-speed and particle size distributions. Although the model could provide prognostic specific rain and snow water contents at least for the stratiform precipitation, these are only available from the nonlinear forecast model, and not from its tangent-linear and adjoint, which instead uses a diagnostic cloud scheme also for stratiform precipitation. To illustrate the issues around the conversion from mass-flux to mixing ratio, we have run single column model simulations that are forced by large-scale tendencies derived from the TWP-ICE convection measurement campaign near Darwin, Australia (Fridlind et al., 2012; Lin et al., 2012). One simulation is run without the deep convection scheme, meaning that convection is resolved and precipitation is generated by the prognostic stratiform cloud scheme. The second simulation is run with the standard Cycle 43r3 model configuration with the deep convection scheme active.

Figure 18a shows the resolved convection generated by the stratiform precipitation scheme, which can predict both the flux and the mass mixing ratio of the precipitation. Converting the prognosed fluxes

to a mass mixing ratio using the parametrisation from the all-sky observation operator is no more than 10% to 30% different from the true prognostic mass mixing ratio. These conversions imply fall speeds of roughly 4 and 0.8 m s^{-1} for rain and snow: since snow falls slower than rain, it has relatively higher mixing ratios. The fluxes simulated using the convection scheme in Fig. 18b are expected to be broadly comparable, though the effect of strong updraft transport leads to more top heavy frozen particle flux profiles (see also the Giga LES results by Dauhut et al., 2016, their Fig. 10), while precipitation driven downdrafts affect the rain flux profiles. There is also a difference in the height of the melting level between the stratiform and the convective simulation because the stratiform integrations develop a warm bias, shifting the melting level up from the initial value of 530 hPa while the convective integrations develop a cold bias shifting the melting level down to 600 hPa by day 6. However, the convective rain flux is similar to that generated in the stratiform-only run, as is the mass-mixing ratio. In contrast, the fluxes and mixing ratios of the frozen particles are top heavy and significantly larger.

For a similar case study and time period, Wang et al. (2009) estimated ice and snow mixing ratios of O(1 g kg^{-1}). Furthermore, maximum frozen particle contents averaged over a very intense convective system are not expected to exceed 4 g kg^{-1} and the ratio between the total frozen particle mixing mixing ratio just above the melting level and the rain mixing ratio below should not exceed a factor of 2 or 3 (see e.g. Chern et al., 2016; Dauhut et al., 2016, Fig. 8 or Fig. 10 respectively). We therefore think that the values of the grid mean convective snow content of 2 g kg^{-1} in Fig. 18b, made using the parametrisation from the observation operator, are too high by roughly a factor of two. In future we will try to correct for this overestimation by using an implied average fall speed of 1-2 m s^{-1} instead of 0.8 m s^{-1} for frozen particles in convection. This would be more in line with the values used in the convective updraft computations. It is not clear whether this is explained simply by the frozen convective particles being denser and smoother than their stratiform counterparts, and thus having higher fall speeds, or whether we need to develop a more sophisticated representation of the suspension and precipitation of frozen particles in updrafts and downdrafts.

To improve the quality of simulations at 10 GHz, currently it is thought that accounting for the projection effect is most likely to improve the quality of our modelling of 10 GHz brightness temperatures (and at higher microwave frequencies too) and that convective area fraction and conversion from flux to density are not to blame in this case. However, we have seen that the modelling of convective frozen particles might need substantial revision, which could have a large effect on the 183 GHz humidity sounding radiances that are already assimilated in large quantities. Further, both the examples shown in this section should have illustrated the importance of sub-grid heterogeneity in correctly modelling all-sky radiances, alongside the probably more well-known sensitivity to microphysical assumptions.

3.4   Microphysical and sub-grid consistency throughout the modelling chain

Although the forecast model and the observation operators have sensitivities to many similar aspects of the microphysics and sub-grid heterogeneity of cloud and precipitation, the assumptions are usually made locally, and in general they are not consistent with each other. To illustrate the scale of the problem, Tab. 1 makes a non-exhaustive survey of the assumptions being made in the different parts of the modelling chain. In the forecast model, that includes the radiation scheme as well as the cloud and convection schemes. Across the main observation operators, the microwave, infrared and radar/lidar forward modelling has developed largely independently, meaning that differing assumptions have been made here too.

Those parts of the system that need to represent cloud and precipitation overlap generally use a mix of maximum-random and exponential-exponential approaches. However, the convection scheme is a special

Table 1: Microphysical and sub-grid heterogeneity assumptions in the forecast model and observation operators

Assumption	Forecast model components			Observation operators		
	Large-scale	Convection	Radiation	Microwave	Infrared	Radar/Lidar
Precipitation overlap	Maximum-random overlap between precipitation fraction and cloud fraction	Maximum	Exponential-exponential (rain ignored)	Maximum implicit in Geer et al. (2009) approach	Maximum implicit in CMSS approach	Maximum-Random
Cloud overlap	Not needed	Not needed	Exponential-exponential	Maximum, as above	Maximum, as above	Maximum-Random
Convective fraction	Not needed	5%	Not represented	5%	Not represented	10%
Snow particle	Sphere	Not represented	Hexagonal column	Liu (2008) sector snowflake	Not represented	Aggregate
Cloud ice particle	Sphere	Not represented	Hexagonal column	Sphere, density 900 kg m^{-3}	Baran parametrization	6-bullet rosette
Rain particle	Sphere	Not represented	Not represented	Sphere	Not represented	Sphere
Cloud water particle	Sphere	Not represented	Sphere	Sphere	Sphere	Sphere
Snow size distribution	Cox (1988)	Not represented	Based on aircraft observations	Field et al. (2007)	Not represented	Field et al. (2007)
Cloud ice size distribution	Cox (1988)	Not represented	Based on aircraft observations	Modified-Gamma	Baran parametrization	Field et al. (2007) with fixed temperature
Rain size distribution	Abel and Boutle (2012)	Not represented	Not included	Marshall-Palmer	Not represented	Field et al. (2007)
Cloud water size distribution	Not needed	Not represented	Modified-Gamma	Modified-Gamma	Monodisperse (effective radius)	Lognormal (fixed number concentration)

case where maximum overlap usually makes sense due to the near-vertical orientation of convective plumes. The microwave and infrared observation operators only as yet represent two sub-columns within any field of view, but the way these are constructed currently implies maximum overlap. Further, Sec. 3.3 has already illustrated importance of the convection fraction in the observation operator. The radar/lidar observation operator is assuming a 10% fraction, whereas the all-sky microwave uses 5%, which is consistent with the convection modelling. Convective hydrometeors in the updraft are not yet represented within either the radiation scheme or the infrared observation operator, but they probably should be in the future. However, updraft fraction is implicit in a mass flux scheme, and the assumption is needed only for subcloud rain evaporation within that scheme. This might give scope for an improved approach, perhaps using a fraction that varies with height, such as in Fig. 17. More generally, there would be great benefit to creating a single cloud and precipitation overlap and fraction generator for use as a pluggable module in all parts of the modelling chain, and eventually to use the same approaches throughout.

The modelling of frozen hydrometeor particle shapes is one of the most diverse areas: both for snow and cloud ice, there is a mix of spheres, columns, snowflakes and aggregates being used in different areas. One unifying factor (not shown on the table) is that these particles are all assumed to have random orientations; this may change in the future as we start to take orientation into account to better fit microwave observations. As with the use of the sector snowflake particle model in the microwave observation operator (Geer and Baordo, 2014) some of these choices may have been made to achieve the best fit between model and observations. However, in other cases the variety of particle shapes reflects the lack of any detailed knowledge of the microphysical properties of such particles, and the novelty of the ongoing scientific developments that hope to resolve these issues. It is hoped that over the next few years, partly through the assimilation of observations from many different sources, we can start to constrain this better. In contrast, cloud water and rain are universally represented by spheres (not shown) but if in future we want to represent some of the oblateness and orientation of these particles, it should ideally be done in a coordinated way across the modelling chain. Finally, particle size distributions are another area where there is great diversity across the modelling chain, also in need of rationalisation.

3.5   Future developments in the forecast model

Previous sections have illustrated the dependence of cloud- and precipitation-sensitive observations to a wide range of microphysical and sub-grid properties, some of which are prognosed or diagnosed, but many of which are assumed. Additionally, state-dependent systematic errors could be addressed by further development of the forecast model. Hence the long-term development path of the moist physics is of great interest for the future use of all-sky observations, and these observations may drive some of the developments. Current plans in the moist physics are first towards a more integrated approach for turbulent diffusion, convection and cloud schemes, and second, towards improved microphysical processes and cloud-radiation interactions. This is being done in the context of the existing moist physics schemes, and it already benefits from comparisons to assimilated all-sky observations as well as to independent data sources. However, with moves towards higher horizontal resolution planned, and increasing use of cloud- and precipitation-sensitive observations, it is also worth considering the possibility of more radical developments in the longer term (e.g. 5 – 10 years).

Starting with the shorter-term developments, the need for convergence of microphysical and macro-physical representations between the convection, cloud and radiation schemes (as well as the forward operators used in all-sky assimilation) is clear. Within the moist physics, areas needing attention due to either outdated assumptions or inconsistencies between different parts of the model are cloud overlap (e.g. representing wind shear Giuseppe and Tompkins, 2015), sub-grid heterogeneity of cloud conden-

sate (Ahlgrimm and Forbes, 2016), effective radius, and representation of 3D effects (Hogan et al., 2016). From the point of view of observations, there is already a lot to be gained from generating more of this information diagnostically from our existing moist physics. In addition, as suggested in Sec. 3.3, convective hydrometeors could be supplied to the observation operator as mixing ratios rather than fluxes, removing any need for the observation operator to make assumptions of particle fall speed, although this would require additional work in the tangent-linear and adjoint models. Also there may be scope for a more sophisticated representation of convective updraft cloud fraction, again largely for the benefit of the observation operator.

Looking to the longer term, with the launch of ICI in 2022, operating at sub-mm frequencies, along with the routine assimilation of all-sky infrared and solar radiances, there will be even greater need for detailed information on ice-phase hydrometeors. As with existing all-sky microwave sensors, these are sensitive to particle size, habit (e.g. cloud ice, snow, aggregates, graupel and hail) and orientation. Relative to the existing all-sky sensors, the higher frequencies (smaller wavelengths) make these newer instruments particularly sensitive to the details of the smaller particles. Future developments in the moist physics will revisit the representation of the ice-phase hydrometeors and their particle properties, including the improved representation of pristine ice crystals and snow aggregates as either separate single or double-moment categories or a combined double-moment hydrometeor category which represents the range of particles with evolving properties from small crystals to large aggregates (as observed ice particle size distributions show little evidence of a particle size scale break; Field et al., 2005).

For higher resolutions, as the model increasingly represents resolved convection, the importance of explicitly modelling graupel and hail increases. Traditionally this is done with additional discrete hydrometeor categories, but alternative approaches consider the prediction of particle properties, such as density and shape (e.g. Morrison and Milbrandt, 2015). However, in the next 10 years, even as ECMWF progresses to 5 km resolutions and lower, the majority of convective ice-phase hydrometeors will still likely be generated through parametrised convection. Therefore, we may also need to look for increased sophistication in the mass-flux parametrization. In particular, we do not yet explicitly represent graupel or hail, although much of the 'snow' modelled in the convection scheme is likely in this form, and the existing all-sky microwave observations are strongly sensitive to these hydrometeors and their microphysical details (Geer and Baordo, 2014). Graupel forms by riming, when ice particles are falling through and accreting significant numbers of supercooled liquid water droplets; significant graupel production is usually only found in strong updrafts associated with deep convection. Repeated riming, melting and refreezing of ice particles, associated with the strongest convective updrafts, forms hail. Hence there is potential to treat graupel and hail as diagnostic outputs from the existing convection scheme; benefits to the convection modelling would come from better representing fall speeds (which are faster for these dense particles than for snow aggregates, for example) and more quickly removing water from the atmospheric column through riming.

For both short-term and longer-term developments, the aim is to improve the realism of the forecast model's cloud and precipitation at the same time as improving forecast skill, but this is not always straight forward. For example, it has proven difficult to address the supercooled liquid water bias in the forecast model (Forbes et al., 2016) without affecting temperature biases in the tropics (although Cycle 45r1 will include some progress on this issue). Other examples have been the large sensitivity to 2-metre temperature over northern Europe to subtle details of the large-scale cloud scheme (Ahlgrimm and Forbes, 2014) and how changes to the evaporation of rain and sublimation of snow can strongly affect the dynamics through diabatic cooling and changes to atmospheric stability (Forbes and Clark, 2003). Complicating the situation, there are also often compensating biases in different processes. Further, adding complexity brings no guarantee of improving forecasts: this has been demonstrated, for example, by

testing the super-parametrisation approach of Subramanian and Khairoutdinov by embedding a cloud re-solving model into the IFS. However, there can be benefit from adding the complexity needed to support assimilation of cloud and precipitation-sensitive observations if this complexity can be constrained by the observations. Hence, we do envisage substantial developments in the moist physics where they can be guided by observations and made within the limits of computational cost.

3.6 Future developments in the observation operator

For the observation operators, there is plenty we can do within the next 5 years to improve the existing (microwave) all-sky observation usage and to prepare for the new observations that are planned within that timeframe (e.g. infrared, space-borne cloud radar, and sub-mm microwave such as ICI). Longer-term (5–10 year) developments, as well as refining further the existing operators, would also add new types of observation operators, such as for solar radiances, as has been described in Sec. 2. Hence we concentrate here on the shorter term. A further difference compared to the forecast model is that we can more easily consider scientific developments that may increase the computational cost of the observation operators, given they are now such a small part of the total cost of 4D-Var (Lean et al., 2016).

Within the all-sky microwave observation operator, we have seen that there are many ways in which we could represent convection better. The flux-to-mixing ratio conversion is likely incorrect for convective hydrometeors, giving mixing ratios that are too large by around a factor of two. Also, the convective fraction of 5% is likely unrealistic in the upper (glaciated) parts and could be replaced with a more sophisticated, vertically-varying convection fraction. However, we would need to repeat the detailed study of Geer and Baordo (2014) to choose a new snow particle shape model to get the best fit between observations and model. It might also become necessary to treat convective and large-scale precipitation as separate hydrometeors from the point of view of the radiative transfer - for example, frozen particles in convection might be better represented by a densely rimed aggregate model, or a hail or graupel particle if a good one can be found, but large scale snow would probably need a less-dense particle. Since 2014, the availability of particle scattering models has mushroomed, so any new exercise in choosing a particle shape will have enormous choice and variety to consider. As part of this, it may also be necessary to include melting particles (e.g. Bauer, 2001; Johnson et al., 2016). However, revising the treatment of convection will be complicated. Further, despite its issues, the existing treatment in the observation operator has worked well enough to support all the forecast benefits currently provided by all-sky microwave data assimilation. Such a major revision to the observation operator may need to wait until sufficient resources are available; however, its benefits will be to help us focus even more closely on constraining convection in the forecast model.

A major scientific investigation is needed to address particle orientation, and not just for ICI when it is launched in 2022. It is becoming clear that neglecting orientation, and hence the polarisation of scattering, may give errors of around 10 K even in existing instruments in low-frequency channels like 37 GHz (e.g. Gong and Wu, 2017). However, without a major increase in the complexity and cost of RTTOV-SCATT (going to fully-polarised radiative transfer, i.e. treatment of the full Stokes vector) it may not be possible to address this. Substantial initial work will need to be done to better assess the size of the errors and the possibility of reducing these errors in the current non-polarised modelling framework. It might be possible to start by using different particle optical properties in different polarisations, although without representing the transfer of energy from one polarisation to another.

A more urgent task in the all-sky microwave will be to address the projection effect, which could reduce forward modelling errors by 10 K to 20 K in some situations. This will benefit both the future assimilation of 10 GHz channels, regarding tropical rain, but also help better understand the model-observation biases

in maritime stratocumulus regions. The most likely solution would involve using a cloud generator to fill a number of vertical sub-columns, and then to trace slanted independent columns through these (e.g Bauer et al., 1998). This potentially implies the addition of more sub-columns, and a higher cost to the observation operator. It will also mean abandoning the effective cloud fraction approach of Geer et al. (2009), possibly for something like the O'Dell et al. (2007) approach. Again, this would be a major change to the observation operator and it could take some years to get it fully working. This will likely be a first priority in the context of the current work to develop the use of 10 GHz channels.

Finally, for the all-sky microwave it is clear that after a number of resolution upgrades, the scale of cloud and precipitation in the forecast model has become smaller that the current superobbing resolution applied to microwave imager observations. These are averaged over an area of roughly 80 km x 80 km, whereas the simulated brightness temperature is calculated using a vertical profiles from a single grid point and nowadays the effective model resolution is around 30-40 km. It is not desirable to abandon superobbing altogether, as it helps unify the fields-of-view of different frequencies onto a single spatial resolution (e.g. Lean et al., 2017), helps avoid correlated observation error, and reduces the amount of spurious precipitation 'noise' in the analysis (Geer and Bauer, 2010). However, it should be possible to reduce the size of the superobs down to around 40 km by 40 km. Given that the raw resolution of some of the microwave instruments (including low-frequency channels on microwave imagers, and cross-track scanners like MHS) is no better than 40 km, we will in future not be looking to superob this data, but rather to consider 'supermodelling', i.e. computing the observation equivalent as the average of computations across the multiple grid points within the instrument's field of view. This will ensure the model resolution stays compatible with observation resolution as the model resolution is increased in future. It may be possible to achieve this reasonably cheaply using the same model-to-observation interpolation framework that supports the slant-path heterogeneity modelling applied to clear-sky radiances and the computation of limb paths for GPSRO.

For the infrared observation operator, the main priority is to address cloud overlap in a better way than the simplified two-subcolumn approach that has been adopted for initial testing, and that has only limited validity, even for upper-tropospheric channels. The full cloud overlap approach available in RTTOV is far too expensive and memory-intensive. This is one of the key developments required to progress the all-sky assimilation of IR radiances.

Finally, as indicated earlier, we need to start working to unify the microphysical and sub-grid assumptions across all the observation operators, and also to make these compatible with the physics. This is best achieved by a unification of the codebase that represents these things. One part of this will be to add a radar capability to RTTOV-SCATT, so that it can potentially replace the existing ZmVar operator in the observation operator to be used for EarthCARE cloud radar.

4 Data assimilation

4.1 Introduction

The current strategy for development of ECMWF's data assimilation system (Bonavita et al., 2017) is a continuation and further enhancement of the 4D-Var algorithm. The main difference between 4D-Var and alternatives such as 4D-EnVar and Ensemble Kalman Filter (EnKF) is how the error covariances are evolved in time. In 4D-Var they are implicitly evolved through the physical knowledge incorporated in a linear model and its adjoint. In the ensemble approach, the time-evolution of error covariances is computed from an ensemble of non-linear model integrations. Given the limited ensemble sizes that are

affordable in global NWP the ensemble approach suffers from significant sampling errors and the related issues connected to the need of defining and propagating in time the localisation operator (Desroziers et al., 2016; Bocquet and Carrassi, 2017; Lorenc, 2017). Another class of algorithm designed to handle non-linearity and, related, non-Gaussian errors is the particle filter. However Bonavita et al. (2017) concluded that current formulations are neither mature enough nor practical for operational development of high order systems. A main advantage to ECMWF in using 4D-Var is the availability of a very good tangent linear model (and its adjoint) including moist processes. A further advantage of 4D-Var for all-sky assimilation is the ability to handle substantial nonlinearity through the incremental formulation: as illustrated by Bauer et al. (2010), the multiple non-linear outer loops allow the evolving analysis, for example, to create convection in places it does not exist in the first guess. This important ability of incremental 4D-Var has more recently been demonstrated at the convection-resolving scale in another system (Wang et al., 2013). Ensemble approaches can be adapted to handle greater nonlinearity (e.g. Bocquet and Sakov, 2014) but at potentially large computational cost. For example the equivalent of relinearisation in 4D-Var would be to re-run the ensemble of prior forecasts. Hence the existing framework of incremental 4D-Var combined with tangent-linear and adjoint moist physics has been essential to support the development of assimilation of sensitive to cloud and precipitation, and Sec. 4.2 will investigate the tangent-linear and adjoint moist physics further.

In 4D-Var, the modelling of background error covariances and the choice of control variable are as important for cloud and precipitation assimilation as they are for other variables. In the vicinity of precipitation, error correlation lengths can be very short, and the balances between atmospheric variables can be very different compared to clear-sky areas (e.g. Montmerle and Berre, 2010; Michel et al., 2011). However, much of the heterogeneity of the background error is likely already captured within the hybrid 4D-Var framework, where the background error covariances are computed by combining climatological and ensemble-derived information. One question for cloud and precipitation assimilation at ECMWF has been whether to add control variables for cloud. So far, all-sky assimilation has worked well despite the only control variables being those related to temperature, horizontal wind, humidity and surface pressure. Section 4.3 examines developments in the background errors and control variables.

A final area of importance to cloud and precipitation assimilation is the observation error formulation. As described in Sec. 1.5 the successful assimilation of all-sky microwave observations has relied on an observation error model that represents the dominance of representation error associated with cloud and precipitation mislocation. The all-sky observation error models do not yet represent observation error correlation, which is a major limitation. Observation error correlations become large in cloudy areas, with significant correlations between channels and in space and time (Bormann et al., 2011). We are moving towards representing inter-channel observation error correlations, originally just for clear-sky radiances (e.g. Bormann et al., 2016) but in the future, also for all-sky radiances. However, the mislocation-representation error has many of the characteristics of background error or model error, and it may ultimately be necessary to move to a generalised global framework similar to the representation of background errors, so as to model time and space correlations in observation error as well. Sec. 4.4 examines this further.

Before moving on, some of the ideas presented in ECMWF's data assimilation strategy (Bonavita et al., 2017) can be discussed in the context of assimilating observations sensitive to cloud and precipitation. The proposed move towards a saddle-point and generalised weak constraint formulation of 4D-Var gives the ability to run sub-windows of the tangent linear and adjoint integrations in parallel, which can make 4D-Var more scaleable. The main cost of 4D-Var is in the tangent-linear and adjoint of the forecast model, so this could allow us to use more expensive versions of the linearised moist physics in the future. Although the cost of the all-sky microwave observation operator is no longer of any concern (e.g.
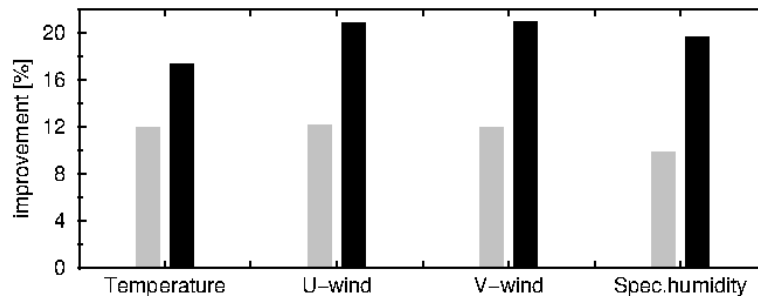
Figure 19: Global relative improvement [%] of the tangent-linear approximation for temperature, wind and specific humidity coming from including: (a) dry physical parametrization schemes (i.e. vertical diffusion, gravity wave drag, non-orographic gravity wave and radiation) alone (grey bars) and (b) in combination with moist processes (i.e. convection and large-scale cloud parametrization schemes - black bars) into the linearized model compared to the purely adiabatic tangent linear model. Evaluations done for 12-hour integration at T255 L91 resolution.

Lean et al., 2016), infrared and solar observation operators may be more expensive, and hence could also benefit from the generalised weak-constraint approach. This formulation can also support longer window 4D-Var (e.g. 24 h) whilst also reducing the timescales over which the tangent linear approximation needs to be valid, by using sub-windows. The sub-window also defines the maximum time over which the forecast model needs to be able to maintain predictability of cloud and precipitation. Hence, it should reduce the size of the representation (cloud mislocation) error and/or allow some of it to be represented as model error, although that would require representation within a new model error matrix, with potentially similar features and complexity to the background error matrix.

4.2 Tangent-linear and adjoint modelling

At ECMWF, an extensive set of linearised physical parametrizations (Janisková and Lopez, 2013) has been developed for the global data assimilation system and for sensitivity diagnostics (e.g Rabier et al., 1996; Cardinali and Buizza, 2004; Cardinali, 2009). It comprises dry parametrization schemes (radiation, vertical diffusion, orographic gravity wave drag and non-orographic gravity wave activity) and moist parametrizations (moist convection, large-scale condensation/precipitation). It is believed to be the most comprehensive linearized physics package currently used in operational global data assimilation. It describes the whole set of physical processes and their interactions almost as accurately as in the nonlinear (NL) model, just slightly simplified and/or regularized. Regularization procedures are particularly crucial in the parametrization of convection, large-scale cloud scheme as well as vertical diffusion. A compromise must constantly be achieved between linearity, computational efficiency and realism, to ensure that the best analysis and forecast performance are obtained.

As has been shown earlier, in 4D-Var the representation of moist processes in the adjoint model is essential for the assimilation of observations sensitive to clouds and precipitation. The TL model should be a good approximation of its full NL counterpart. Figure 19 shows that taking into account dry physical processes improves the quality of the TL approximation and that the inclusion of moist processes (including cloud-radiation interactions) leads to additional significant improvement. The TL model including all physical processes performs remarkably better than its dry version. Janisková and Cardinali (2017) also confirmed that a full comprehensive description of the moist physical processes in the adjoint model is necessary to properly propagate backward in time and space the humidity component of the forecast
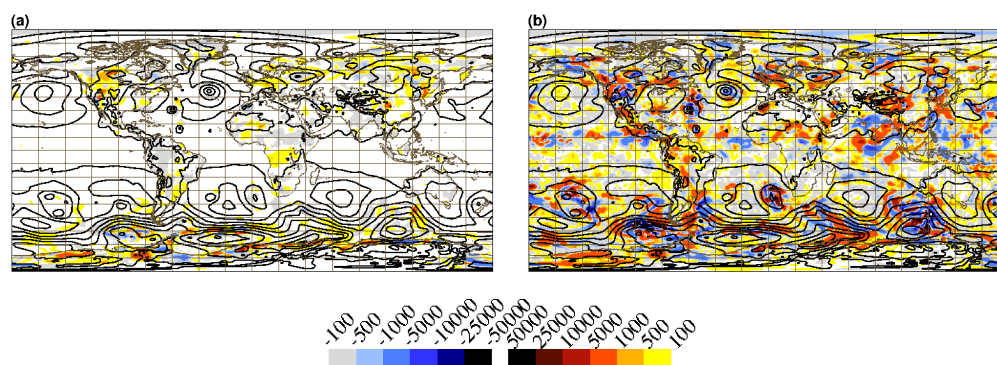
Figure 20: Adjoint sensitivity of the 24-hour forecast error to initial conditions in specific humidity ($J\,kg^{-1}/(g\,kg^{-1})$) at the lowest model level for the situation on 28 August 2010 at 21:00 UTC. The results from computations performed at the resolution T255 L91 are presented for (a) an experiment with dry parametrization schemes used in the adjoint model and (b) with moist processes also included. Sensitivities are shown with colour shading. Black isolines represent mean-sea-level pressure (hPa).

error. Fig. 20 displays the adjoint sensitivity of the 24-hour forecast error to the initial conditions, i.e. to the analysis. The sensitivity with respect to specific humidity at the lowest model level indicates that sensitivity to specific humidity is quite small and localized in areas of strongest dynamical activity when using only dry parametrization schemes in the adjoint computation. Adding moist processes in the adjoint model brings additional structures to the sensitivity in areas affected by large-scale condensation/evaporation and convection. Therefore, using a more sophisticated adjoint model also provides more flow-dependent and more realistic sensitivities in 4D-Var.

The maintenance and improvement of our simplified, linearized forecast models is essential to support 4D-Var in the future. It is also a difficult task requiring dedicated resources in the simplification and regularization of the linearized physics and in monitoring the quality of the TL approximation and the correctness of the adjoint whenever the NL forecast model is changed (i.e. at every new model release). To make further use of observations sensitive to cloud and precipitation, we have described plans to extend the nonlinear physics to support more detailed microphysical and sub-grid representation (Sec. 3) and the possibility of adding new sensitivities, such as to effective radius. These developments would likely need to be matched in the linearised physics, and certainly any required sensitivities would need be added.

4.3 Control variables and background errors

All-sky observations are sensitive to humidity and cloud variables whose errors can vary by orders of magnitude over short distances, in particular in the upper troposphere. Hence, an accurate background error formulation is required that takes into account the special nature of cloud and precipitation assimilation, and generates the correct weighting in the analysis between the background field and the observation departure.

In the ECMWF 4D-Var, the background errors are modelled with a wavelet model (Fisher, 2003) which is updated each analysis cycle with the errors of the day obtained from an EDA system consisting of 25 members at half the operational resolution. The background error model consists of three steps: spatial variances, vertical correlation matrices, and a balance operator. The spatial variances are fully flow-dependent and are determined from the EDA of the day. The balance operator accounts for horizontal correlations as well as for correlation between errors of different variables. The balance operator sub-

tracts out the correlated part of the errors, leaving 'unbalanced' variables for which the correlation matrix is block-diagonal. The background error correlation matrices are flow-dependent, though due to the limited number of ensemble members, the correlation samples of the day are blended with at climatological correlation matrix, with 30% contribution from the daily samples up to waveband T63, increasing gradually to 93% contribution from the daily samples at T399. The full set of control variables is vorticity and ozone together with the unbalanced components of divergence, temperature, logarithm of surface pressure and relative humidity. At the moment, the formulation of the humidity background errors is the most relevant to the assimilation of cloud and precipitation sensitive observations. For the future, the question is whether to extend the control vector to include cloud or precipitation variables, and how to represent the effect of cloud and precipitation on the correlations between different variables.

The formulation of humidity background errors was changed in Cycle 43r3, so that it now uses fully flow-dependent relative humidity variances from the EDA, which were already in place for all other variables. This replaced the previous humidity formulation of Hólm et al. (2002) which generated flow-dependency using climatologically-determined function of relative humidity and model level. The EDA-derived relative humidity variances generated improvements in tropical winds in particular, highlighting the extraction of wind information from humidity-sensitive observations. The simplified humidity-temperature saturation adjustment (Hólm et al., 2002) is still used to model balances between humidity and temperature, and this does not yet account for correlations between humidity and dynamics. Background cloud cover is needed and is modelled with a statistical regression, as a function of relative humidity and model level, which is reasonably close to the nonlinear model cloud cover, but used in preference due to its smooth variation.

To model the correlations between humidity errors and errors of temperature, surface pressure, wind and hydrometeors in the future, one possibility is to use a statistical regression (e.g. Berre, 2000; Descombes et al., 2015) but this approach neglects the way the correlation between humidity and other errors varies dynamically and is different inside and outside cloudy/precipitating regions. This was recognized by Montmerle and Berre (2010) who derived a hybrid formulation with different regressions inside and outside these cloudy/precipitating areas, but the resulting patchwork of analyses would be difficult to unify. A better approach is to model the correlations analytically, as has been done in the nonlinear balance and omega-equation operators of Fisher (2003). Pagé et al. (2007) tested a more comprehensive operator derived from the full nonlinear omega-equation including diabatic tendencies in a limited area model, although their operator is too complex for inclusion in the current IFS. A simpler operator (Asai, 1965; Hólm, 2015) consists of a linear saturation adjustment where humidity and temperature increments are adjusted, optionally giving balanced contribution to cloud liquid water and cloud ice increments as well when these are included as control variables.

Compared with the current simplified saturation adjustment of Hólm et al. (2002), the proposed formulation means that not only humidity but also temperature increments can be created from a pure humidity control variable increment. For the final link with the dynamic balance operator, the linearized saturation adjustment can be performed before the omega-equation in the balance operator, which gives final divergence that dynamically supports the in-cloud balance changes. This is seen in Fig. 21, which shows that the proposed balance operator formulation can set up a secondary circulation to support the in-cloud changes. The tangent linear evolution of the new increments remains balanced throughout the window (not shown) and the changes in humidity result in balanced changes to wind and temperature which should carry the information from the observations further into the forecast than humidity alone could.

Cloud liquid water and cloud ice water will in future be added as control variables and in the background errors, following the formulation of Hólm (2015). Figure 22 illustrates the need: the current assimilation system is unable to generate sufficient cloud increments towards the beginning of the assimilation
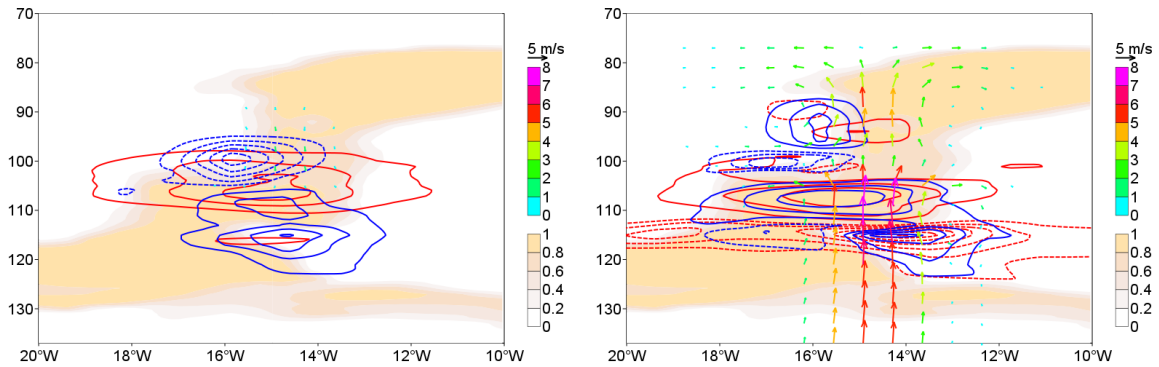
Figure 21: Analysis increments from a single profile of microwave all-sky observations in Cycle 43r3 (which includes EDA humidity variances, left) and with added linearized saturation adjustment before the ω-equation in the balance operator (right). Shown are u-w wind increments (arrows, m s^{-1}), temperature increments (red lines, isoline interval 0.2 K, solid positive, dashed negative), humidity increments (blue lines, isoline interval 0.1 g kg^{-1}, solid positive, dashed negative) and background cloud cover (shaded).

Figure 22: Standard deviation of analysis increments at GMI observation locations, binned as a function of time through window (30 minute bin size) and normalised so that the value is 1 at the end of the assimilation window. TCWV, CWP, IWP, RWP and SWP are the integrated column amounts of water vapour, cloud water, cloud ice, rain and snow (in kgm^{-1} before normalisation) and THETA700 is the 700 hPa potential temperature.

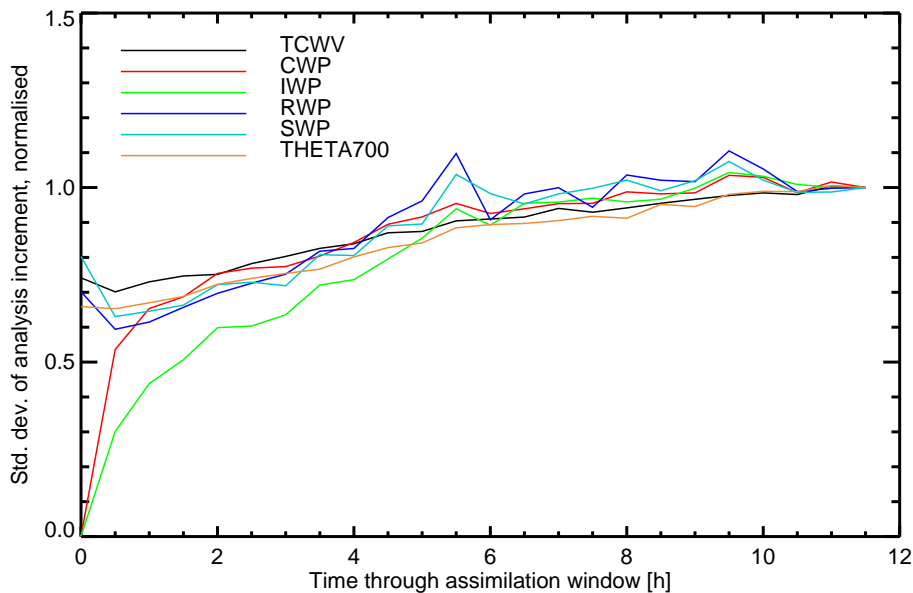window in cloud water and particularly for cloud ice. The problem is not apparent in the precipitation variables, which usually have short lifetimes and also (for data assimilation) are generated using diagnostic moist physics parametrizations. In contrast clouds are longer-lived phenomena, so towards the beginning of the window it must be possible to modify them directly in the analysis. Starting with cloud liquid and ice (as opposed to precipitation or cloud fraction) also makes sense as these variables have more linear physics and are more closely connected to humidity. Alternatively it has been proposed to use a total water variable together with a splitting operator to retrieve the water and ice increments (e.g. Sharpe, 2007; Migliorini et al., 2017). However, experience at ECMWF with prototype tangent linear models including cloud liquid and ice (P. Lopez, personal communication) show these variables have quite distinct evolution – in particular they are reduced differently by precipitation. It is thus difficult to keep track of their evolution if they are treated as total water, leading to inaccuracies in their splitting. Treating them as two separate variables is much simpler if the tangent linear model has been extended to include them. With cloud condensate variables in the analysis special treatment is also needed for the variances and the adjustment of cloud cover. Following ideas in Wilson and Gregory (2003) cloud cover can be adjusted nonlinearly at outer loop level as an extension of the saturation adjustment, and the cloud condensate variances can be limited to a minimum value outside cloudy areas which will prevent numerical problems due to division by zero and leave a small chance for clouds to form at the start of the assimilation window under all conditions.

4.4 Observation error modelling

Observation error is the sum of measurement error, representation error and forward model error. For observations of cloud and precipitation, the measurement error is typically negligible and instead representation errors dominate due to the widespread mislocation of cloud and precipitation in the forecast (as illustrated in Sec. 1). The 'symmetric' observation error model addresses this by inflating observation error in cloudy and precipitating areas(Geer and Bauer, 2010, 2011) and has also been used in many external studies of all-sky assimilation (e.g. Zhu et al., 2016; Harnisch et al., 2016; Okamoto, 2017). Other studies have indicated the need for situation-dependent error inflation in all-sky assimilation, but have used alternative approaches to determine observation error (e.g. Deblonde et al., 2007; Zhang et al., 2016; Minamide and Zhang, 2017). Not all of the first-guess departure in cloudy and precipitating areas is due to representation or observation error, but for all-sky observations the background error appears to be a relatively small part of the total error budget compared to the contribution from representation error (see also Harnisch et al., 2016). Hence, in an all-sky symmetric observation error model, predicted standard deviation of the first-guess departure is typically used as the observation error itself.

The development of assimilation for cloud radar and lidar demonstrates another alternative to the symmetric error model: a physically based estimate of the observation error can be obtained by estimating the measurement error, representation error and forward model error. The representation error is modelled using the local variability along the radar transect combined with correlation from a climatology. The new method has been validated using synthetic data and MODIS radiances (Fielding and Janisková, 2017) and has similar performance to a more complex method based on look-up tables (Stiller, 2010). Estimates of forward model error are generated with a Monte Carlo approach (similar to, e.g., Kulie et al., 2010; Di Michele et al., 2012), where microphysical assumptions are perturbed within their physical ranges. This physically based estimate of observation error has the advantage of being independent from the model background errors. Figure 23 shows the mean observation error calculated for one month of CloudSat and CALIPSO observations. For CloudSat radar reflectivity, representation error tends to dominate over tropical areas, while forward model error dominates the extra-tropics, particularly in stratiform regimes. Conversely, for CALIPSO lidar backscatter, the observation error tends to be lower in the

CloudSAT

mean observation error

CALIPSO

mean observation error

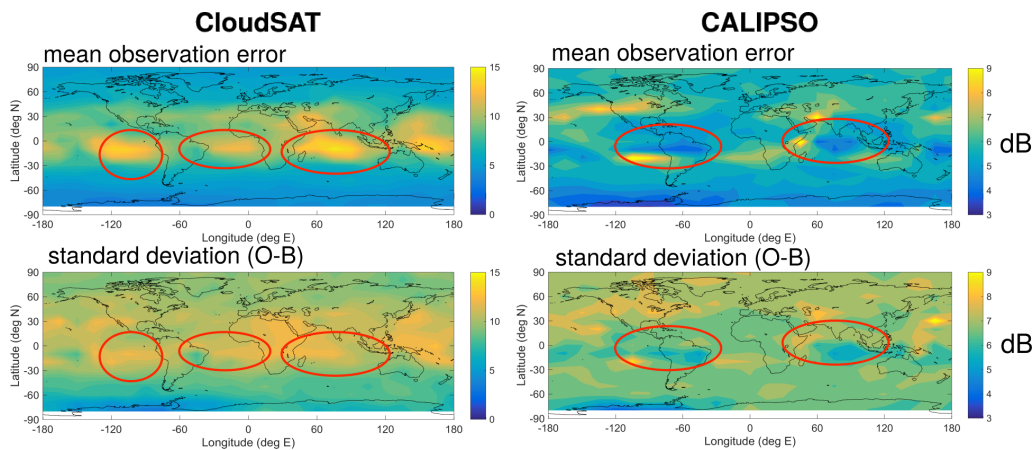standard deviation (O-B)

standard deviation (O-B)

Figure 23: A comparison of global maps of CloudSat radar (left side) and CALIPSO lidar (right side) mean expected observation errors (sum of instrument, operator and representation errors; top) versus the standard deviation of first guess departure errors (bottom). The red ovals are to aid comparison.

tropics as the lidar has the smallest errors for regions associated with ice cloud, such as those formed by convective outflow. Physically-based observation error estimates have also been tried in the context of clear-sky hyperspectral assimilation but diagnostic methods (e.g. Bormann et al., 2016) have given the best results in trials and are currently preferred. Once the direct assimilation of cloud radar and lidar has been demonstrated in 4D-Var, there may be more evidence in favour of the physical approach.

For the moment, the assimilation of all-sky satellite radiances will use the successful 'symmetric' approach, which is well-proven in operational use. One development will be to account for the differences in predictability of convection and large-scale precipitation; currently the representation errors are a little small for the tropics and a little too large for the midlatitudes. However, the main focus is the inclusion of inter-channel observation error correlations, which are not yet modelled. Bormann et al. (2011) demonstrated strong inter-channel error correlations in all-sky radiances in cloudy conditions. The development of all-sky hyperspectral IR radiance assimilation has already had to confront the problem given that the clear-sky assimilation already includes inter-channel error correlations (Bormann et al., 2016). By combining the techniques of eigenvector decomposition with the error variance inflation used in the symmetric error model, it is possible to simultaneously inflate the error variance and to generate stronger inter-channel error correlations in cloudy areas (Fig. 24). This technique will be tested also with the all-sky microwave humidity-sensitive instruments, where it is hoped it might allow additional weight to be put on the observations, such as with the use of additional channels or more instruments. It will be a good test to see if it can help improve the use of a set of observations that already has a large and beneficial impact in our system. However, inter-channel error correlations are only the start of the process. As mentioned earlier, the representation error in cloud and precipitation may ultimately need to be modelled with a full-featured spatial-temporal error covariance matrix along the lines of the background errors.

5 Verification and validation

The development of cloud and precipitation assimilation is closely linked to that of forecast verification and validation. It has been difficult to verify the short and medium-range forecast impacts on the basic forecast fields (e.g. temperature, wind and humidity) particularly in the tropics. Many NWP centres have seen this during their development of all-sky assimilation (e.g. Geer et al., 2017b). Assimilating
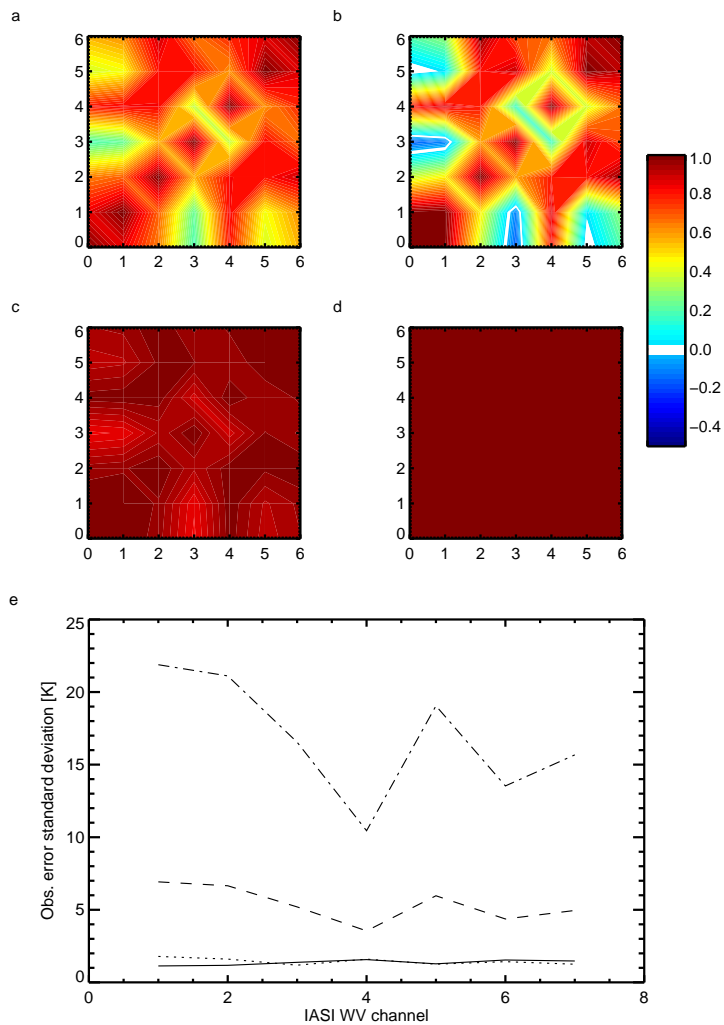
Figure 24: An error covariance model for all-sky IASI, covering the 7 upper-tropospheric humidity channels, compared to the existing clear-sky error covariance model. Left: (a) current clear-sky correlation matrix; (b-d) correlation matrices at different states of cloudiness from fully clear to fully cloudy. Right (e): observation error variances for current clear-sky model (solid) and at different states of cloudiness from clear (dotted) through to fully cloudy (dot-dash).

cloud and precipitation generates small-scale analysis increments that appear like degradations in many measures of short-range forecast quality. A well-known example is the apparent degradation of own-analysis forecast scores in the tropics, although it is usually possible to show improvement in first guess fits to other observations (e.g. Chambon and Geer, 2017). Further, it has never been easy to measure the direct impact of cloud- and precipitation-sensitive observations on the cloud and precipitation variables themselves. Despite many developments over the years (e.g. Roberts, 2008; Hogan et al., 2009) cloud and precipitation verification is not a standard part of forecast quality assessments performed at ECMWF. However, the cloud and precipitation observations we are adding to the data assimilation system are themselves part of the solution. Once in the system, they can be used for verification, as well as for model validation and development as described in Sec. 3.

We have three possible approaches to verification and validation against observations:

1. **Comparison to retrieved quantities:** this is popular for model evaluation and development for obvious reasons, as it enables comparison in terms of the model variables, rather than difficult-to-interpret radiances and reflectivities. Also, retrievals are sophisticated enough to combine different instruments such as radar and lidar to improve retrieval quality and to provide a useful evaluation tool (e.g. Delanoë et al., 2011). However, there are well-known limitations: (i) assumptions (including microphysical assumptions) are being outsourced to the retrieval developers; (ii) the a-priori may be aliased into the retrieval in regions of low information content; (iii) where there is ambiguity in the sensitivity of observations to physical quantities, retrievals cannot on their own resolve the ambiguity; (iv) retrievals may only represent certain times of day (e.g. that of the satellite overpass) and there may be sampling limitations (for example some retrievals only work well on some cloud types) and these can incur sampling and representation errors. Although careful work can mitigate many of these problems, and current model errors may in some cases be so large that retrieval errors are unimportant, these are all good reasons to move towards evaluation in observation space.

2. **Offline comparisons in observation space:** these rely on the MARS archive containing sufficient information to compute the observed radiances, and are limited by the archiving frequency, which may imply time-offsets of up to 3 h between the forward simulation and the observation. However, vital cloud and precipitation-related quantities are not yet archived. An example outside ECMWF was that of Rysman et al. (2016) who attempted to compare all-sky microwave brightness temperatures simulated from a climate model to observations from MHS. However, because the convective hydrometeor water contents had not been archived (despite these being critical to replicating the MHS observations) the comparisons were of less value. Despite its issues, the offline route is a straightforward and accessible way of doing observation-space verification and evaluation, particularly for external researchers who may not have access to the ECMWF data assimilation framework.

3. **Using the data assimilation framework:** this should be the ultimate goal, as it leverages all the efforts already made to provide the best quality of time interpolation (the forecast model), horizontal interpolation and data movement and sophisticated observation operators with known microphysical assumptions, consistent with the forecast model. However, one thing that would make it easier for scientists to interpret the results would be to provide conversions back into an approximate physical space.

Hence the data assimilation framework itself is the optimal tool for forecast verification and validation. This is a large part of the motivation for developments like the passive monitoring of top-of-the-atmosphere radiation fluxes (Sec. 2.7) even if we have no great expectations from the active assimilation

of such data. The 'model to observation' approach is also increasingly recognised for climate model evaluation (e.g. Matsui et al., 2014) but the great advantage of a model like the IFS is that its data assimilation system already provides the model-to-observation functionality.

We do still recommend additional archiving of data in MARS, so that there is sufficient information to be able to reproduce standard cloud and precipitation observations offline from archived forecast data. This requires the archiving of convective as well as large-scale hydrometeors in order to replicate passive microwave and radar observations, and the archiving of effective radius for IR, solar radiance and lidar forward modelling. Further, the archiving of hourly surface precipitation accumulations throughout the forecast range would allow much more comprehensive verification against rain gauges, particularly those that accumulate over non-standard time periods and report their accumulations outside of the usual synoptic hours. The solution, with minimal additional archiving requirements, is simply to archive the hourly accumulated precipitation, making it possible to compute observation equivalents for almost all the world's rain gauges.

However, offline verification in observation space will always have limitations. First, following the philosophy of 'microphysical convergence' explored in Sec. 3 the set of additional microphysical and sub-grid variables required to accurately replicate observations could grow quite large, and the archived values in MARS may remain in a state of catch-up compared to what is used in the observation operators in the data assimilation. Second, it will never be possible to archive every timestep of the model, yet especially for cloud and precipitation observations it is important to take model inputs at the closest possible time and location. It is likely cheaper to recreate the additional variables and intermediate timesteps by re-running the forecast model. This also means the observation operators can be run at the same time, from within the data assimilation system. Such a framework is already available at ECMWF (e.g. Dahoui et al., 2016) but it is relatively cumbersome and expensive (requiring complicated additional experiments) and it does not yet feed into forecast verification tools. However, if this framework can be streamlined, made more economic, and integrated with our verification tools, it would be of great utility, particularly for verifying cloud and precipitation.

6 Conclusion

All-sky assimilation is a major success, but it needed ECMWF to take the long view. The ability to do cloud and precipitation assimilation is founded on choices made 15–20 years ago. ECMWF decided to invest in developing a simplified, linearised physics package that is now the most advanced in the world, and to explore the assimilation of a wide range of observations sensitive to cloud and precipitation. These early investments have fed through to an operational assimilation of all-sky microwave observations which now provide around 20% of all forecast impact from observations and significant benefit to medium range forecasts, using the 4D-Var tracing effect to infer dynamical initial conditions from water vapour, cloud and precipitation. While these developments were ongoing, it was often hard to demonstrate their full benefit, and often ECMWF chose to go operational with an early version of a new capability knowing that it could be improved over subsequent years from within the operational system. It is not easy getting forecast benefit from new cloud and precipitation observations, and rather it depends on continued detailed improvements in the scientific quality of the whole system. This includes observation operators incorporating science at the forefront of research (for example using detailed particle scattering models), developing a forecast model able to represent cloud and precipitation with great realism, and adapting the data assimilation framework to handle observations affected by nonlinearity and large representation errors. Cloud and precipitation assimilation therefore requires cooperation across all branches of NWP research, inside and outside of ECMWF.

Continuing the development of cloud and precipitation assimilation would bring three main benefits to ECMWF: (1) the ability to use existing satellite observations in all states of the atmosphere, bringing increased coverage in the areas most sensitive to forecast quality; (2) for the forecasts to benefit from further improvements to initial conditions that can now be inferred from a range of new cloud and precipitation data, from ground based radar to solar radiances; (3) to develop even further the cooperation between observation, assimilation and model scientists using cloud and precipitation observations to help constrain and improve the model's moist physics parametrisations. This can give benefit at all forecast time ranges by helping to improve the modelling of phenomena as diverse as wintertime continental boundary layer cloud, midlatitude and tropical cyclones, and convectively-coupled tropical waves. An aim is to move towards 'sub-grid and microphysical closure' where as much as possible, the sub-grid heterogeneity and microphysics of the forecast model is constrained by observations.

We should have the ambition to bring all possible observations related to cloud and precipitation into our assimilation system. So far only around 25% of the satellite radiance types assimilated at ECMWF have been transferred into an all-sky framework. The process that began with microwave imagers and humidity sounders will be continued, with continuing efforts to use all-sky microwave temperature-sounding radiances, and all-sky infrared humidity radiances. However, there is a far greater availability of observations including radar, rain gauge and lightning observations on the ground, and radar, lidar, lightning, earth radiation budget and solar radiances from space platforms. There are also novel channels from microwave and infrared sensors whose main sensitivities are to cloud and precipitation, including the 10 GHz microwave for heavy rain over ocean and EUMETSAT's future sub-mm ICI instrument for ice cloud globally. Among these novel observational sources, the 10 GHz passive microwave and space-based radar from EarthCARE are a current priority for active assimilation. For the other observation types an initial passive monitoring capability will benefit model validation and verification, and provide a platform for developing active assimilation in the long term. With sufficient development, all of these observation types should be able to contribute to medium-range forecast quality directly through their assimilation. Further, the great diversity of these observations will allow us to constrain increasingly large parts of the cloud and precipitation modelling – for example from rain on the ground (gauges) to rain and large frozen particles in the atmosphere (radar and microwave) to the liquid and ice clouds (microwave, lidar, infrared, solar). For observations such as ground-based radar, the main limitation is not internal to ECMWF but the availability of data. Even regions such as Europe still need more cooperation and investment to develop quality-controlled, near-real-time meteorological radar observation networks suitable for global weather forecasting.

We will continue to rely on further development of RTTOV as the main observation operator for space-based observations sensitive to cloud and precipitation, with support within the EUMETSAT NWP-SAF. This helps us benefit from development and maintenance activities that are shared across European NWP centres (and beyond) and similarly helps us share our developments. It also gives a framework to ensure microphysical and sub-grid consistency in observation operators from microwave to solar frequencies, and for both active and passive applications. A more detailed work-plan for the microwave includes (i) treatment of the projection effect; (ii) urgent investigation of the effects of polarised scattering, and their implications on the future development of RTTOV for example the need for fully polarised radiative transfer; (iii) cooperation between the model physics and observation operator developers to do a better job of convection, considering the interface (issues of convective fraction, flux and mixing ratio) and the particle types (the potential need for graupel and hail hydrometeors, and scattering models and particle size distributions to support this). For the infrared, the priority is clear: a better treatment of cloud overlap, but without the cost of a many-independent column approach. Developments in support of capabilities for radar, cloudy solar radiances and sub-mm instruments (ICI) will also continue in the RTTOV framework, with many of these developments coming from other NWP centres.

A major benefit of cloud and precipitation assimilation is to better constrain the forecast model, and to contribute to forecast model developments, but this also means the forecast model needs to evolve in support of the observations. Even at forecast ranges where most of the impact of initial conditions has been lost, an improved forecast model will still have smaller systematic error in its cloud and precipitation fields. This is a main motivation for missions like EarthCARE where the amount of data is small, but the constraint on the model is strong. To support this, the modelling chain must be thought of as an integrated whole, with 'sub-grid and microphysical closure' between the model and the observation operators. Practically, this means more sharing of components (such as sub-grid cloud generators) and making more consistent microphysical and sub-grid assumptions wherever possible. More complicated microphysics (such as double-moment) or more sophisticated representations of convection will continue to be considered as the model resolution increases, but more complexity does not necessarily guarantee major improvement in model biases or predictability. History (such as the difficulty in developing a solution to the lack of liquid water in cold-air outbreaks) shows how difficult it is to make progress. Regardless, there will continue to be a drive to increase the physical realism in all the parametrization schemes which will be of benefit in the long term for both model forecast accuracy and making the best use of observations in the assimilation system. There is already scope for providing more diagnostic variables to the observation operators, such as measures of the particle size distribution (perhaps effective radius for the infrared) or improved representation of the convective precipitation mass-mixing ratios and sub-grid fraction. Following this, further diagnostic information for the observation operators such as ice particle shape, or a representation of graupel/hail in the convection scheme, could be explored. We should aim to provide full tangent-linear/adjoint sensitivities to any of these new variables through the model and observation operator, so that they can be constrained by observations in 4D-Var.

On the data assimilation side, we need continued investment in tangent-linear/adjoint modelling, more sophisticated observation error models, and we should move towards cloud ice and water control variables. The recent data assimilation strategy (Bonavita et al., 2017) is fully compatible with further development of cloud and precipitation assimilation. However we should note again the importance of the simplified linearised moist physics modelling as the underlying basis of all our cloud and precipitation assimilation activities. There are both difficulties and great benefits in keeping it maintained and supporting future developments of the nonlinear moist physics, and offering new observational sensitivities (such as to cloud effective radius). It is also becoming clearer that we do need to invest in cloud ice and water control variables, and the associated modelling of cloud-related background error balances. For example, cloud ice seems to have up to a 6-hour memory of the initial conditions; this may prevent us assimilating all-sky infrared radiances in the first half of the assimilation window unless there is a cloud ice control variable. Finally, observation error model developments will continue using the 'symmetric' framework for variance inflation in cloudy conditions, and new capability will be developed to model the way that inter-channel error correlations also become greater in cloudy conditions. However, these observation error correlations (coming from representation error, i.e. the mislocation of cloud and precipitation features) also have spatial and temporal correlations that would in the long term benefit from a model of the observation error covariances of similar complexity to the background errors, and may in the short-term benefit from representation of the model error term in a weak-constraint framework.

To make use of cloud and precipitation observations for forecast verification and validation, we need to develop the data assimilation framework as the main tool for mapping model states to observation space. For forecast model development, we should also ensure that the MARS archive contains sufficient information to generate offline comparisons to cloud and precipitation observations. This is partly to support validation activities internally, but also to allow outside researchers to compare ECMWF cloud and precipitation forecasts to observations in observation space. Here, the MARS archiving of convective hydrometeor profiles and precipitation fraction (for passive and active microwave),
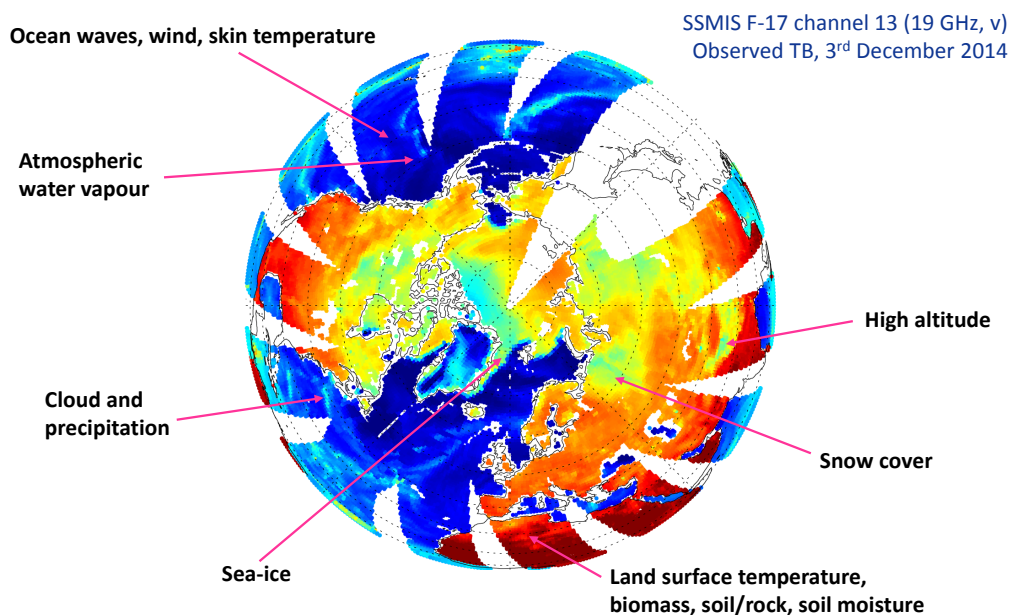
Figure 25: SSMI/S observations in the 19GHz v-polarised channel. Currently we make use of the wind, water vapour, cloud and precipitation information content over ocean, but there is much more available for earth-system assimilation.

cloud effective radius (for infrared and radiation modelling) and hourly surface precipitation accumulations at all forecast ranges (for rain gauges) would be a good first step. However, the best place to use these observations for verification and validation is within the existing data assimilation framework. Essentially, there needs to be a convergence of data assimilation, model validation and forecast verification activities. The current framework for generating model − observation departures at arbitrary forecast ranges (rather than just at first-guess) needs to become faster, cheaper and easier to run, as well as more integrated within the verification systems of ECMWF. The OOPS project should help make it easier to use the data assimilation tools such as interpolation to observation space, observation operators and quality control, but inside a verification framework.

All-sky is a template for other complex earth system assimilation problems. Satellite radiances are sensitive to not just the atmosphere, but also other aspects of the earth system. For example (Fig. 25) microwave imager radiances are sensitive to SST, sea-ice coverage (and ice structure and thickness), snow cover (and snowpack structure), soil moisture (and soil temperature and structure) and flooding coverage. Infrared and visible observations can also bring sensitivity to aerosol, potentially helping further constrain the particle size distributions of cloud and precipitation. The ideal future path is to include the assimilation of these quantities into the main analysis system just as we are doing successfully for cloud and precipitation. Lessons to draw from all-sky assimilation are to move towards a unified analysis (analyse mass, wind, hydrometeors and earth-system variables simultaneously), and we have also seen the benefits of direct assimilation of observed quantities like radiances and reflectivities, rather than assimilation of retrievals. This also requires the use of physically-based observation operators. A tangent-linear and adjoint capability is needed not just for these observation operators but also for the new earth-system model components.

Following the success of all-sky microwave humidity radiance assimilation, we expect an ever-wider variety of observations sensitive to cloud and precipitation will become increasingly important for deter-

mining atmospheric initial conditions, for improving medium-range forecasts, and for helping to develop cloud and precipitation modelling.

Acknowledgements

Satellites and sensors

AIRS	Atmospheric Infrared Sounder
AMSR2	Advanced Microwave Scanning Radiometer 2
AMSU-A	Advanced Microwave Sounding Unit-A
ATMS	Advanced Technology Microwave Sounder
CALIPSO	Cloud-Aerosol Lidar and Infrared Pathfinder Satellite Observations
CrIS	Cross-track Infrared Sounder
DMSP	Defense Meteorological Satellite Program
DPR	Dual-frequency Precipitation Radar
EarthCARE	Earth, Clouds, Aerosols and Radiation Explorer
FY	Feng-Yun
GCOM-W	Global Change Observation Mission - Water
GLM	Geostationary Lightning Mapper
GMI	GPM Microwave Imager
GOES	Geostationary Operational Environmental Satellite
GPM	Global Precipitation Measurement
GPSRO	GPS radio occultation
IASI	Infrared Atmospheric Sounding Interferometer
ICI	Ice Cloud Imager
LI	Lightning Imager
LIS	Lightning Imaging Sensor
LMI	Lightning Mapping Imager
MHS	Microwave Humidity Sounder
MODIS	Moderate Resolution Imaging Spectroradiometer
MTG	Meteosat Third Generation
MWHS-2	MicroWave Humidity Sounder-2
MWS	Microwave Sounder
MWTS-2	MicroWave Temperature Sounder-2
NOAA	National Oceanic and Atmospheric Administration
OTD	Optical Transient Detector
SAPHIR	Sondeur Atmosphérique du Profil d'Humidité Intertropicale par Radiométrie
SSMIS	Special Sensor Microwave Imager/Sounder
Suomi-NPP	Suomi National Polar-orbiting Partnership
TMI	TRMM Microwave Imager
TRMM	Tropical Rainfall Measuring Mission

References

Abel, S. J. and I. A. Boutle (2012). An improved representation of the raindrop size distribution for single-moment microphysics schemes. *Quarterly Journal of the Royal Meteorological Society 138*(669), 2151–2162.

Ahlgrimm, M. and R. Forbes (2014). Improving the representation of low clouds and drizzle in the ECMWF model based on ARM observations from the Azores. *Mon. Wea. Rev. 142*, 668–685.

Ahlgrimm, M. and R. M. Forbes (2016). Regime dependence of cloud condensate variability observed at the atmospheric radiation measurement sites. *Quarterly Journal of the Royal Meteorological Society 142*(697), 1605–1617.

Allen, D. R., K. W. Hoppel, G. E. Nedoluha, D. D. Kuhl, N. L. Baker, L. Xu, and T. E. Rosmond (2013). Limitations of wind extraction from 4D-Var assimilation of ozone. *Atmos. Chem. Phys. 13*, 3501–3515.

Andersson, E., P. Bauer, A. Beljaars, F. Chevallier, E. Hólm, M. Janisková, P. Kållberg, G. Kelly, P. Lopez, A. McNally, E. Moreau, A. J. Simmons, J.-N. Thépaut, and A. M. Tompkins (2005). Assimilation and modeling of the atmospheric hydrological cycle in the ECMWF forecasting system. *Bull. Am. Met. Soc. 86*, 387–402.

Andersson, E., A. Hollingsworth, G. Kelly, P. Lönnberg, J. Pailleux, and Z. Zhang (1991). Global observing system experiments on operational statistical retrievals of satellite sounding data. *Mon. Weath. Rev. 119*(8), 1851–1865.

Andersson, E., E. Hólm, P. Bauer, A. Beljaars, G. A. Kelly, A. P. McNally, A. J. Simmons, J.-N. Thépaut, and A. Tompkins (2007). Analysis and forecast impact of the main humidity observing systems. *Quart. J. Roy. Meteorol. Soc. 133*, 1473–1485.

Asai, T. (1965). A numerical study of the air-mass transformation over the Japan Sea in winter. *J. Meteorol. Soc. Japan. 43*(1), 1–15.

Auligné, T., A. P. McNally, and D. P. Dee (2007). Adaptive bias correction for satellite data in a numerical weather prediction system. *Quart. J. Roy. Meteorol. Soc. 133*, 631–642.

Baordo, F. and A. J. Geer (2016). Assimilation of SSMIS humidity-sounding channels in all-sky conditions over land using a dynamic emissivity retrieval. *Quart. J. Roy. Meteorol. Soc. 142*, 2854–2866.

Bauer, P. (2001). Including a melting layer in microwave radiative transfer simulation for cloud. *Atmos. Res. 57*, 9–30.

Bauer, P., T. Auligné, W. Bell, A. Geer, V. Guidard, S. Heillette, M. Kazumori, M.-J. Kim, E. H.-C. Liu, A. P. McNally, B. Macpherson, K. Okamoto, R. Renshaw, and L.-P. Riishøjgaard (2011). Satellite cloud and precipitation assimilation at operational NWP centres. *Quart. J. Roy. Meteorol. Soc. 137*, 1934–1951.

Bauer, P., A. J. Geer, P. Lopez, and D. Salmond (2010). Direct 4D-Var assimilation of all-sky radiances: Part I. Implementation. *Quart. J. Roy. Meteorol. Soc. 136*, 1868–1885.

Bauer, P., P. Lopez, A. Benedetti, D. Salmond, and E. Moreau (2006a). Implementation of 1D+4D-Var assimilation of precipitation-affected microwave radiances at ECMWF. I: 1D-Var. *Quart. J. Roy. Meteorol. Soc. 132*, 2277–2306.

Bauer, P., P. Lopez, D. Salmond, A. Benedetti, S. Saarinen, and E. Moreau (2006b). Implementation of 1D+4D-Var assimilation of precipitation-affected microwave radiances at ECMWF. II: 4D-Var. *Quart. J. Roy. Meteorol. Soc. 132*, 2307–2332.

Bauer, P., P. Lopez, D. Salmond, and A. J. Geer (2006c). Assimilation of cloud and precipitation affected microwave radiances. *ECMWF Tech. Memo., 502, available from http://www.ecmwf.int*.

Bauer, P., E. Moreau, F. Chevallier, and U. O'Keeffe (2006d). Multiple-scattering microwave radiative transfer for data assimilation applications. *Quart. J. Roy. Meteorol. Soc. 132*, 1259–1281.

Bauer, P., L. Schanz, and L. Roberti (1998). Correction of three-dimensional effects for passive microwave remote sensing of convective clouds. *Journal of Applied Meteorology 37*(12), 1619–1632.

Bechtold, P., M. Köhler, T. Jung, M. Leutbecher, M. Rodwell, F. Vitart, and G. Balsamo (2008). Advances in predicting atmospheric variability with the ECMWF model. *Quart. J. Roy. Meteorol. Soc.* (134), 1337–1351.

Bechtold, P., N. Semane, P. Lopez, J.-P. Chaboureau, A. Beljaars, and N. Bormann (2014). Representing equilibrium and nonequilibrium convection in large-scale models. *J. Atmos. Sci. 71*(2), 734–753.

Benedetti, A. and M. Janisková (2008). Assimilation of MODIS cloud optical depths in the ECMWF model. *Mon. Wea. Rev. 136*, 1727–1746.

Benedetti, A., P. Lopez, P. Bauer, and E. Moreau (2005). Experimental use of TRMM precipitation radar observations in 1D+4D-Var assimilation. *Quart. J. Roy. Meteorol. Soc. 131*, 2473–2495.

Bengtsson, L. and K. Hodges (2005). On the impact of humidity observations in numerical weather prediction. *Tellus 57A*, 701–708.

Bennartz, R. and T. Greenwald (2011). Current problems in scattering radiative transfer modelling for data assimilation. *Quart. J. Roy. Meteorol. Soc. 137*, 1952–1962.

Berre, L. (2000). Estimation of synoptic and mesoscale forecast error covariances in a limited-area model. *Mon. Weath. Rev. 128*(3), 644–667.

Bi, L., A. Collard, E. H. Liu, J. Jung, and J. Derber (2016). Towards the assimilation of all-sky infrared radiances for selected humidity sensitive IASI channels at NCEP/EMC. Fourth IASI (Infrared Atmospheric Sounding Interferometer) Conference, Antibes Juan-les-Pins, France.

Birman, C., J.-F. Mahfouf, M. Milz, J. Mendrok, S. A. Buehler, and M. Brath (2017). Information content on hydrometeors from millimeter and sub-millimeter wavelengths. *Tellus A: Dynamic Meteorology and Oceanography 69*(1), 1271562.

Bocquet, M. and A. Carrassi (2017). Four-dimensional ensemble variational data assimilation and the unstable subspace. *Tellus A 69*(1), 1304504.

Bocquet, M. and P. Sakov (2014). An iterative ensemble kalman smoother. *Quarterly Journal of the Royal Meteorological Society 140*(682), 1521–1535.

Bonavita, M., Y. Trémolet, E. Holm, S. T. K. Lang, M. Chrust, M. Janisková, P. Lopez, P. Laloyaux, P. de Rosnay, M. Fisher, M. Hamrud, and S. English (2017). A strategy for data assimilation. *ECMWF Research Department Memorandum 800*.

Bormann, N., M. Bonavita, R. Dragani, R. Eresmaa, M. Matricardi, and A. McNally (2016). Enhancing the impact of IASI observations through an updated observation-error covariance matrix. *Quart. J. Roy. Meteorl. Soc. 142*(697), 1767–1780.

Bormann, N., A. Fouilloux, and W. Bell (2013). Evaluation and assimilation of ATMS data in the ECMWF system. *J. Geophys. Res.: Atmos. 118*(23).

Bormann, N., A. Geer, and P. Bauer (2011). Estimates of observation error characteristics in clear and cloudy regions for microwave imager radiances from NWP. *Quart. J. Roy. Meteorol. Soc. 137*, 2014–2023.

Buehler, S. A., C. Jimenez, K. Evans, P. Eriksson, B. Rydberg, A. Heymsfield, C. Stubenrauch, U. Lohmann, C. Emde, V. John, et al. (2007). A concept for a satellite mission to measure cloud ice water path, ice particle size, and cloud altitude. *Quart. J. Roy. Meteorol. Soc. 133*(S2), 109–128.

Cardinali, C. (2009). Monitoring the observation impact on the short-range forecast. *Quart. J. Roy. Meteorol. Soc. 135*(638), 239–250.

Cardinali, C. and R. Buizza (2004). Observation sensitivity to the analysis and the forecast: A case study during ATreC targeting campaign. In *In Proceedings of the First THORPEX International Science Symposium, 6-10 December 2004, Montreal, Canadan WMO TD 1237 WWRP/THORPEX N. 6.*

Caumont, O., V. Ducrocq, É. Wattrelot, G. Jaubert, and S. Pradier-Vabre (2010). 1D + 3DVar assimilation of radar reflectivity data: a proof of concept. *Tellus A 62*(2), 173–187.

Chambon, P. and A. J. Geer (2017). All-sky assimilation of Megha-Tropiques/SAPHIR radiances in the ECMWF numerical weather prediction system. *ECMWF Research Department Memorandum 802*.

Chern, J.-D., W. K. Tao, S. E. Lang, T. Natsui, J.-L. Li, K. I. Mohr, G. M. Skofronick-Jackson, and C. D. Peters-Lidard (2016). Performance of the Goddard multiscale modeling framework with Goddard ice microphysical schemes. *J. Adv. Mod. Earth Syst. 8*, 66–95.

Chevallier, F. and G. Kelly (2002). Model clouds as seen from space: Comparison with geostationary imagery in the 11-μm window channel. *Mon. Wea. Rev. 130*, 712–722.

Chevallier, F., P. Lopez, M. A. Tompkins, M. Janisková, and E. Moreau (2004). The capability of 4D-Var systems to assimilate cloud-affected satellite infrared radiances. *Quart. J. Roy. Meteorol. Soc. 130*, 917–932.

Cox, G. P. (1988). Modelling precipitation in frontal rainbands. *Quarterly Journal of the Royal Meteorological Society 114*(479), 115–127.

Dahoui, M., G. Radnoti, S. Healy, L. Isaksen, and T. Haiden (2016). Use of forecast departures in verification against observations. *ECMWF newsletter* (149), 30–33.

Dauhut, T., J.-P. Chaboureau, J. Escobar, and P. Mascart (2016). Giga-LES of the Hectot the Convector and its two tallest updrafts up to the stratosphere. *J. Atmos. Sci. 73*(12), 5041–5060.

Deblonde, G., J.-F. Mahfouf, B. Bilodeau, and D. Anselmo (2007). One-dimensional variational data assimilation of SSM/I observations in rainy atmospheres at MSC. *Mon. Wea. Rev. 135*, 152–172.

Dee, D. (2004). Variational bias correction of radiance data in the ECMWF system. In *ECMWF workshop proceedings: Assimilation of high spectral resolution sounders in NWP, 28 June – 1 July, 2004*, pp. 97–112. Eur. Cent. for Med. Range Weather Forecasts, Reading, UK, available from http://www.ecmwf.int.

Dee, D. P., S. M. Uppala, A. J. Simmons, P. Berrisford, P. Poli, S. Kobayashi, U. Andrae, M. A. Balmaseda, G. Balsamo, P. Bauer, P. Bechtold, A. C. M. Beljaars, L. van de Berg, J. Bidlot, N. Bormann, C. Delsol, R. Dragani, M. Fuentes, A. J. Geer, L. Haimberger, S. Healy, H. Hersbach, E. V. Hólm, L. Isaksen, P. Kållberg, M. Köhler, M. Matricardi, A. P. McNally, B. M. Monge-Sanz, J.-J. Morcrette, C. Peubey, P. de Rosnay, C. Tavolato, J.-N. Thépaut, and F. Vitart (2011). The ERA-Interim reanalysis: Configuration and performance of the data assimilation system. *Quart. J. Roy. Meteorol. Soc. 137*(656), 553–597.

Delanoë, J., R. J. Hogan, R. M. Forbes, A. Bodas-Salcedo, and T. H. M. Stein (2011). Evaluation of ice cloud representation in the ECMWF and UK Met Office models using CloudSat and CALIPSO data. *Quart. J. Roy. Meteorol. Soc. 137*(661), 2064–2078.

Descombes, G., T. Auligné, F. Vandenberghe, D. Barker, and J. Barre (2015). Generalized background error covariance matrix model (GEN_BE v2. 0). *Geosci. Model Dev. 8*(3), 669–696.

Desroziers, G., E. Arbogast, and L. Berre (2016). Improving spatial localization in 4DEnVar. *Quart. J. Roy. Meteorol. Soc.*.

Di Michele, S., M. Ahlgrimm, R. Forbes, M. Kulie, R. Bennartz, M. Janiskova, and P. Bauer (2012). Interpreting an evaluation of the ECMWF global model with CloudSat observations: ambiguities due to radar reflectivity forward operator uncertainties. *Quart. J. Roy. Meteorol. Soc. 138*, 2047–2065.

ECMWF (2017). Radiation in numerical weather prediction. *Paper to 46th session of the ECMWF Scientific Advisory Committee, 9–11 October 2017*, ECMWF/SAC/46(17)13.

English, S., T. McNally, N. Bormann, K. Salonen, M. Matricardi, A. Horanyi, M. Rennie, M. Janisková, S. Di Michele, A. Geer, E. Di Tomaso, C. Cardinali, P. de Rosnay, J. Muñoz Sabater, M. Bonavita, C. Albergel, R. Engelen, and J.-N. Thépaut (2013). Impact of satellite data. *ECMWF Tech. Memo., 711, available from http://www.ecmwf.int*.

Errico, R. M., L. Fillion, D. Nychka, and Z.-Q. Lu (2000). Some statistical considerations associated with the data assimilation of precipitation observations. *Quart. J. Roy. Meteorl. Soc. 126*(562), 339–359.

Field, P. R., A. J. Heymsfield, and A. Bansemer (2007). Snow size distribution parameterization for midlatitude and tropical ice clouds. *J. Atmos. Sci. 64*, 4346 – 4365.

Field, P. R., R. J. Hogan, P. R. A. Brown, A. J. Illingworth, T. W. Choularton, and R. J. Cotton (2005). Parameterization of ice-particle size distributions for midlatitude stratiform cloud. *Quart. J. Roy. Meteorol. Soc. 131*, 1997 – 2017.

Fielding, M. D. and M. Janisková (2017). Observation quality monitoring and pre-processing. WP-2000 report for the project Operational Assimilation of Space-borne Radar and Lidar Cloud Profile Observations for Numerical Weather Prediction, 4000116891/16/NL/LvH. pp.

Fillion, L. and R. Errico (1997). Variational assimilation of precipitation data using moist convective parameterization schemes: A 1D-Var study. *Mon. Weath. Rev. 125*(11), 2917–2942.

Fisher, M. (2003). Background error covariance modelling. *Proc. ECMWF Seminar on Recent Developments in Data Assimilation for Atmosphere and Ocean, 8–12 September 2003, Reading, UK, pp.45–63.*

Forbes, R., A. Geer, K. Lonitz, and M. Ahlgrimm (2016). Reducing systematic errors in cold-air outbreaks. *ECMWF newsletter* (146), 17–22.

Forbes, R. M. and P. A. Clark (2003). Sensitivity of extratropical cyclone mesoscale structure to the parametrization of ice microphysical processes. *Quarterly Journal of the Royal Meteorological Society 129*(589), 1123–1148.

Forbes, R. M. and A. M. Tompkins (2011). An improved representation of cloud and precipitation. *ECMWF Newsletter No. 129*, 13–18.

Forbes, R. M., A. M. Tompkins, and A. Untch (2011). A new prognostic bulk microphysics scheme for the IFS. *ECMWF Technical Memorandum 649.*

Fridlind, A. M., A. S. Ackermann, J.-P. Chaboureau, J. Fan, W. W. Grabowski, A. A. Hill, T. R. Jones, M. M. Khaiyer, G. Liu, P. Minnis, H. Morrison, L. Nguyen, S. Park, J. C. Petch, J.-P. Pinty, C. Schumacher, B. J. Shipway, A. C. Varble, X. Wu, S. Xie, and M. Zhang (2012). A comparison of TWP-ICE observational data with cloud-resolving models. *J. Geophys. Res. 117*, doi: 10.1029/2011JD016595.

Galligani, V. S., D. Wang, M. A. Imaz, P. Salio, and C. Prigent (2017). Analysis and evaluation of WRF microphysical schemes for deep moist convection over Southeastern South America (SESA) using microwave satellite observations and radiative transfer simulations. *Atmos. Meas. Tech. 10*, 3627–3649.

Geer, A. J. (2013). All-sky assimilation: better snow-scattering radiative transfer and addition of SSMIS humidity sounding channels. *ECMWF Tech. Memo., 706, available from http://www.ecmwf.int.*

Geer, A. J. and F. Baordo (2014). Improved scattering radiative transfer for frozen hydrometeors at microwave frequencies. *Atmos. Meas. Tech. 7*, 1839–1860.

Geer, A. J., F. Baordo, N. Bormann, and S. English (2014). All-sky assimilation of microwave humidity sounders. *ECMWF Tech. Memo., 741, available from http://www.ecmwf.int.*

Geer, A. J., F. Baordo, N. Bormann, S. English, M. Kazumori, H. Lawrence, P. Lean, K. Lonitz, and C. Lupu (2017a). The growing impact of satellite observations sensitive to humidity, cloud and precipitation. *Quart. J. Roy. Meteorol. Soc.*, accepted, doi:10.1002/qj.3172.

Geer, A. J. and P. Bauer (2010). Enhanced use of all-sky microwave observations sensitive to water vapour, cloud and precipitation. *Published simultaneously as ECMWF Technical Memoranda 620 and ECMWF/EUMETSAT fellowship reports 20.*

Geer, A. J. and P. Bauer (2011). Observation errors in all-sky data assimilation. *Quart. J. Roy. Meteorol. Soc. 137*, 2024–2037.

Geer, A. J., P. Bauer, and S. J. English (2012). Assimilating AMSU-A temperature sounding channels in the presence of cloud and precipitation. *Published simultaneously as ECMWF Technical Memoranda 670 and ECMWF/EUMETSAT fellowship reports 24.*

Geer, A. J., P. Bauer, and P. Lopez (2007). Lessons learnt from the 1D+4D-Var assimilation of rain and cloud affected SSM/I observations at ECMWF. *Published simultaneously as ECMWF Technical Memoranda 535 and ECMWF/EUMETSAT fellowship reports 17.*

Geer, A. J., P. Bauer, and P. Lopez (2008). Lessons learnt from the operational 1D+4D-Var assimilation of rain- and cloud-affected SSM/I observations at ECMWF. *Quart. J. Roy. Meteorol. Soc. 134*, 1513–1525.

Geer, A. J., P. Bauer, and P. Lopez (2010). Direct 4D-Var assimilation of all-sky radiances: Part II. Assessment. *Quart. J. Roy. Meteorol. Soc. 136*, 1886–1905.

Geer, A. J., P. Bauer, and C. W. O'Dell (2009). A revised cloud overlap scheme for fast microwave radiative transfer. *J. App. Meteor. Clim. 48*, 2257–2270.

Geer, A. J., R. Forbes, and P. Bauer (2009). Cloud and precipitation overlap in simplified scattering radiative transfer. *EUMETSAT/ECMWF Fellowship Programme Research Report 18.*

Geer, A. J., R. Forbes, P. Bauer, and F. Baordo (2011). Big temperature increments in the 37r3 esuite coming from all-sky observations in the southern winter. *ECMWF Research Department Internal Memorandum R48.3/AG/11110.*

Geer, A. J., K. Lonitz, P. Weston, M. Kazumori, K. Okamoto, Y. Zhu, E. H. Liu, A. Collard, W. Bell, S. Migliorini, P. Chambon, N. Fourrié, M.-J. Kim, C. Köpken-Watts, and C. Schraff (2017b). All-sky satellite data assimilation at operational weather forecasting centres. *Quart. J. Roy. Meteorol. Soc.*, in review.

Giuseppe, F. D. and A. M. Tompkins (2015). Generalizing cloud overlap treatment to include the effect of wind shear. *Journal of the Atmospheric Sciences 72*(8), 2865–2876.

Gong, J. and D. L. Wu (2017). Microphysical properties of frozen particles inferred from global precipitation measurement (GPM) microwave imager (GMI) polarimetric measurements. *Atmos. Chem. Phys. 17*(4), 2741–2757.

Guerbette, J., J.-F. Mahfouf, and M. Plu (2016). Towards the assimilation of all-sky microwave radiances from the SAPHIR humidity sounder in a limited area NWP model over tropical regions. *Tellus A 68*, 28620.

Harnisch, F., M. Weissmann, and Á. Periáñez (2016). Error model for the assimilation of cloud-affected infrared satellite observations in an ensemble data assimilation system. *Quart. J. Roy. Meteorol. Soc. 142*(697), 1797–1808.

Hogan, R. J., E. J. O'Connor, and A. J. Illingworth (2009). Verification of cloud-fraction forecasts. *Quart. J. Roy. Meteorol. Soc. 135*(643), 1494–1511.

Hogan, R. J., S. A. K. Schafer, C. Klinger, J.-C. Chiu, and B. Mayer (2016). Representing 3D cloud-radiation effects in two-stream schemes: 2. Matrix formulation and broadband evaluation.Verification of cloud-fraction forecasts. *J. Geophys. Res. Atmos. 121*, 8583–8599.

Hólm, E. (2015). Balance operator including linear saturation adjustment and cloud condensate. *The 3rd Joint JCSDA-ECMWF Workshop on Assimilating Satellite Observations of Clouds and Precipitation into NWP Models. NCWCP, College Park, Maryland, December 1–3, 2015. Available at https://www.jcsda.noaa.gov/documents/meetings/EC-JC_Wkshp2015/Holm_EC_JC.*

Hólm, E., E. Andersson, A. Beljaars, P. Lopez, J.-F. Mahfouf, A. Simmons, and J.-N. Thepaut (2002). Assimilation and modelling of the hydrological cycle: ECMWF's status and plans. *ECMWF Tech. Memo., 383, available from http://www.ecmwf.int.*

Illingworth, A. et al. (2015). The earthcare satellite: The next step forward in global measurements of clouds, aerosols, precipitation, and radiation. *Bulletin of the American Meteorological Society 96*(8), 1311–1332.

Janisková, M. (2015). Assimilation of cloud information from space-borne radar and lidar: Experimental study using 1D+4D-Var technique. *Q. J. R. Meteorol. Soc.* **141**, 2708–2725.

Janisková, M. and C. Cardinali (2017). On the impact of the diabatic component in the Forecast Sensitivity Observation Impact diagnostics. In *Data Assimilation for Atmospheric, Ocean and Hydrological Applications (Vol III), Springer-Verlag Berline Heidelberg*, pp. 483–511.

Janisková, M., S. Di Michele, and E. Martins (2014). Support-to-Science-Elements (STSE) Study - EarthCARE Assimilation. ESA Contract Report on Project 4000102816/11/NL/CT. 225 pp.

Janisková, M. and P. Lopez (2013). Linearized physics for data assimilation at ECMWF. In *S.K. Park and L. Xu (Eds), Data Assimilation for Atmospheric, Ocean and Hydrological Applications (Vol II), Springer-Verlag Berline Heidelberg*, pp. 251–286, doi:10.1007/978–3–642–35088–7–11.

Janisková, M., O. Stiller, S. Di Michele, R. Forbes, J.-J. Morcrette, M. Ahlgrimm, P. Bauer, and L. Jones (2010). QuARL - Quantitative Assessment of the Operational Value of Space-Borne Radar and Lidar Measurements of Cloud and Aerosol Profiles. ESA Contract Report on Project 21613/08/NL/CB. 329 pp.

Janisková, M., J.-N. Thépaut, and J.-F. Geleyn (1999). Simplified and regular physical parameterizations for incremental four-dimensional variational assimilation. *Mon. Weath. Rev. 127*(1), 26–45.

Johnson, B., W. Olson, and G. Skofronick-Jackson (2016). The microwave properties of simulated melting precipitation particles: sensitivity to initial melting. *Atmospheric Measurement Techniques 9*(1), 9–21.

Joiner, J. and A. Da Silva (1998). Efficient methods to assimilate remotely sensed data based on information content. *Quart. J. Roy. Meteorol. Soc. 124*(549), 1669–1694.

Karbou, F., É. Gérard, and F. Rabier (2006). Microwave land emissivity and skin temperature for AMSU-A and -B assimilation over land. *Quarterly Journal of the Royal Meteorological Society 132*(620), 2333–2355.

Kazumori, M., A. J. Geer, and S. J. English (2016). Effects of all-sky assimilation of GCOM-W/AMSR2 radiances in the ECMWF numerical weather prediction system. *Quart. J. Roy. Meteorol. Soc. 142*, 721–737.

Klein, M. and A. J. Gasiewski (2000). Nadir sensitivity of passive millimeter and submillimeter wave channels to clear air temperature and water vapor variations. *J. Geophys. Res. 105*(D13), 17481 – 17511.

Kollias, P., E. E. Clothiaux, M. A. Miller, B. A. Albrecht, G. L. Stephens, and T. P. Ackerman (2007). Millimeter-wavelength radars: New frontier in atmospheric cloud and precipitation research. *Bulletin of the American Meteorological Society 88*(10), 1608–1624.

Kostka, P. M., M. Weissmann, R. Buras, B. Mayer, and O. Stiller (2014). Observation operator for visible and near-infrared satellite reflectances. *Journal of Atmospheric and Oceanic Technology 31*(6), 1216–1233.

Kulie, M. S., R. Bennartz, T. J. Greenwald, Y. Chen, and F. Weng (2010). Uncertainties in microwave properties of frozen precipitation: implications for remote sensing and data assimilation. *J. Atmos. Sci. 67*, 3471–3487.

Kummerow, C. (1998). Beamfilling errors in passive microwave rainfall retrievals. *J. Appl. Meteor. 37*, 356–370.

Langland, R. H. and N. L. Baker (2004). Estimation of observation impact using the NRL atmospheric variational data assimilation adjoint system. *Tellus A 56*(3), 189–201.

Lawrence, H., N. Bormann, A. Geer, Q. Lu, and S. English (2016). An evaluation of FY-3C MWHS-2 at ECMWF. *Quart. J. Roy. Meteorol. Soc.*, in review.

Lean, P., A. Geer, and K. Lonitz (2017). Assimilation of Global Precipitation Mission (GPM) Microwave Imager (GMI) in all-sky conditions. *ECMWF Tech. Memo. 799, available from http://www.ecmwf.int*.

Lean, P., A. Geer, D. Salmond, and J. Hague (2016). The cost and scalability of observation processing in IFS; implications for future observation usage. *ECMWF RD internal memo. RD16-045*.

Lin, Y., L. J. Donner, J. Petch, P. Bechtold, J. Boyle, S. A. Klein, T. Komori, K. Wapler, M. Willett, X. Xie, M. Zhao, S. Xie, and S. A. McFarlane (2012). TWP-ICE global atmospheric model intercomparison: convection responsiveness and resolution impact. *J. Geophys. Res. 117*, doi: 10.1029/2011JD017018.

Liu, G. (2008). A database of microwave single-scattering properties for nonspherical ice particles. *Bull. Am. Met. Soc. 111*, 1563–1570.

Lonitz, K. and A. Geer (2015). New screening of cold-air outbreak regions used in 4D-Var all-sky assimilation. *EUMETSAT/ECMWF Fellowship Programme Research Report, 35, available from http://www.ecmwf.int*.

Lonitz, K. and A. Geer (2017). Effect of assimilating microwave imager observations in the presence of a model bias in marine stratocumulus. *EUMETSAT/ECMWF Fellowship Programme Research Report, 44, available from http://www.ecmwf.int*.

Lopez, P. (2011). Direct 4D-Var assimilation of NCEP stage IV radar and gauge precipitation data at ECMWF. *Mon. Weath. Rev. 139*(7), 2098–2116.

Lopez, P. (2013). Experimental 4D-Var assimilation of SYNOP rain gauge data at ECMWF. *Mon. Wea. Rev. 141*(5), 1527–1544.

Lopez, P. (2014). Comparison of NCEP Stage IV precipitation composites with ECMWF model. *ECMWF Tech. Memo., 728, available from http://www.ecmwf.int*.

Lopez, P. (2016). A lightning parameterization for the ECMWF Integrated Forecasting System. *Mon. Wea. Rev. 144*, 3057–3075.

Lopez, P. and P. Bauer (2007). "1D+4D-Var" assimilation of NCEP stage IV radar and gauge hourly precipitation data at ECMWF. *Mon. Wea. Rev. 135*, 2506–2524.

Lopez, P. and E. Moreau (2005). A convection scheme for data assimilation: Description and initial tests. *Quart. J. Roy. Meteorol. Soc. 131*, 409–436.

Lorenc, A. C. (2017). Improving ensemble covariances in hybrid variational data assimilation without increasing ensemble size. *Quart. J. Roy. Meteorol. Soc. 143*(703), 1062–1072.

Lupu, C. and A. McNally (2012). Assimilation of cloud-affected radiances from Meteosat-9 at ECMWF. *EUMETSAT/ECMWF Fellowship Programme Research Report No. 25, available from http://www.ecmwf.int*.

Lupu, C. and T. Wilhelmsson (2016). A guide to simulated satellite images in the IFS. *ECMWF RD internal memo., RD16-064, 10 pp.*.

Mahfouf, J.-F. (1999). Influence of physical processes on the tangent-linear approximation. *Tellus A 51*(2), 147–166.

Marécal, V., J.-F. M. and P. Bauer (2002). Comparison of TMI rainfall estimates and their impact on 4D-Var assimilation. *Quart. J. Roy. Meteorol. Soc. 128*, 2737–2758.

Martinet, P., N. Fourrié, V. Guidard, F. Rabier, T. Montmerle, and P. Brunel (2013). Towards the use of microphysical variables for the assimilation of cloud-affected infrared radiances. *Quart. J. Roy. Meteorol. Soc. 139*(674), 1402–1416.

Matricardi, M. (2005). The inclusion of aerosols and clouds in RTIASI, the ECMWF fast radiative transfer model for the infrared atmospheric sounding interferometer. *ECMWF Tech. Memo., 474, available from http://www.ecmwf.int*.

Matricardi, M. (2006). The second phase of the merge of RTIASI/RTTOV. *EUMETSAT Contract report EUM/CO/06/1504/PS*.

Matsui, T., J. Santanello, J. Shi, W.-K. Tao, D. Wu, C. Peters-Lidard, E. Kemp, M. Chin, D. Starr, M. Sekiguchi, et al. (2014). Introducing multisensor satellite radiance-based evaluation for regional earth system modeling. *J. Geophys. Res.: Atmos. 119*(13), 8450–8475.

McNally, A. (2002). A note on the occurrence of cloud in meteorologically sensitive areas and the implications for advanced infrared sounders. *Quart. J. Roy. Meteorol. Soc. 128*(585), 2551–2556.

McNally, A. (2009). The direct assimilation of cloud-affected satellite infrared radiances in the ECMWF 4D-Var. *Quart. J. Roy. Meteorol. Soc. 135*, 1214–1229.

Michel, Y., T. Auligné, and T. Montmerle (2011). Heterogeneous convective-scale background error covariances with the inclusion of hydrometeor variables. *Mon. Wea. Rev. 139*(9), 2994–3015.

Migliorini, S., A. C. Lorenc, and W. Bell (2017). A moisture incrementing operator for the assimilation of humidity- and cloud-sensitive observations. *Q. J. R. Meteorol. Soc.* (under review).

Migliorini, S., C. Piccolo, and C. D. Rodgers (2008). Use of the information content in satellite measurements for an efficient interface to data assimilation. *Mon. Weath. Rev. 136*(7), 2633–2650.

Minamide, M. and F. Zhang (2017). Adaptive observation error inflation for assimilating all-sky satellite radiance. *Mon. Weath. Rev. 145*, 1063–1081.

Montmerle, T. and L. Berre (2010). Diagnosis and formulation of heterogeneous background-error covariances at the mesoscale. *Quart. J. Roy. Meteorol. Soc. 136*, 1408–1420.

Moreau, E., P. Bauer, and F. Chevallier (2003). Variational retrieval of rain profiles from spaceborne passive microwave radiance observations. *J. Geophys. Res. 108*, 10.1029/2002JD003315.

Moreau, E., P. Lopez, P. Bauer, A. M. Tompkins, M. Janisková, and F. Chevallier (2004). Variational retrieval of temperature and humidity profiles using rain rates versus microwave brightness temperatures. *Quart. J. Roy. Meteorol. Soc. 130*, 827–852.

Morrison, H. and J. A. Milbrandt (2015). Parameterization of cloud microphysics based on the prediction of bulk ice particle properties. Part I: Scheme description and idealized tests. *Journal of the Atmospheric Sciences 72*(1), 287–311.

O'Dell, C. W., P. Bauer, and R. Bennartz (2007). A fast cloud overlap parametrization for microwave radiance assimilation. *J. Atmos. Sci. 64*, 3896–3909.

Okamoto, K. (2017). Evaluation of IR radiance simulation for all-sky assimilation of Himawari-8/AHI in a mesoscale NWP system. *Quart. J. Roy. Meteorol. Soc. 143*, 1517–1527.

Okamoto, K., A. P. McNally, and W. Bell (2014). Progress towards the assimilation of all-sky infrared radiances: an evaluation of cloud effects. *Quart. J. Roy. Meteorol. Soc. 140*(682), 1603–1614.

Pagé, C., L. Fillion, and P. Zwack (2007). Diagnosing summertime mesoscale vertical motion: implications for atmospheric data assimilation. *Mon. Weath. Rev. 135*(6), 2076–2094.

Pangaud, T., N. Fourrié, V. Guidard, M. Dahoui, and F. Fabier (2009). Assimilation of AIRS radiances affected by mid to low level clouds. *Mon. Weath. Rev. 137*, 4276–4292.

Pavelin, E. G., S. J. English, and J. R. Eyre (2008). The assimilation of cloud-affected infrared satellite radiances for numerical weather prediction. *Quart. J. Roy. Meteorol. Soc. 13*, 737–749.

Pearson, K. J., S. Lister, C. E. Birch, R. P. Allan, R. J. Hogan, and S. J. Woolnough (2014). Modelling the diurnal cycle of tropical convection across the 'grey zone'. *Quart. J. Roy. Meteorol. Soc. 140*(B), 491–499.

Peubey, C. and A. P. McNally (2009). Characterization of the impact of geostationary clear-sky radiances on wind analyses in a 4D-Var context. *Quart. J. Roy. Meteorol. Soc. 135*, 1863 – 1876.

Prigent, C., F. Aires, D. Wang, S. Fox, and C. Harlow (2016). Sea-surface emissivity parametrization from microwaves to millimetre waves. *Quart. J. Roy. Meteorol. Soc.*.

Prigent, C., J. R. Pardo, and W. B. Rossow (2006). Comparisons of the millimeter and submillimeter bands for atmospheric temperature and water vapor soundings for clear and cloudy skies. *J. Appl.Meteorol. Clim. 45*(12), 1622–1633.

Rabier, F., E. Klinker, P. Courtier, and A. Hollingsworth (1996). Sensitivity of forecast errors to initial conditions. *Quart. J. Roy. Meteorol. Soc. 122*(529), 121–150.

Riishøjgaard, L. P. (1996). On four-dimensional variational assimilation of ozone data in weather-prediction models. *Quart. J. Roy. Meteorol. Soc. 122*, 1545–1571.

Roberts, N. (2008). Assessing the spatial and temporal variation in the skill of precipitation forecasts from an NWP model. *Meteorol. Appl. 15*(1), 163–169.

Rysman, J.-F., S. Berthou, C. Claud, P. Drobinski, J.-P. Chaboureau, and J. Delanoë (2016). Potential of microwave observations for the evaluation of rainfall and convection in a regional climate model in the frame of HyMeX and MED-CORDEX. *Clim. Dyn.*, 1–19.

Saltikoff, E., P. Lopez, A. Taskinen, and S. Pulkkinen (2015). Comparison of quantitative snowfall estimates from weather radar, rain gauges and a numerical weather prediction model. *Boreal Env. Res 20*, 667–678.

Scheck, L., P. Frèrebeau, R. Buras-Schnell, and B. Mayer (2016). A fast radiative transfer method for the simulation of visible satellite imagery. *J. Quant. Spectr. Rad. Trans. 175*, 54–67.

Schomburg, A., C. Schraff, and R. Potthast (2015). A concept for the assimilation of satellite cloud information in an ensemble kalman filter: Single-observation experiments. *Quart. J. Roy. Meteorol. Soc. 141*, 839–908.

Sharpe, M. C. (2007). Incrementing liquid & frozen cloud water and grid-box cloud fraction for VAR observation operator and UM initialization. *Unpublished VAR Scientific Documentation Paper 61, UK Met. Office*.

Sieron, S. B., E. E. Clothiaux, F. Zhang, Y. Lu, and J. A. Otkin (2017). Comparison of using distribution-specific versus effective radius methods for hydrometeor single-scattering properties for all-sky microwave satellite radiance simulations with different microphysics parameterization schemes. *J. Geophys. Res.: Atmos. 122*(13), 7027–7046. 2017JD026494.

Smith, E. A., P. Bauer, F. S. Marzano, C. D. Kummerow, D. McKague, A. Mugnai, and G. Panegrossi (2002). Intercomparison of microwave radiative transfer models for precipitating clouds. *IEEE Trans. Geosci. Remote Sensing 40*, 541–549.

Stephens, G., D. Vane, R. Boain, G. Mace, K. Sassen, Z. Wang, A. Illingwort, E. O'Connor, W. Rossow, and S. Durden (2002). The CloudSat mission and the A-train. *Bull. Am. Meteorol. Soc. 83*(12), 1771–1790.

Stiller, O. (2010). A flow-dependent estimate for the sampling error. *J. Geophys. Res.* **115** (D22), doi: 10.1029/2010JD013934.

Tiedtke, M. (1989). A comprehensive mass flux scheme for cumulus parameterization in large-scale models. *Monthly Weather Review 117*(8), 1779–1800.

Tiedtke, M. (1993). Representation of clouds in large-scale models. *Mon. Wea. Rev. 128*, 1070–1088.

Tompkins, A. M., K. Gierens, and G. Rädel (2007). Ice supersaturation in the ECMWF integrated forecast system. *Quart. J. Roy. Meteorol. Soc. 133*(622), 53–63.

Tompkins, A. M. and M. Janisková (2004). A cloud scheme for data assimilation: Description and initial tests. *Quart. J. Roy. Meteorol. Soc. 130*, 2495–2517.

Wang, H., J. Sun, X. Zhang, X.-Y. Huang, and T. Auligné (2013). Radar data assimilation with WRF 4D-Var. Part I: System development and preliminary testing. *Mon. Wea. Rev. 141*(7), 2224–2244.

Wang, W., L. Xiaohong, S. Xie, J. Boyle, and A. Sally (2009). Testing ice microphysics parameterizations in the NCAR community atmospheric model verasion 3 using tropical warm pool-international cloud experiment data. *J. Geophys. Res.* **114** *(D22)*, doi: 10.1029/2008JD011220.

Wattrelot, E., O. Caumont, and J.-F. Mahfouf (2014). Operational implementation of the 1D+3D-Var assimilation method of radar reflectivity data in the AROME model. *Mon. Weath. Rev. 142*(5), 1852–1873.

Wilson, D. and D. Gregory (2003). The behaviour of large-scale model cloud schemes under idealized forcing scenarios. *Quart. J. Roy. Meteorol. Soc. 129*(589), 967–986.

Winker, D., M. Vaughan, A. Omar, Y. Hu, K. Powell, Z. Liu, W. Hunt, and S. Young (2009). Overview of the CALIPSO mission and CALIOP data processing algorithms. *J. Atmos. and Ocean. Tech.* **26***(7)*, 2310–2323.

Zhang, F., M. Minamide, and E. E. Clothiaux (2016). Potential impacts of assimilating all-sky infrared satellite radiances from GOES-R on convection-permitting analysis and prediction of tropical cyclones. *Geophys. Res. Let. 43*(6), 2954–2963.

Zhu, Y., E. H. Liu, R. Mahajan, C. Thomas, D. Groff, P. van Delst, A. Collard, D. Kleist, R. Treadon, and J. Derber (2016). All-sky microwave radiance assimilation in the NCEP's GSI analysis system. *Mon. Wea. Rev. 144*, 4709 – 4735.